ABSTRACT

Developing a Method to Quantify Cyclic Motion Patterns Using Smart Phone Technology

Heather J. King

Director: Brian A. Garner, Ph.D.

Cyclic motion patterns are those that repeat in a periodic sequence. Researchers have traditionally quantified cyclic patterns using high-quality optical or video motion capture systems that are often expensive and cumbersome. However, the modern emergence of accelerometers and gyroscopes embedded within common smart phones has inspired new research efforts to characterize motion patterns from these less expensive and more broadly-available tools. While many recent studies have focused on acceleration data, the present study seeks to derive the positional translation and orientation patterns from the smart phone data. A primary challenge with deriving positional data from accelerometer sensors is that the data must be integrated twice with respect to time, and data noise accumulates into substantial drift. For this study, the motion pattern of a mechanical horse was simultaneously recorded with a high-quality video motion capture system and with iPhone sensors. Positional data was derived from the iPhone data using an algorithm that capitalized on the known fact that the motion pattern was cyclic. Comparison of the motion-capture and iPhone-derived data sets revealed that the algorithm was very successful at reproducing the patterns of angular orientation, but not successful at completely eliminating drift from the positional translation pattern.

APPROVED BY DIRECTOR OF HONORS THESIS

____

Dr. Brian A. Garner, Department of Mechanical Engineering

APPROVED BY THE HONORS PROGRAM

____

Dr. Andrew Wisely, Director

DATE: ______________________________

DEVELOPING A METHOD TO QUANTIFY CYCLIC MOTION PATTERNS USING SMART PHONE TECHNOLOGIES

A Thesis Submitted to the Faculty of

Baylor University

In Partial Fulfillment of the Requirements for the

Honors Program

By

Heather King

Waco, Texas

May 2015

TABLE OF CONTENTS

TABLE OF FIGURES

ACKNOWLEDGMENTS

First, I would like to express my deepest gratitude to my advisor, Dr. Brian Garner, for his continuous guidance through my Honors Thesis research and development. Dr. Garner provided me with an excellent environment for conducting research and taught me more than I ever thought possible. Most importantly, his humble spirit and perpetual desire to serve was an inspiration to me throughout my journey at Baylor University.

I would also like to take this opportunity to thank the other members of my Honors Thesis Defense Committee: Dr. Lesley Wright and Dr. Yang Li for their flexibility, insightful comments, and challenging inquiries.

Last, but certainly not least, I would like to thank family for their continued support and encouragement throughout my time at Baylor University. My father taught me the value of being an excellent writer, and helped me hone the necessary skills to be one. My mother taught me the value of hard work and organization, two skills that carried me through this project. My little brother became a leader amongst his peers and inspired to do the same amongst my own. Without them, I would not be where I am today.

Most of all, I thank the good Lord for His continued blessings in my life…for good fortune of studying at Baylor University, for the mentors that have guided my personal and professional growth, the friends who encouraged me when all seemed hopeless, and the family members who always believed I could accomplish anything.

"For I can do all things through Christ, who strengthens me." Philippians 4:13

CHAPTER ONE

Introduction

Background Information

Cyclic motion patterns are readily apparent in both natural and synthetic applications. These patterns vary in complexity, ranging from the simple motion of a pendulum swing to the more complex cycles of humans in motion. Corporal movement patterns created by humans during routine activities such as walking have generated the interest of researchers in diverse fields, ranging from computer programming to mechanical engineering.

Applications of Motion Pattern Quantification

As the fields of computer vision and graphics have grown exponentially over the last few years, so too has the interest in quantifying human motion patterns. In these fields, motion patterns can be used for a variety of applications, including the development of more accurate human animations in the film & digital media industry, the improvement of visual surveillance software in security industry, and the enhancement of computer-user interfaces in technology development industries (Fuentes et al.).

Moreover, the quantification of movement patterns is also of great interest in the field of biomedicine and biomechanical engineering. For example, the movement patterns of elite athletes can provide a plethora of valuable information about the condition of the athlete's body. Motion pattern analysis of athletes may provide information about their range of motion, flexibility, and other performance indicators (Ellison, Rose, and Sahrmann). This information may help athletic trainers better develop training programs for their athletes. Likewise, irregular motion patterns may be indicative of developing injuries that are too subtle for typical diagnosis. This can alert physicians and help them avoid injury progression. The same concept can be applied to the health and performance monitoring of elite race horses. Much time, effort, and money is spent to maintain their health and ensure they are at peak performance. Unlike human athletes, however, animals cannot articulate their pain or injuries to their veterinarians. However, subtle changes in the horse's movement patterns may reveal such injuries and thus alert owners and veterinarians of potential problems.

In addition to these sports medicine applications, the quantification of movement patterns is also valuable in the rehabilitation and therapy arena. In this field, movement patterns can help determine post-therapy patient progress. For example, Timed-Up-and-Go (TUG) tests, trials commonly used to assess balance in elderly people, currently use devices that measure gait and movement (Milosevic, Jovanov, and Milenkovic). Quantifying these motion patterns (sitting, standing, and walking), can help therapists to more accurately assess the specific balance impairments (Milosevic, Jovanov, and Milenkovic). Similarly, therapists can measure balance therapy progress by comparing motion patterns in this test before and after therapy. Alternately, movement pattern quantification can be used to enhance other types of therapy. For example, hippotherapy is a treatment strategy that incorporates horseback riding. Hippotherapy has proven beneficial for individuals living with various forms of neuromuscular disability. Hippotherapists will select a particular horse that provides certain movement qualities and features they feel will best serve the client receiving the treatment. The ability to quickly and effectively quantify the features of these movement patterns will facilitate the analysis, study, and sharing of which pattern may prove most effective for a given disability. It can even facilitate the development of therapeutic devices that may also provide similar types of movements. Overall, the quantification of movement patterns has valuable applications in a variety of industries.

Movement Pattern Quantification Methods

In addition to the numerous applications for movement patterns, there are also several methods for measuring movement patterns. Traditionally, movement is assessed using data collected from sophisticated video motion capture systems. The data from these video motion capture systems can be processed and used to recognize certain types of motion (Chiu et al.). Researchers have explored several different methods to classify motion and improve motion recognition. Among these methods are KFD algorithms, Bayesian/neural networks, support vector machines, and decision trees (Chiu et al.)

While video is the most popular motion capture system, other systems use either magnetic or inertial variations to measure changes in motion. Magnetic motion capture systems measure the magnetic flux of a low-frequency magnetic field that is generated by a transmitter (Meta Motion). Inertial motion capture systems attach accelerometers, gyroscopes, and magnetometers to the subject to measure the motion of the subject. Although easy to setup and use, quality inertial motion capture systems, are often very expensive (Roetenberg, Luinge, and Slycke). Similarly, sophisticated video and magnetic motion capture systems are often expensive, complex, or time-consuming to setup. Thus, many researchers have begun to investigate simpler methods of motion capture by using the same tools as inertial motion capture systems (accelerometers and gyroscopes), but in a less expensive framework.

Smart Phone Inertial Sensors

The use of accelerometers in motion capture applications has begun to gain in popularity, especially with the rapid escalation in the availability of smart phone technology. The most recent smart phone technologies all contain a variety of sensors, including three-dimensional accelerometers, three-dimensional gyroscopes, magnetometers, and location/GPS sensors. While the purpose of these sensors is to enhance the computer-user interface and improve usability of smart phone applications, their data output has potential motion capture utility as well. Both iPhone and Android phones have applications (Sensor Data and Sensor Kinetics, respectively) that permit data collection from the phone's internal sensors (Wavefront Labs). The accelerometers measure translational acceleration in the x, y, and z planes, while gyroscopes measure 3-plane rotational acceleration (Wavefront Labs). Magnetometers provide information about the magnetic data that is used in conjunction with GPS input to produce location information (latitude, longitude, course, speed, and altitude) (Milosevic, Jovanov, and Milenkovic; Wavefront Labs).

Some researchers have already begun using these sensor applications for motion pattern analysis. For example, a group of researchers at the University of Alabama at Huntsville developed an application to use the iPhone's accelerometers and gyroscopes to conduct the TUG test (Milosevic, Jovanov, and Milenkovic). The sensors in the phone, which is attached to the subject's chest, measure the acceleration and orientation of the subject. By comparing this to known acceleration/orientation patterns, the application (sTUG) was able to recognize whether the person was sitting, standing, or walking (Milosevic, Jovanov, and Milenkovic).

Problem

Although some groups have started using smart phone accelerometer data for motion pattern analysis and recognition, to our knowledge no studies have yet determined whether the accelerometer data can be accurately manipulated to produce *position* data. Producing position data would enable simplified analysis of the cyclic features of the motion pattern being measured. One can obtain position by integrating the accelerometer data twice with respect to time.

However, this integration provides some challenges. Smart phone sensors produce accelerometer data that includes noise associated with the signal. When that data is integrated twice in time to acquire the position data, the noise accumulates and causes the position data to drift dramatically from the actual motion pattern being measured. Fortunately, the true value of a cyclic motion pattern lies in the local features that are repeated over the period of motion. Hence, the absolute positions are not critical, and the drifts can be ignored (factored out of the data). A Baylor research group led by Dr. Brian Garner has begun to develop an algorithm to process the raw accelerometer data and extract only the relative, periodic motion features that provide value in this analysis.

Purpose

The purpose of the present study is to verify the accuracy of the algorithm being developed by Dr. Garner. This study will test the accuracy of the finalized algorithm by comparing motion data produced from a smart phone to known motion patterns that have been measured using a video motion capture system. Overall, this study aims to develop and test a quick, simple, accessible, and reliable method to measure, quantify, and analyze the cyclic movement patterns of humans and animals.

Solution

Experimental Overview

The first step of this study of cyclic movement pattern quantification is collecting raw data. The team will use the application entitled "Sensor Data" to access and collect information from the accelerometers and gyroscopes embedded in an iPhone. The second step is to process the raw data, so that the cyclic movement pattern features can be extracted, analyzed, and interpreted. The team will use Dr. Garner's algorithm to factor out signal noise and highlight the local, cyclic features of the motion pattern. The final step of this study is to test and verify the cyclic movement pattern quantification methodology. Our team will use a mechanical horse device that produces a known and carefully controlled, complex three-dimensional movement pattern similar to that of riding a live horse. We will attach the iPhone, running the Sensor Data application, to this device to measure the accelerometer data. We will simultaneously record the motion using a sophisticated motion capture system. Subsequently, the team will process the information provided by the Sensor data application using our algorithm. Results will then be compared to the motion data of the mechanical horse that is collected by the motion capture system.

Thesis Overview

This thesis is organized into four chapters, with this Introduction serving as Chapter One. Chapter Two will explore existing research that relates to this thesis and illuminates the value of the results of the current study. Chapter Three will detail the experimental methods and materials used to collect data from the iPhone, measure motion patterns with video motion capture systems, and process the data from both systems. Chapter Four will detail the results of the experiment and the comparison analyses between known motion patterns and those produced by the iPhone sensors. The final chapter, Chapter Five, will discuss the results, describe the implications of the research, detail the limitations of the study, and present possibilities for future research.

CHAPTER TWO

Literature Review

Recently, inertial motion capture systems have grown in popularity, especially in the gaming, film, and digital media industries. Professionals in these industries typically use inertial sensors to conduct ambulatory motion analysis in order to accurately recreate human motion in a digital framework. Inertial systems offer a plethora of benefits compared to other motion capture systems. First, high quality inertial motion capture systems are typically simple to assemble and configure. For example, one popular inertial motion capture system, Xsens MVN, consists of a full body suit that is embedded with 17 inertial and magnetic sensors (Roetenberg, Luinge, and Slycke). These sensors wirelessly transmit their signal to a computer where the data is loaded into visualization software. The assembly and configuration of this system takes less than 10 minutes, yet yields excellent results (Roetenberg, Luinge, and Slycke). Moreover, inertial motion capture systems are better suited for a wider range of environments. Optical motion capture systems typically require specialized lighting in order to ensure that the all of the optical markers are clearly identifiable. Inertial motion capture systems have no such limitations, and are thus suited for both indoor and outdoor purposes (Roetenberg, Luinge, and Slycke). However, the benefits offered by a quality inertial motion capture system come at a significant cost. Quality systems can range from $5000-$80000, depending on the complexity (Meta Motion).

Yet, the core components of the inertial motion capture systems—inertial sensors and gyroscopes—are available at a fraction of the cost. Many researchers have begun to use such accelerometers and gyroscopes for their research in cyclic motion patterns. Yet, each study that utilizes inertial sensors is unique because the accelerometer data in each investigation is processed and applied through different techniques. Primarily, researchers have developed two primary methods for processing the raw accelerometer data into useful motion data. Typically, researchers will use the accelerometer data in conjunction with pattern matching and motion recognition algorithms. However, some researchers integrate the accelerometer data to acquire position or velocity data and develop a more traditional motion pattern. Each method introduces different challenges and limitations.

Some researchers have sought to simplify inertial motion capture by using smart phone accelerometers in their research efforts to quantify cyclic motion patterns. The data from smart phone accelerometers can be processed in a manner similar to regular accelerometers. However, smart phone accelerometers produce their own set of challenges. For example, smart phone inertial sensors tend to be lower quality and thus introduce more noise into the signals. Thus, it is helpful to test the accuracy of smart phone accelerometers by comparing the motion data they produce to the motion data produced by a higher quality motion capture system. However, this task itself introduces complications since there is currently not a standardized method of comparing different motion patterns.

The present study utilizes smart phone accelerometers to measure cyclic movement patterns and must address many of the issues discussed above. Before examining the methods that the current study uses to process and utilize accelerometer data, however, it is helpful to review related studies and research. This chapter is broken into three sections. The first details research that utilizes accelerometers to measure motion patterns, examines their data processing techniques, and highlights any challenges they experienced. The second section details research that utilizes smart phone accelerometers to measure motion patterns, examines their data processing techniques, and highlights any challenges they experienced. The final section addresses research that attempts to develop a standardized method of comparing cyclic motion patterns.

Accelerometer Research & Data Analysis

As mentioned above, there are a variety of ways to process accelerometer data, depending on the desired information and available computational resources. By far, the majority of researchers utilized pattern-matching algorithms or motion recognition software to match the accelerometer data against known motion patterns. Each research study described below highlighted a different motion recognition method, and revealed the complexity of using accelerometers to measure cyclic motion patterns.

A 2008 study by Slyper and Hodgins attempted to create a simplified, less expensive version of the Xsens inertial motion capture systems. The researchers affixed five accelerometers to a shirt that could be worn by the subject during tests. The acceleration data sets from the shirt sensors transmit to a computer program employing a wavelet-matching algorithm (Slyper and Hodgins). This algorithm matched the accelerometer readings to known, preprocessed motion patterns. Whenever a match was found, the system would recreate the motion on a digital rendering of the human subject.

Slyper and Hodgins discovered that their method relied heavily on repeatable accelerations. In other words, the system easily recognized distinct motions that were repeated for a period of time (such as jumping jacks), but had difficulty recognizing smaller, quicker movements (Slyper and Hodgins).

A 2011 study by Mesbah, et al, utilized several 3-axis accelerometers to monitor fetal movement episodes. The accelerometer data from each axis was then used to calculate the root mean square of the acceleration magnitudes (Mesbah et al.). If the RMS value was greater than a predetermined threshold value, the motion was classified as a fetal movement. This study's limitations included the fact that the method could only identify fetal activity from inactivity. Moreover, the study did not offer any method to differentiate between fetal movements and small maternal movements (Mesbah et al.).

A 2012 study conducted by Yao, et al, similarly utilized multiple 3-axis accelerometers to monitor sleep positions, in an effort to improve research on obstructive sleep apnea syndrome. The accelerometer sensors were attached to the forehead and chest of the patient. The raw accelerometer data collected from each axis was then converted into the angular domain using a CORDIC algorithm (Yao et al.). This algorithm produced the tilt angles relating to the patient's head inclination or rotation. When used in conjunction with other research, the tilt angles produced from the accelerometer data may help clinicians identify and correct early symptoms of obstructive sleep apnea syndrome (Yao et al.).

All of these research efforts used accelerometers to measure different aspects of movement patterns. Each study processed the accelerometer data differently, but all of them compared the processed acceleration data to known motion patterns. However, some other researchers used the acceleration data to produce *position* data.

For example, a 2013 study conducted by Cho and Shieh involved the design and testing of a smart belt that detects the gait of human walking or running at various speeds. The researchers desired that the smart belt be able to detect acceleration, velocity, and absolute position of the human subject. The relative acceleration data was used to identify the type of gait (standing, walking, running, etc), but obtaining position data proved more difficult. The researchers recognized that simply integrating the acceleration data twice with respect to time to obtain position would yield significant error in the absolute position of the signal (Yao et al.). Thus, Cho and Shieh instead partitioned the acceleration data into small time intervals that could be treated as a continuous system without accuracy losses. For each window, they calculated the average velocity. The distance the subject moved during each window was then calculated by multiplying the velocity by the time of the interval. The sum of the distance moved during each time interval yielded the distance that the subject moved during the entire test (Yao et al.).

A 2004 study by Grimnes, et al, involved suturing an accelerometer to the left ventricle of a pig's heart. Grimnes then applied a Butterworth high-pass filter to the acceleration data to remove any inaccuracies (Grimnes et al.). The filtered data was then integrated twice using a trapezoidal integral approximation, with the high-pass filter applied after each integration (Grimnes et al.). Similarly, a 2013 study conducted by Li used accelerometers to calculate velocity and position data for welding techniques. Li used similar processing methods as Grimnes to filter the acceleration data and integrate for position data. However, both of these studies were concerned primarily with obtaining approximations of the absolute position. Our current study is concerned with producing a repeatable, cyclic motion pattern that represents relative motion.

Smart Phone Accelerometer Research

In addition to the above research involving motion capture with accelerometers, there are also several researchers that are beginning to utilize smart phone accelerometers in their studies. In order to better understand the benefits/drawbacks of employing smart phone accelerometers, several studies were reviewed.

A 2012 study by Cho, et al, employed a smart phone as a handheld game controller for a digital game of tennis. The researchers accessed the acceleration data produced by the smart phone's inertial systems and created a pattern-matching algorithm that enabled the smart phone to recognize the player's strokes based on the accelerations produced (Cho et al.). Cho noted that their algorithm would not be able to differentiate between two movements that produced similar acceleration vectors.

Another 2012 study by Bai, et al, worked towards the design and implementation of a fall monitor system. Smart phones are uniquely suited for fall detection because almost everyone has access to a smart phone that contains inertial sensors. Moreover, acceleration patterns of a falling individual are very unique, and thus easily recognized by a computer program (Bai, Wu, and Tsai). Once the acceleration patterns are matched to known fall acceleration patterns, GPS can be activated to determine where the fall occurred (Bai, Wu, and Tsai). This application would be of significant help to elderly individuals at risk for severe injury upon falling.

Yet another 2012 study by Ryu, et al, utilized a smart phone, attached to the back of a human subject, to conduct ambulatory gait analysis. In this study, Ryu applied a low-pass filter to the initial acceleration data in order to remove any irregularities. In order to obtain position displacement, the acceleration data was integrated twice with respect to time and a high-pass filter was applied to remove integration drift (Ryu et al.). This study was particularly helpful because it highlighted some of the issues that typically arise when using smart phones as motion capture devices. Namely, smart phone accelerometer signals may have irregular sampling intervals, present alignment problems, and introduce other inaccuracies not seen with regular accelerometers (Ryu et al.).

Standardized Motion Capture Comparison

Several of the studies highlighted above compare their inertial motion capture data to data captured from a quality optical motion capture system. For example, the 2012 study by Ryu used optical motion capture data verify the gait analysis they conducted with smart phone accelerometers (Ryu et al.). The 2011 study by Mesbah used an ultrasound system to verify the accuracy of accelerometers in the detection of fetal movements (Mesbah et al.). However, to our knowledge, no studies developed a standardized method to compare motion patterns produced by accelerometers to those produced by optical motion capture systems.

CHAPTER THREE

Materials & Methods

Data Collection

To collect the requisite data for this experiment, we used both three-dimensional video motion capture and smart phone accelerometer technology. Although both the accelerometers and the motion capture system could be used to record virtually any motion, we chose to model the mechanical horse designed and built by Dr. Brian Garner and his graduate students (shown below). Measuring the mechanical horse's motion

Figure 1: Mechanical horse designed and constructed by Dr. Brian Garner and his graduate students.

served a dual purpose. First, the horse's motion produces a sufficiently complex, yet also cyclic pattern. We were able to capture both a known motion pattern from the video motion capture system and an experimental motion pattern from the smart phone accelerometers. Since the video and inertial motion capture systems can easily measure this cyclic motion, it is ideal for testing the validity of the algorithm used to process the smart phone accelerometer data. Second, accurate measurement of the mechanical horse motion may foster additional research in this subset of biomechanics. For example, the ability to quickly and easily quantify a horse's motion pattern using smart phone technology may improve practices in fields such as hippotherapy and equine racing.

Motion Capture System Trials

Three-dimensional video motion capture systems typically use a series of cameras and a set of markers to record motion. The cameras surround the observation space, and may connect to each other in a "daisy-chain" pattern. A computer, connected to the lead camera, synchronizes all cameras via an electrical signal. The markers—typically small spheres wrapped in reflective tape or small light sources (such as an LED bulb)—are attached to the subject using adhesive tape. The position of any given marker can be accurately triangulated only when sensed by at least two cameras. Additionally, the system must be properly calibrated. After proper configuration and calibration, the motion capture software will process the data retrieved from each reflective marker and return the position of the marker (x, y, and z) throughout the test.

In this study, we configured Baylor University's PhaseSpace IMPROV (PhaseSpace, Inc., San Leandro, CA) video motion capture system in the Human Health & Sciences laboratory. Eight cameras were arranged into a semi-circle array, with Camera 1 serving as the lead camera. The system was calibrated using a reflective wand and PhaseSpace Calibration software.

Figure 2: PhaseSpace IMPROV drivers and calibration wand.

After calibration, we placed the mechanical horse in the observation space and synchronized the LED markers to a driver. For each trial, the motion capture system returned the three dimensional coordinates (x, y, and z) of each marker at every instant during the capture period. All video trials were conducted at the system's maximum

Figure 3: Cameras were arranged in a semi-circle around the observation space for the motion capture of the mechanical horse's motion patterns

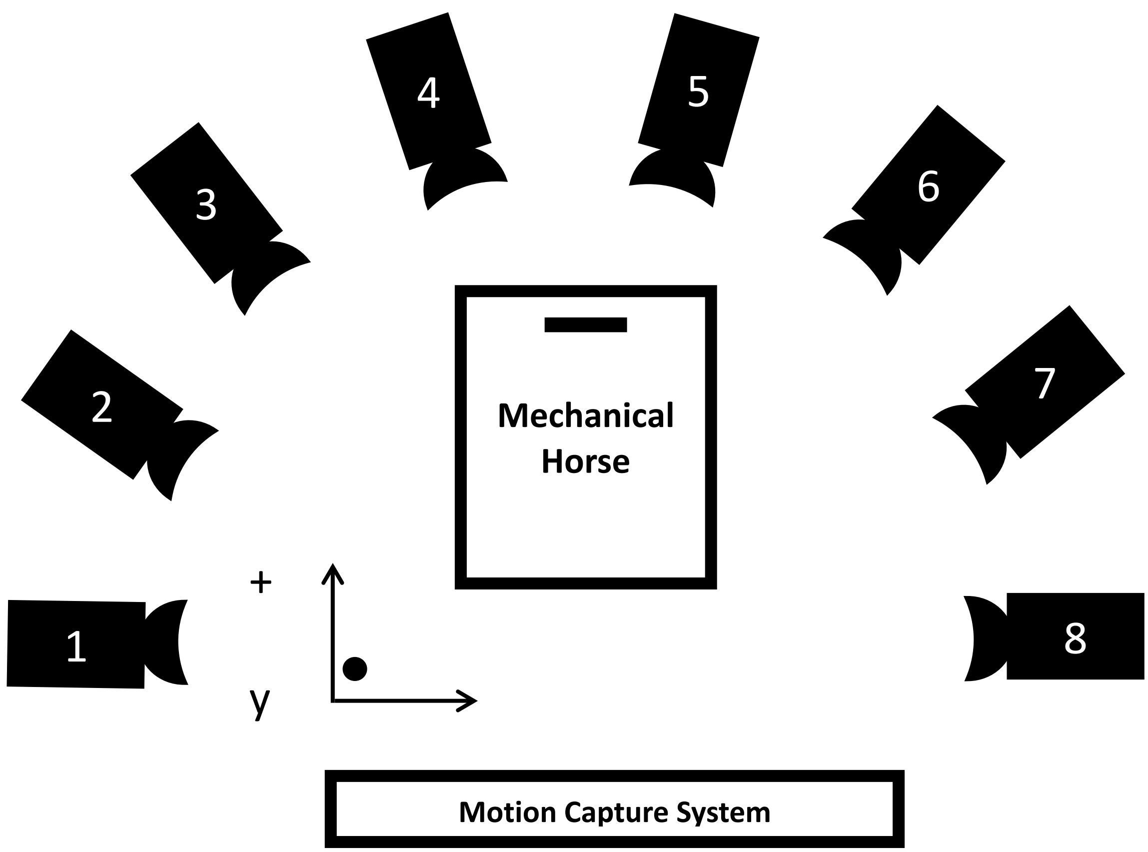

capture rate, 120 Hz. From the computer's frame of reference, the positive *x*-axis refers to forward motion, the positive *z*-axis refers to lateral motion to the right of the horse, and the positive *y*-axis refers to upward motion. For this research study, we used a total of twelve LED markers. The first four were placed on the stationary base of the motion capture system. Since these markers were immobile throughout the test, they were designed to help correlate the motion capture coordinate system to the base coordinate system of the mechanical horse. Three markers were placed on the rear of the mechanical horse's saddle and two were placed on the front of the saddle. One marker was placed on the handle of the mechanical horse. This marker serves as the "origin" of the mechanical horse's coordinate system. The final two markers were affixed to a pelvis belt, consisting of a Velcro strap attached to a rigid metal bar. This pelvis belt was attached the rider to help track the motion of the rider's pelvis more accurately.

Figure 4: Posterior view of the markers on the mechanical horse and rider (right). Anterior view of markers on the mechanical horse saddle/handle with no rider (left). The marker on the handle serves as the origin of the mechanical horse's coordinate system.

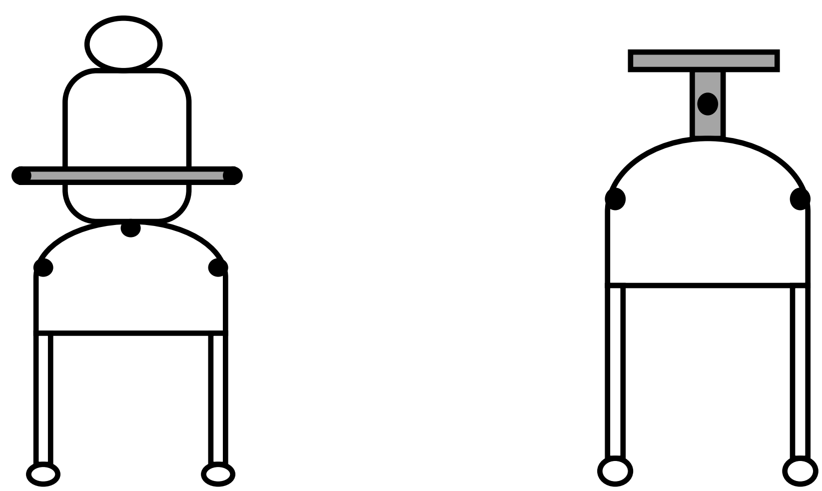

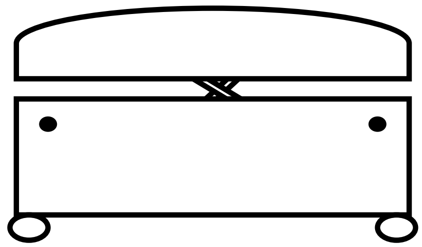

Figure 5: Lateral view of the markers on the base of the mechanical horse--view is identical for both sides of the horse.

After constructing the observation space and configuring the equipment, we conducted two groups of three trials (six total), each lasting approximately 30 seconds. Frequency was set at 30 Hz for the first trial in each group and then increased by 15 Hz for each subsequent trial. The first three trials involved one female, able-bodied adult rider who was 5 ft. 1 in. tall and weighed 120 pounds. Experiments for assessing humans riding on the mechanical horse were approved by the Baylor IRB. The rider wore the pelvis belt described above, to more accurately track her pelvic motion. The last three trials followed the same pattern as the first three, but were conducted without a rider.

Smart Phone Inertial Sensors

Most modern smart phones contain a variety of sensors that help orient it and improve the function of its applications. Among these sensors are three that contribute significantly to motion capture—three-dimensional accelerometers, three-dimensional gyroscopes, and location/GPS sensors. Lately, some application developers have created applications to access and utilize these sensors. One such application, Sensor Data, runs on the iPhone. This application, created by Wavefront Labs, accesses the three-dimensional accelerometers and gyroscopes. Thus, this application allows the iPhone to be used as an inertial motion capture system. The Sensor Data application has two modes of operation—streaming mode and capture mode. Streaming mode sends the stream of sensor data from the device directly to an external computer. This facilitates real-time data collection. Capture mode collects the sensor data at a specified rate (ranging from 1-100 Hz) and stores it in a file on the phone. Each captured data set file can be found in the application “Library”. Additionally, the application creates a website address that allows the user access to the data files from their home computer. These files are CSV (comma-separated values) and thus easily exported into a spreadsheet. Moreover, Sensor

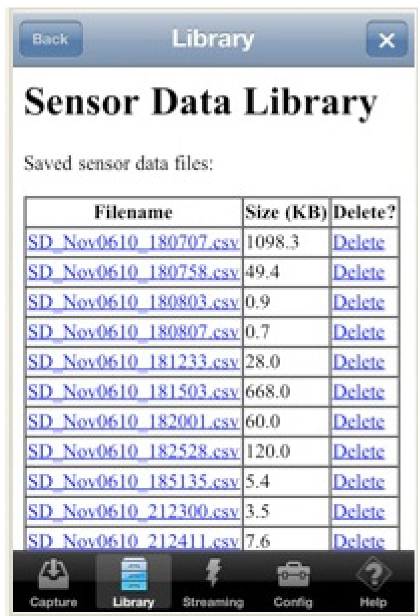

Figure 6: Sample library of data files created by using the capture mode of the Sensor Data application.

Data contains a configuration tab that allows the user to select specific information collected by the application. For example, users can choose to gather accelerometer data while ignoring the latitude/longitude data. This lets the user adapt the application to their individual needs

For the purposes of this study, all available data was collected. However, the *x*, *y*, and *z* accelerations, as well as the roll, pitch and yaw measurements, were of primary interest.

For this research study, we used the latter mode of operation at a sampling frequency of 100 Hz. We conducted thirteen trials using an iPhone 4, with the first six coinciding with the motion capture trials discussed earlier. For the first three trials, the rider placed the iPhone between her legs to secure it. However, we wanted the iPhone to measure the mechanical horse's motion and not the rider's motion. Therefore, she was

Figure 7: User interface of Sensor Data application in the capture mode.

asked to secure the smart phone gently enough that her body's motion did not affect the iPhone. For the next three trials there was no rider, so the smart phone was placed flat on the saddle back, as close to the handle (origin) as possible.

After these six trials, we stopped recording data samples using the motion capture system. However, we took seven more samples using the iPhone 4 Sensor Data application. For three of these trials, the iPhone was placed near the handle and tilted upwards at an angle. The mechanical horse was then operated at 30, 45, and 60 Hz while the iPhone captured data at each frequency. For the next three trials, the iPhone was once again placed near the handle but twisted sideways. The same process was then repeated. Finally, the iPhone was placed flat on the saddle, as far from the handle as possible. Data was collected while operating the mechanical horse at 60 Hz. These last seven samples were collected primarily to give Dr. Garner more data to analyze and help improve his algorithm.

Data Analysis

Processing Motion Capture Data

For each motion capture, the raw data files consisted of the recorded three-dimensional trajectories of each marker throughout the trial duration. The goal was to create a representative, single-cycle movement pattern of the saddle that reflects the translational (*x,y,z*) trajectories of the saddle coordinate system origin, and the angular (roll, pitch, yaw) trajectories of the saddle orientation. This format would allow us to easily compare the motion capture data to the processed iPhone data, or to other motion capture trials. Achieving this goal required the five steps listed below, which were performed on each of the six data sets collected.

1.) ***Orient****:* Each LED marker in the Phasespace IMPROV system is labeled with a specific number, so that the computer can track individual markers. However, these LED's are not labeled with the associated number. Thus, the first step of data processing was to determine where each marker was placed on the mechanical horse. We graphed the top view, lateral view, and frontal view of the motion of each marker. Analyzing these graphs helped us determine where each marker was located. These correlations are summarized in Table 2.1.

2.) ***Change coordinate system****:* Once the markers were defined according to their position on the mechanical horse, we were able to use them to orient the coordinate system of the mechanical horse's base with respect to the motion capture coordinate system. The marker on the handle of the mechanical horse served as the origin of the base coordinate system. Using a rotation matrix, we rotated the x, y, and z coordinates of each marker so as to express them all in terms of the base coordinate system. This allowed us to analyze the actual movement of the mechanical horse, rather than movement from perceived by the motion capture system.

Marker Orientation		
Marker Number	***General Location***	***Specific Location***
39	Rider Pelvis Belt	Right
40	Rider Pelvis Belt	Left
5	Base (Fixed)	Forward Left
16	Base (Fixed)	Back Left
17	Base (Fixed)	Forward Right
15	Base (Fixed)	Back Right
1	Saddle Corners	Forward Left
2	Saddle Corners	Forward Right
3	Saddle Corners	Back Right
4	Saddle Corners	Back Left
6	Saddle	Middle Saddle
0	Handle (Origin)	Front Handle

Table 2.1: Correlation between marker number and location of marker on mechanical horse.

3.) ***Calculate kinematic measurements****:* Once all coordinates were rotated into the base coordinate system, we wanted to model the periodic translational and angular movement of the mechanical horse over the entire trial. The translational motion was easily modeled by plotting the x, y, and z coordinates of Marker 0 (origin marker) over the trial time. The angular shift required some additional, simple calculations. The roll, pitch, and yaw were all calculated by constructing three vectors. One vector pointed from Marker 4 to Marker 1, the second vector pointed from Marker 3 to Marker 2, and the final vector pointed from Marker 6 to Marker 0. Then, the angle between the x and y axes was calculated for each vector. This supplied three estimates for the pitch angle. The average of all three pitch estimates became our pitch angle. Similarly, the angle between the x and z axes was calculated for each vector. This calculation yielded three estimates for the yaw angle and, once again, the average of these estimates became our final representation of yaw. The angle between the *y* and *z* axes yielded only two estimates for roll, as Marker 0 and Marker 6 were assumed to be perfectly aligned in the *yz* plane. The average of the two estimates yielded our final roll angle.

Figure 8: Roll, Pitch, and Yaw of mechanical horse.

These first three data analysis steps were originally performed using a technical computing program called MATLAB. However, these steps were eventually integrated directly into Dr. Garner's algorithm, so that the motion capture data and the iPhone data process simultaneously. This enables the algorithm to output the motion capture data and the iPhone data in an identical format, which simplifies comparison.

Processing Smart Phone Accelerometer Data

The majority of data processing for the iPhone accelerometer data occurred when the data for each trial was imported into Dr. Garner's algorithm. Dr. Garner's algorithm selects the three translational accelerations and three rotational accelerations calculated by the iPhone. It then integrates the selected data twice with respect to time to obtain position data. However, this amplifies any noise found in the original signal. The algorithm then capitalizes on the known cyclic nature of the movement patterns to identify cyclic periods, and factor out the drift component. Details of the algorithm are beyond the scope of this thesis. The final result is a cyclic motion pattern that represents the global motion pattern of the iPhone. At this point, the iPhone data set and the motion capture data sets have identical formats (six vectors consisting of x, y, z, roll, pitch, yaw data), and are prepared for comparison.

Processing Data Sets for Comparison

At this point, the two data sets were imported into MATLAB, for plotting and comparison. Before the two sets could be accurately compared, however, they required some additional processing.

1) ***Normalize Time:*** First, we normalized the time vector. The motion capture and the iPhone data vectors were of different sizes, which made them difficult to compare graphically. The difference in vector size existed for two primary reasons. First, the iPhone and motion capture trials ran for different amounts of time. Second, the sampling rate of the iPhone differed from that of the motion capture system. Normalizing the time vector helped resolve the first difference. Scaling the data sets helped resolve the second difference.
2) ***Scale Data Sets:*** Since the sampling rate of the iPhone was approximately half of the sampling rate of the motion capture system, the iPhone vectors

contained less data points. Thus, when the time vector was normalized, the periodic motion produced by the iPhone appeared to be half the size of the periodic motion produced by the motion capture system. Thus, the iPhone data was scaled to match the motion capture data.

3) ***Shift Data Sets:*** Moreover, the origin of the iPhone differed from that of the motion capture system. Thus, the iPhone data was shifted left to accommodate the differing origins.

After these changes, the iPhone and motion capture data could be easily plotted and compared to each other.

CHAPTER FOUR

Results

As discussed above, the motion of the mechanical horse was recorded on both the optical motion capture system and on the inertial sensors of the iPhone for six separate trials. The first three trials recorded the mechanical horse's motion with a rider at three different speeds (30, 45, 60 Hz). The second three trials recorded the mechanical horse's motion without a rider at the same three speeds (30, 45, 60 Hz). While the team endeavored to synchronize the iPhone recordings with the motion capture recordings, some of the samples were started late, or had to be restarted mid-recording. For this reason, this chapter only presents the results from Trial 2 (with rider) and Trial 5 (without rider). These trials were both recorded at 45 Hz, and did not involve any recording errors.

In sum, graphical results follow, depicting the relative, periodic motion of the mechanical horse in the *x*, *y*, and *z*-coordinate trajectories, as well as the periodic roll, pitch, and yaw angles detected during the trial. Data are shown for the motion of the mechanical horse with a rider and without a rider. Each data set includes the motion of the mechanical horse as recorded by both the optical motion capture system and by the iPhone Sensor Data application.

Figures 9 through 11 show the average spatial translations of the mechanical horse from the perspective of a viewer observing from behind (back view), above (top view), or lateral (side view). The Lissajous plots reflect the magnitude and patterns of the mechanical horse's translations in one spatial direction versus the translations in another spatial direction. The spatial translations recorded by the iPhone are plotted on the same plots as those recorded by the motion capture system.

Figures 12 through 14 show the linear translations of the periodic motion of the mechanical horse. Figures 15 through 17 show the angular measurements of the periodic motion of the mechanical horse. The iPhone data sets are plotted on the same plots as the motion capture data sets to aid visual comparison.

Spatial Views of Mechanical Horse Motion

Figure 9 shows the mechanical horse's translation as viewed from behind the mechanical horse (back view). For this view, the y-coordinate (vertical motion) is plotted versus the z-coordinate (lateral motion). In both Trial 2 and Trial 5, the motion capture system traced a very clear, repeatable butterfly shape. The processed iPhone data, however, did not have a clear pattern and indicated much larger translations in both the lateral and vertical directions. The trial with a rider, Trial 2, indicated a more random pattern with significant outliers in the vertical direction. The trial with no rider, displayed a more repeatable pattern that Trial 2, but was not as a precise as the motion capture system pattern.

Figure 10 shows the mechanical horse's translation as viewed from the side of the mechanical horse (side view). For this view, the y-coordinate (vertical motion) is plotted versus the x-coordinate (forward motion). In both Trial 2 and Trial 5, the motion capture system produced a repeatable, kidney-shaped pattern. This pattern is somewhat evident in the iPhone data from Trial 5, but almost non-existent in Trial 2. Both iPhone data sets indicated significant variations in both the vertical and forward directions, and did not indicate clear repeatability.

Figure 11 shows the mechanical horse's translation as viewed from above the mechanical horse (top view). For this view, the *x*-coordinate (forward motion) is plotted versus the *z*-coordinate (lateral motion). In both Trial 2 and Trial 5, the motion capture data produced a repeatable, figure-8 shape pattern. The iPhone data from the top view displayed a more repeatable pattern than the other two views, but it was still not as precise as the motion capture data. Moreover, the iPhone data from Trial 2 did not display the same figure 8 pattern as the motion capture system. The iPhone data from Trial 5 indicated a more repeatable, figure 8 pattern than Trial 2.

Translation Motion of Mechanical Horse

Figure 12 displays the periodic motion of the mechanical horse in the *x*-direction (forward motion). The motion capture data from both Trial 2 and Trial 5 indicates a clearly periodic motion with one valley and one crest per period. In Trial 2, the iPhone data also indicated a periodic motion. However, in this trial, the periodic motion varies more significantly. The amplitude appears to match that of the motion capture system for the first two periods, but then the amplitude of the iPhone data increases for the next two periods. This pattern continues for the remainder of the trial. Trial 5 matches the periodic motion of the motion capture system very closely, with only a few outliers occurring near the beginning and end of the trial.

Figure 13 displays the periodic motion of the mechanical horse in the *y*-direction (vertical motion). The motion capture data from both Trial 2 and Trial 5 indicates a periodic motion with one valley and two crests per period. Trial 2 shows a periodic motion in the iPhone data, but the features vary from period to period. Some periods demonstrate one crest and one trough, while others appear to have two crests. Additionally, there is a significant trough that occurs approximately 40% of the way through the trial. The iPhone data from Trial 5 has a somewhat more consistent periodic motion with two crests per period. The amplitude of the Trial 5 iPhone data is very close to that of the motion capture data, but the periodic pattern is not as consistent.

Figure 14 displays the periodic motion of the mechanical horse in the *z*-direction (lateral motion). The motion capture data from both Trial 2 and Trial 5 indicates a periodic motion that consists of two crests (one higher than the other) and two valleys (one lower than the other). The iPhone data from both Trial 2 and Trail 5 exhibited a trend similar to the motion capture data, but the features were not as well defined. Moreover, the amplitude of the top crests increased as the trial progressed.

Angular Motion of Mechanical Horse

Figure 15 displays the mechanical horse's periodic roll motion. In Trial 2, there is significant alignment between the motion capture data and the iPhone data. Both appear to have one valley and one crest. However, the amplitude of the iPhone data begins slightly lower than that of the motion capture data and gradually increases to a height greater than the motion capture system. In Trial 5, there is also significant alignment between the motion capture data and the iPhone data. In this trial, both appear to have one valley and one crest, but there is also an additional graphical feature that appears near the origin. This feature is not evident in the Trial 2 graphs.

Figure 16 displays the periodic pitch motion of the mechanical horse. Trial 2 exhibits significant alignment between the motion capture data and the iPhone data. Both have one clear peak and on clear trough per period, but the amplitude of the Trial 2 iPhone peaks fluctuate more than the motion capture peaks. Trial 5 exhibits even better alignment between the motion capture data and the iPhone data. Both sets have one clear trough and one clear peak per period. Neither the iPhone data nor the motion capture data exhibit significant variance in their amplitude, but the iPhone amplitude is consistently less than that of the motion capture data.

Figure 17 displays the periodic, yaw motion of the mechanical horse. Both Trial 2 and Trial 5 exhibit excellent alignment between the motion capture data and the iPhone data. Both appear to have one valley and one crest per cycle. In Trial 5, however, additional features appear at the valleys/crests of both the iPhone and the motion capture data. The Trial 2 data appears smoother, and does not exhibit the finer features seen in the Trial 5 data.

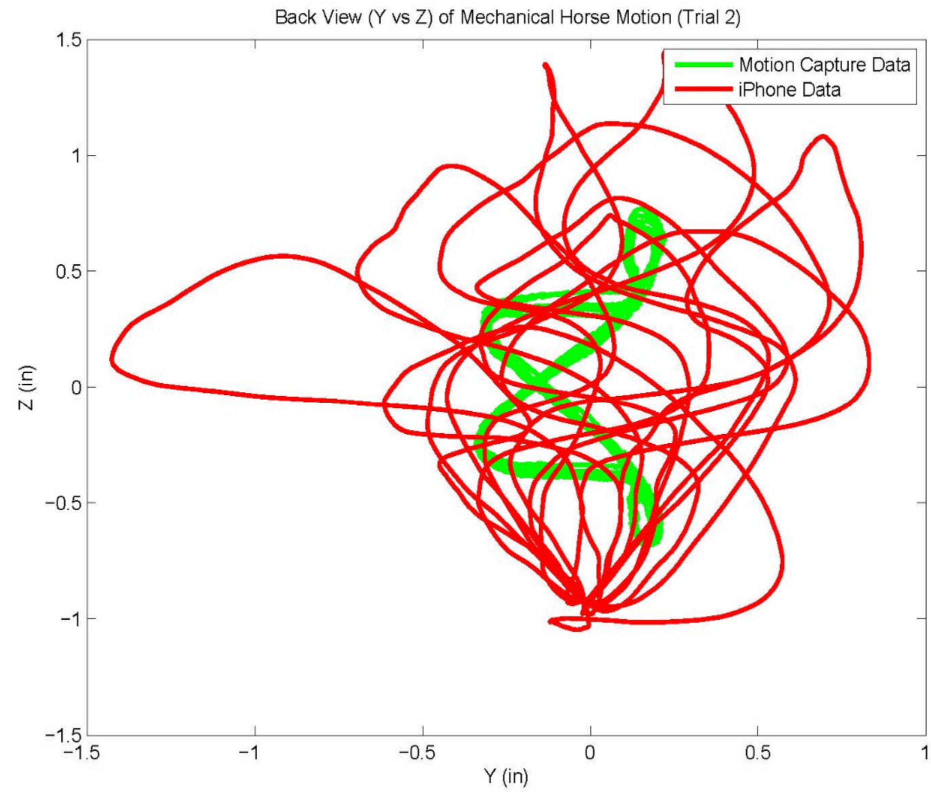

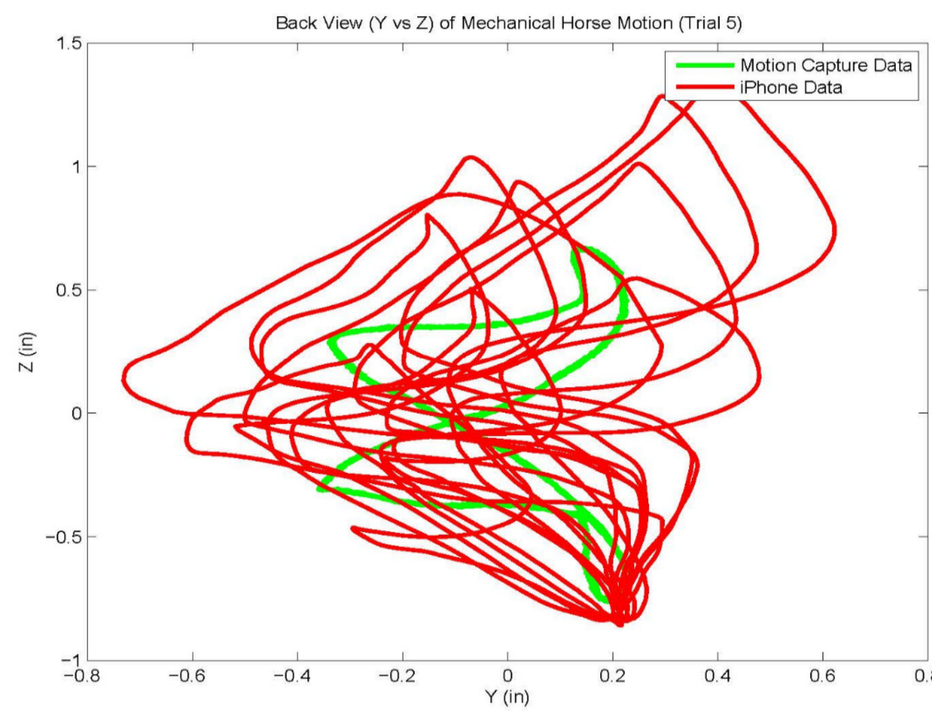

Figure 9: Motion of the mechanical horse as viewed from behind. Motion recorded for a trial with a rider (Trial 2) and a trial without a rider (Trial 5).

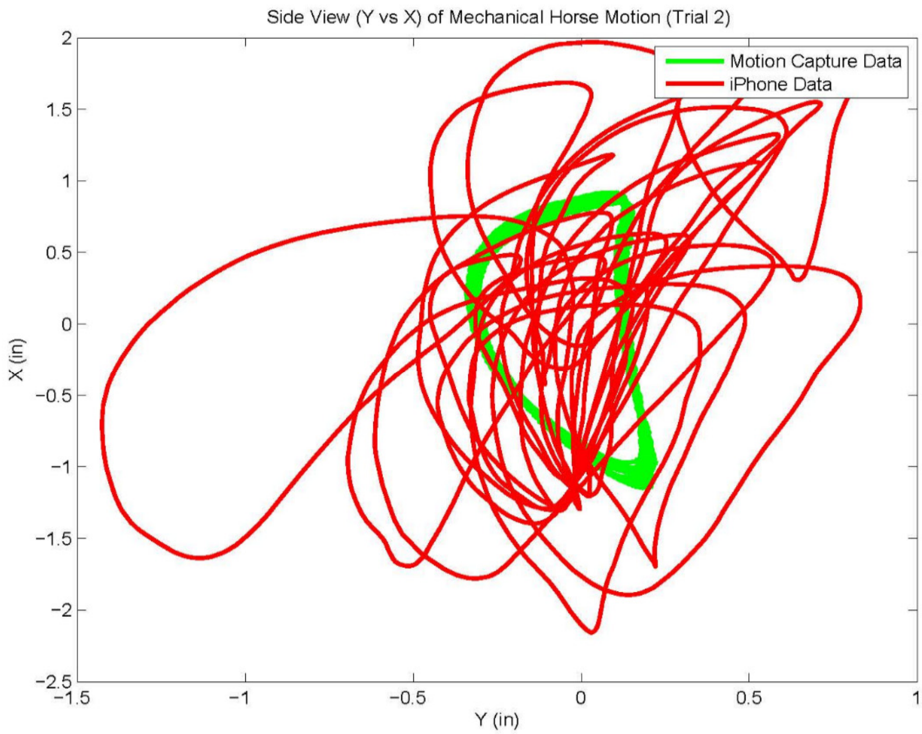

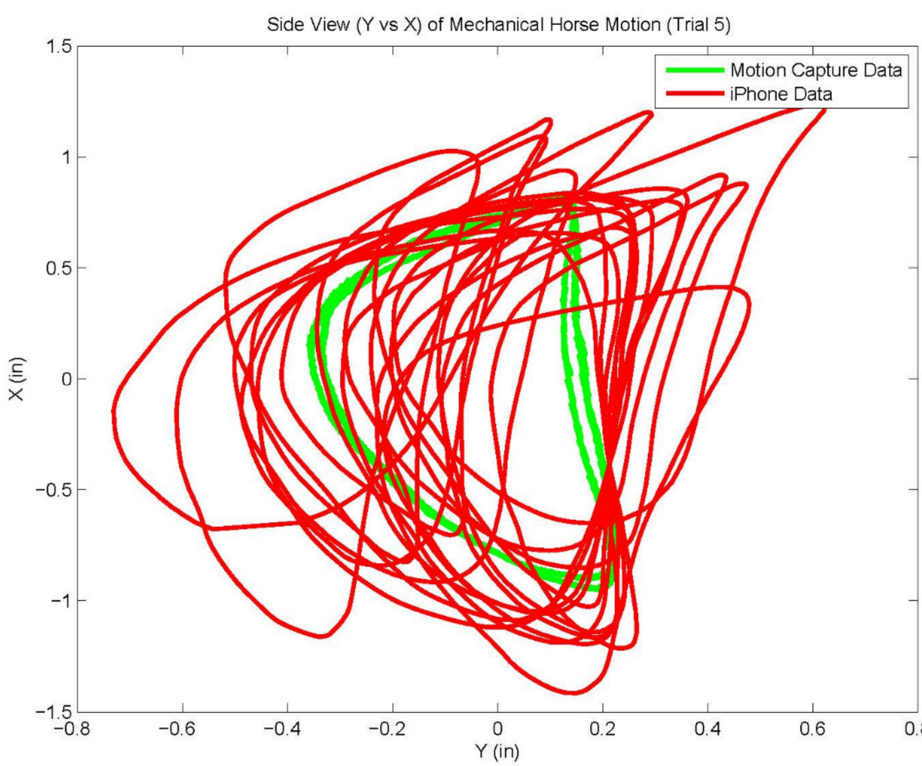

Figure 10: Motion of the mechanical horse as viewed from the side. Motion recorded for a trial with a rider (Trial 2) and a trial without a rider (Trial 5).

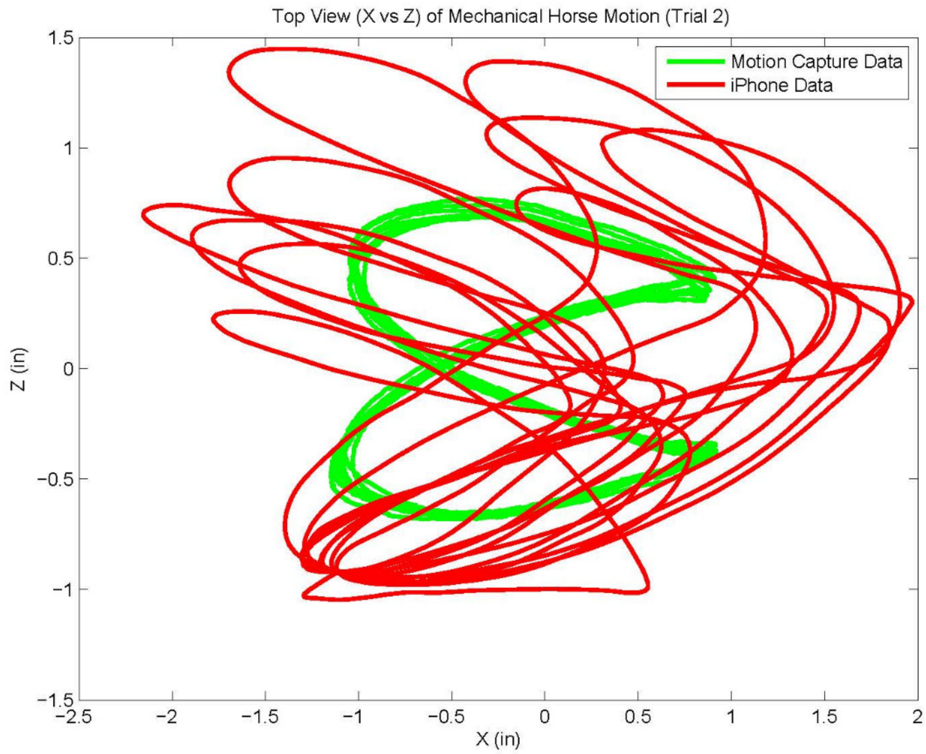

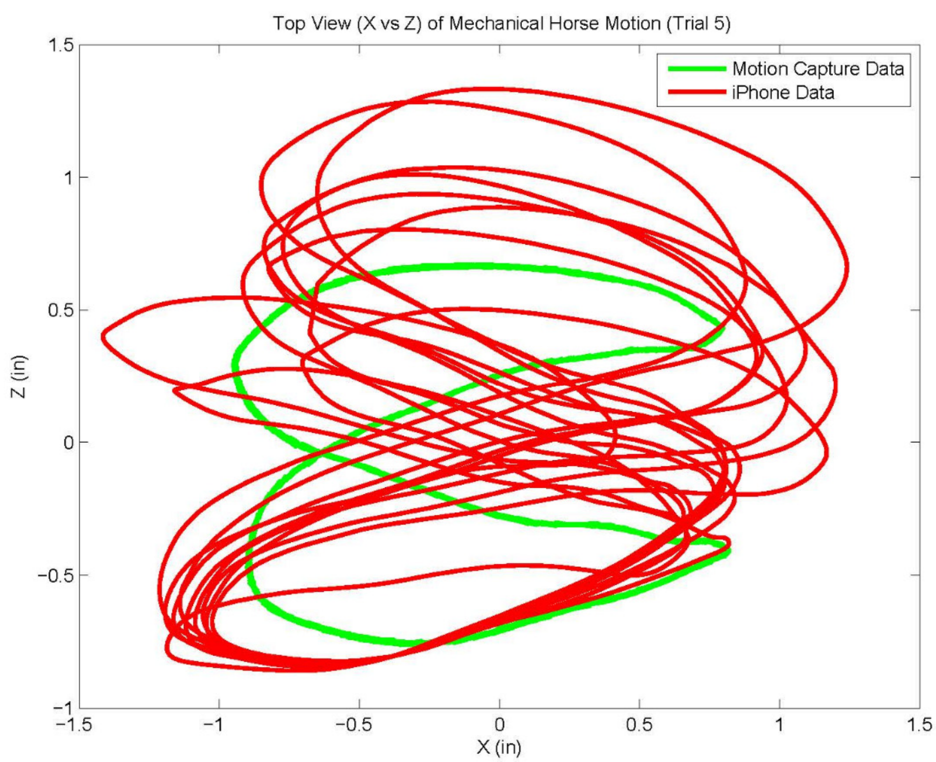

Figure 11: Motion of the mechanical horse as viewed from above. Motion recorded for a trial with a rider (Trial 2) and a trial without a rider (Trial 5).

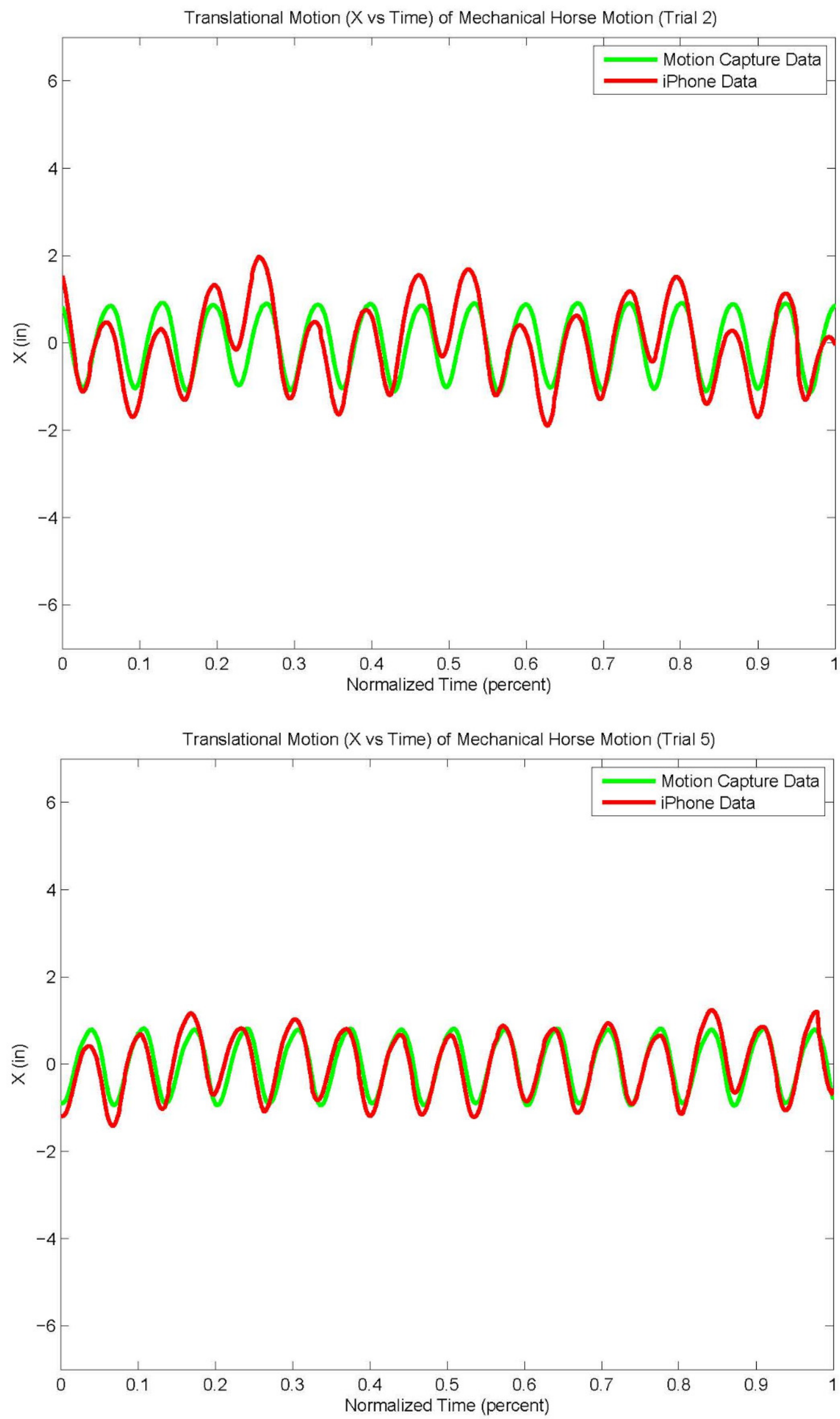

Figure 12: Periodic motion of the mechanical horse in the x-direction. Motion recorded for a trial with a rider (Trial 2) and a trial without a rider (Trial 5).

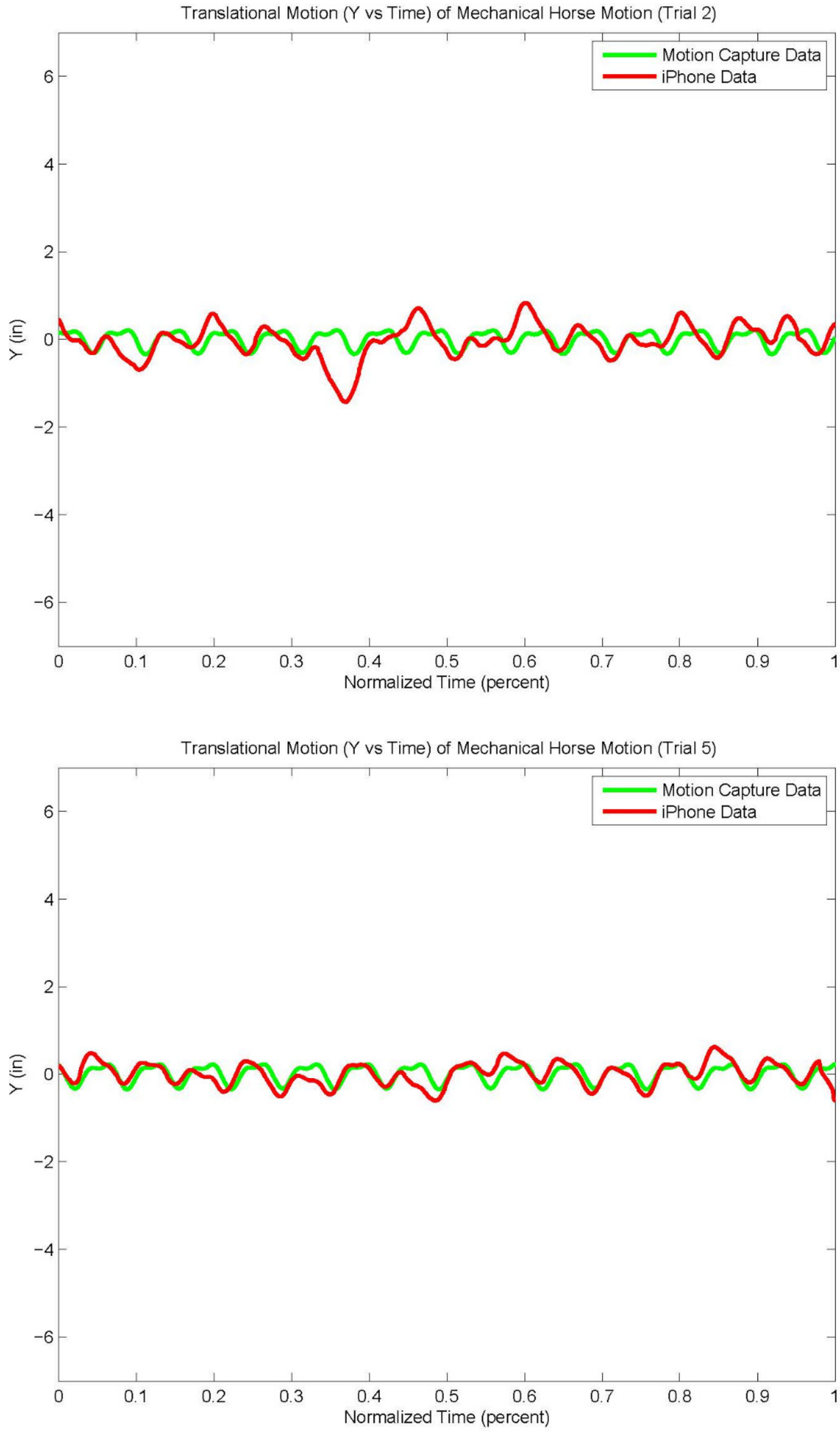

Figure 13: Periodic motion of the mechanical horse in the y-direction. Motion recorded for a trial with a rider (Trial 2) and a trial without a rider (Trial 5).

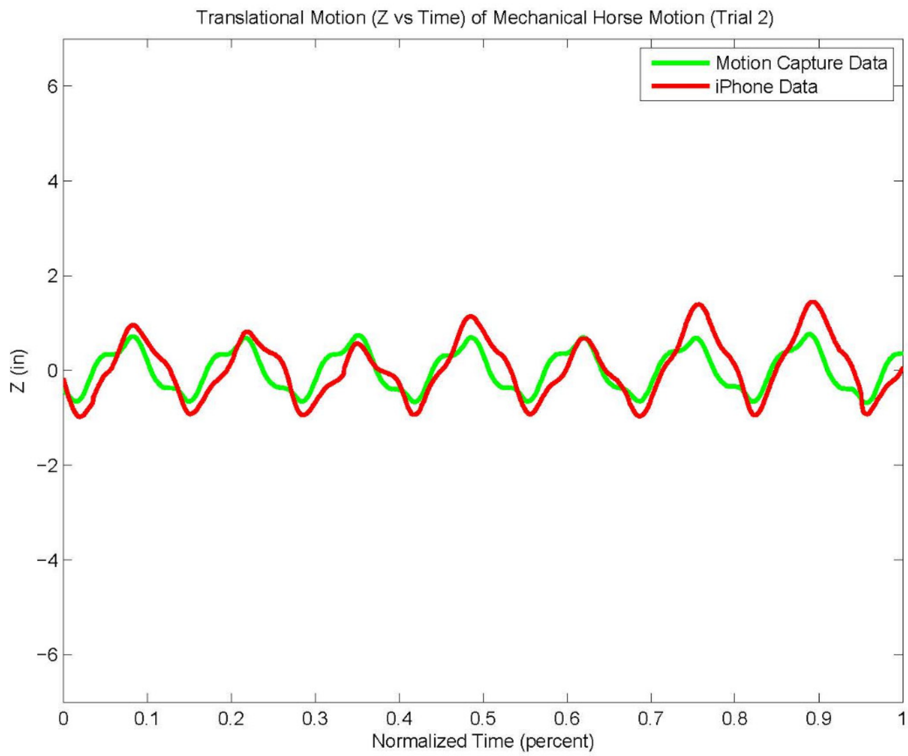

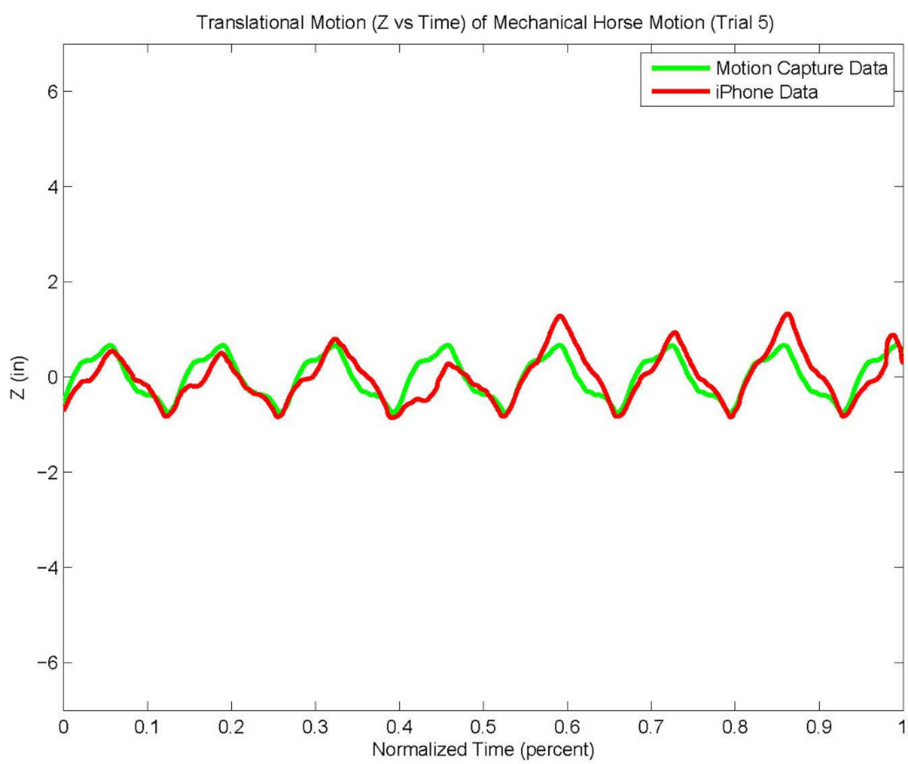

Figure 14: Periodic motion of the mechanical horse in the z -direction. Motion recorded for a trial with a rider (Trial 2) and a trial without a rider (Trial 5).

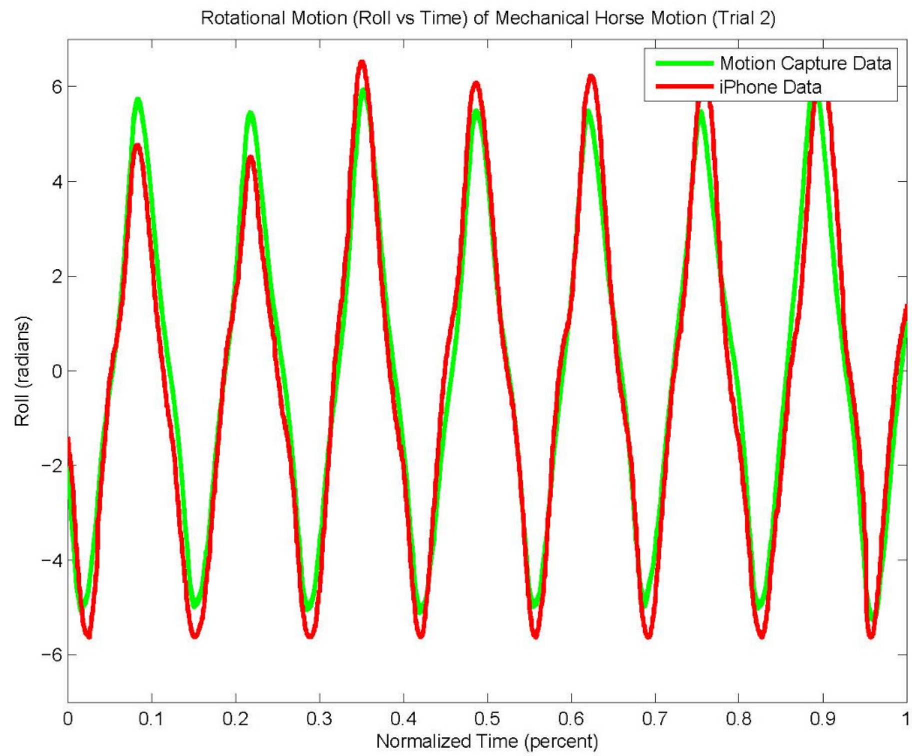

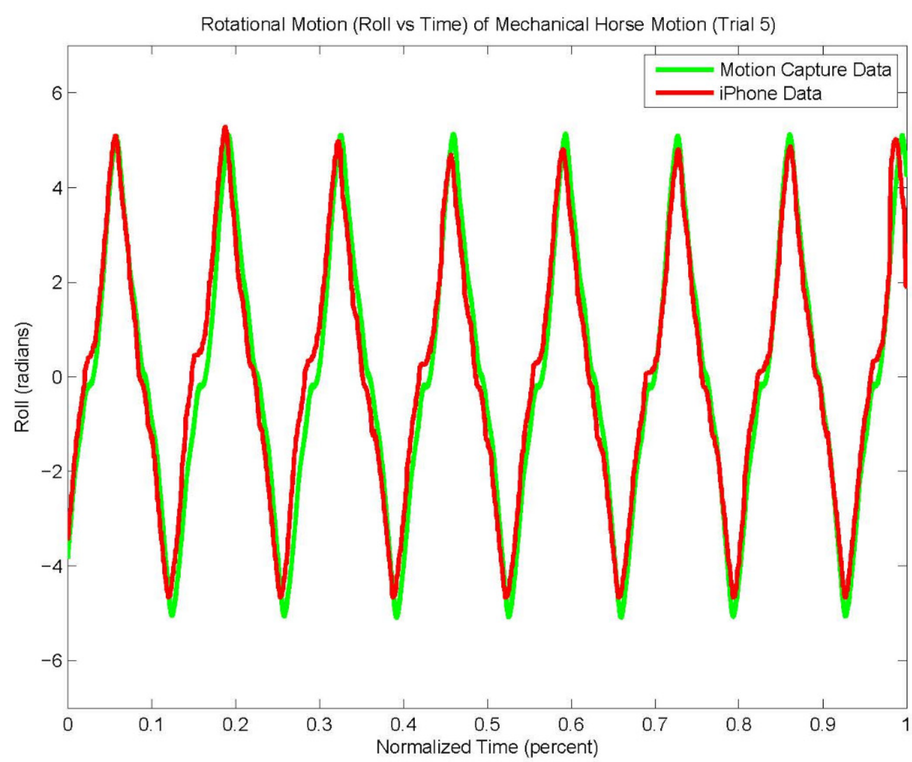

Figure 15: Periodic roll motion of the mechanical horse. Motion recorded for a trial with a rider (Trial 2) and a trial without a rider (Trial 5).

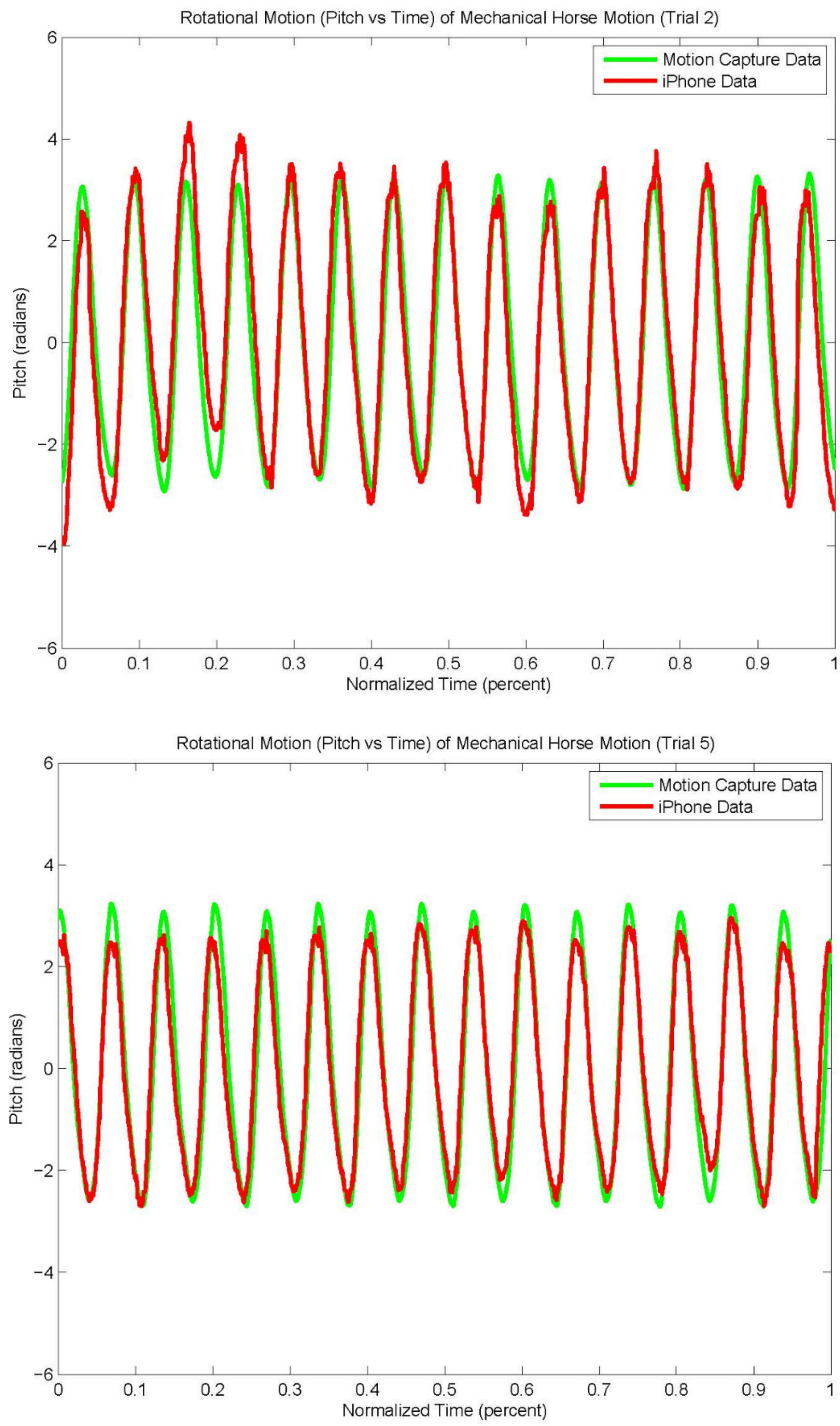

Figure 16: Periodic pitch motion of the mechanical horse. Motion recorded for a trial with a rider (Trial 2) and a trial without a rider (Trial 5).

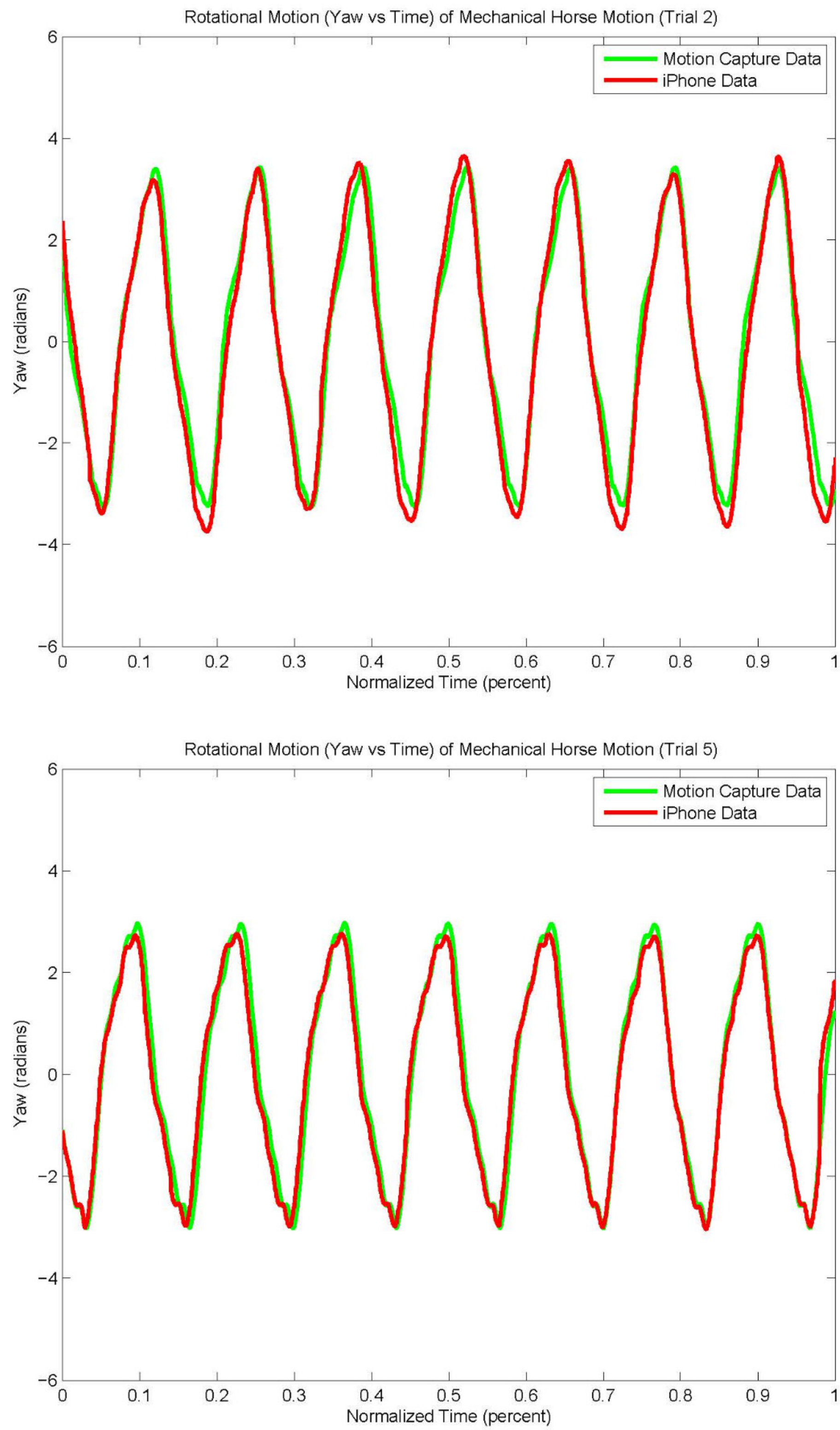

Figure 17: Periodic yaw motion of the mechanical horse. Motion recorded for a trial with a rider (Trial 2) and a trial without a rider (Trial 5).

CHAPTER FIVE

Discussion

The aim of this study is to determine if Dr. Garner's algorithm can adequately process the iPhone data to accurately yield the periodic motion of a complex, cyclic motion. We have focused on the motion of a mechanical horse because this produces a sufficiently complex motion, and may yield valuable results for future research in hippotherapy or equine racing.

Analysis of Results

Similarities are apparent between the motion recorded by the optical motion capture system and the motion recorded by the iPhone. However, most of the data indicated that the processed iPhone data was still much less accurate than that of the motion capture data.

The Lissajous plots revealed that the iPhone could not accurately trace the cyclic motion patterns of the mechanical horse in a spatial framework. For each spatial graph, the amplitude range of the iPhone was much larger than that of the motion capture system. Moreover, the iPhone spatial trace did not follow a repeatable pattern, except in the side view and in the top view. Even in these views, the pattern traced was imprecise and did not demonstrate the same accuracy as the motion capture system. The Lissajous plots also revealed that the rider of the mechanical horse may have interfered with iPhone recording. The spatial traces from the trial without a rider demonstrated a far more repeatable pattern than any of the traces from the trial with a rider. Thus, it appears that the iPhone may have been influenced by the rider's motion.

The periodic translational movement patterns indicated that processed iPhone data could not accurately reveal the cyclic, periodic motion of the mechanical horse. In both the *y*-direction and the *z*-direction, the iPhone data did not accurately trace the data captured by the motion capture system. However, the iPhone was able to more accurately trace the motion in the *x*-direction. This anomaly is likely due to the fact that the motion in the *x*-direction revealed a more continuous curve, with less small graphical features than the *y* and *z* directions. The periodic translational movement patterns also confirmed the theory that the rider's motion may have interfered with the iPhone. The translational motion from the iPhone matches that of the motion capture system much more in the trial without a rider. This is most noticeable in the *x*-direction.

The angular translational movement patterns were the most promising. These motion patterns indicated that the iPhone could accurately reveal the cyclic, periodic motion pattern of the mechanical horse. Moreover, these patterns indicated that the rider's motion had little impact on the iPhone's measurement of the mechanical horse's rotational motion. In both trials, the iPhone accurately traced the roll, pitch, and yaw motion of the mechanical horse. However, both the pitch and yaw motion patterns revealed that the iPhone struggled to accurately measure the finer features of these motions patterns when there was a rider.

Limitations of Study

This preliminary study had several limitations that made it difficult to perform a robust analysis. The most significant limitation was that we did not have the opportunity to accurately identify the error source that caused the processed iPhone data to differ from the motion capture data. There were several possible error sources in this experiment. First, the iPhone was not securely mounted to the mechanical horse and may have shifted slightly during the trials, causing the data to exhibit unwanted motion. Second, during trials with a rider, the iPhone was placed gently between the rider's legs. However, the data strongly indicates that this placement caused the motion of the rider to interfere with the iPhone's capture of the mechanical horse's motion. Third, there is a possibility that the iPhone sensors were not accurately calibrated and thus caused additional drift that was not factored out. Finally, and most probably, there is a possibility that Dr. Garner's algorithm still requires improvement in processing the iPhone data.

There were other minor, difficulties that may have affected the accuracy of the results. First, the exact sampling rate employed by the motion capture system was unknown. Thus, when the data was altered to accommodate the difference between the iPhone sampling rate and the motion capture sampling, the alterations only represented an approximation. Second, it was difficult to synchronize the start of the iPhone capture with the start of the motion capture system. This may have caused slight anomalies in the data near the beginning and the end of the trials. Third, there was not time to adequately analyze the effect that the mechanical horse's speed had on the iPhone's capture of the motion. Higher speeds may have caused the iPhone to move more freely on the mechanical horse, and thus alter the accuracy of the data. Finally, the small scope of this study was one of the most limiting factors. This study only recorded the motion of the mechanical horse, and did not attempt to record other similar, cyclic motions. Further experimentation needed to correct these limitations are described below.

Future Work

Further research must be conducted to verify and improve the results of this study. First, this study should be repeated with a few modifications. First, a mounting system for the iPhone should be developed in order to reduce/remove extraneous motion. Second, special care should be taken to ensure that the rider's motion does not interfere with the iPhone's recording of the mechanical horse's motion. Third, a method should be developed to synchronize the recordings from the motion capture system to that of the iPhone. Fourth, the exact sampling rate of the optical motion capture system should be recorded. Better yet, the sampling rate of the optical motion capture system should be matched to that of the iPhone sensors. These changes will help remove error sources and improve the accuracy of the data.

Moreover, another study should be conducted to identify other possible error sources. First, the iPhone should be used to record other known, quantifiable motion patterns. This data can then be processed through Dr. Garner's algorithm in order to verify its accuracy or illuminate areas of improvement. Second, these experiments should be repeated using other iPhone versions, or other smart phones such as Android or

Windows phones. This may help identify what role, if any, the iPhone's inertial sensors paly in the accuracy of the results.

Conclusion

Overall, the initial results of this study are promising. The processing of the iPhone inertial sensors data by Dr. Garner's current algorithm is not accurate enough to produce precise, global, absolute motion patterns for complex movements. However, it seems promising that the data from these sensors can be processed to reveal the periodic, local movement patterns of complex cyclic motions. The processing method employed by Dr. Garner's algorithm proved to be very accurate for rotational motion (roll, pitch, yaw), but does not yet yield as much accuracy for translational motion (x, y, z). Moreover, the iPhone data appeared to be more accurate when there was no rider on the mechanical horse. Additional research should be conducted to more accurately identify the error sources in this experiment, determine which conditions yield the most accurate iPhone data, and to continue to verify the accuracy of Dr. Garner's algorithm.

APPENDIX

A brief description of the recorded data trials follows. Additionally, this appendix contains the Lissajous plots, the periodic translational motion plots, and the periodic angular motion plots for the four trials not discussed in the Results section.

Trial	**Duration (seconds)**	**Horse Speed (Hz)**	**Conditions/Notes**
1	30	30	Iphone flat, near handle Heather riding the mechanical horse during sample
2	30	45	Iphone flat, near handle Heather riding the mechanical horse during sample
3	30	60	Iphone flat, near handle Heather riding the mechanical horse during sample Sample started late on Iphone
4	40	30	No rider; IPhone flat, near handle Started w/no motion and then re-started w/motion
5	30	45	No rider; IPhone flat, near handle
6	40	60	No rider; IPhone flat, near handle Sample started late

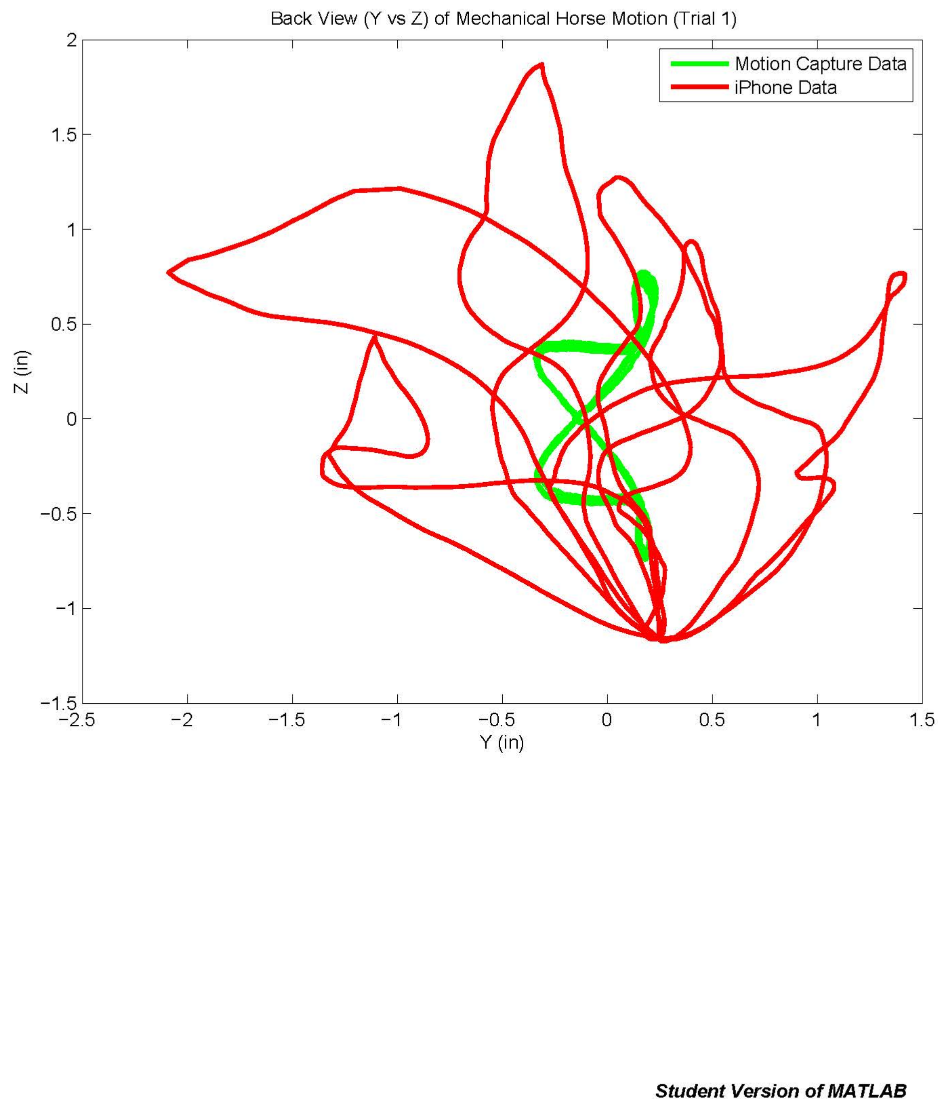

Back View (Y vs Z) of Mechanical Horse Motion (Trial 1)
Motion Capture Data
iPhone Data
Z (in)
Y (in)
2
1.5
1
0.5
0
−0.5
−1
−1.5
−2.5
−2
−1.5
−1
−0.5
0
0.5
1
1.5
Student Version of MATLAB

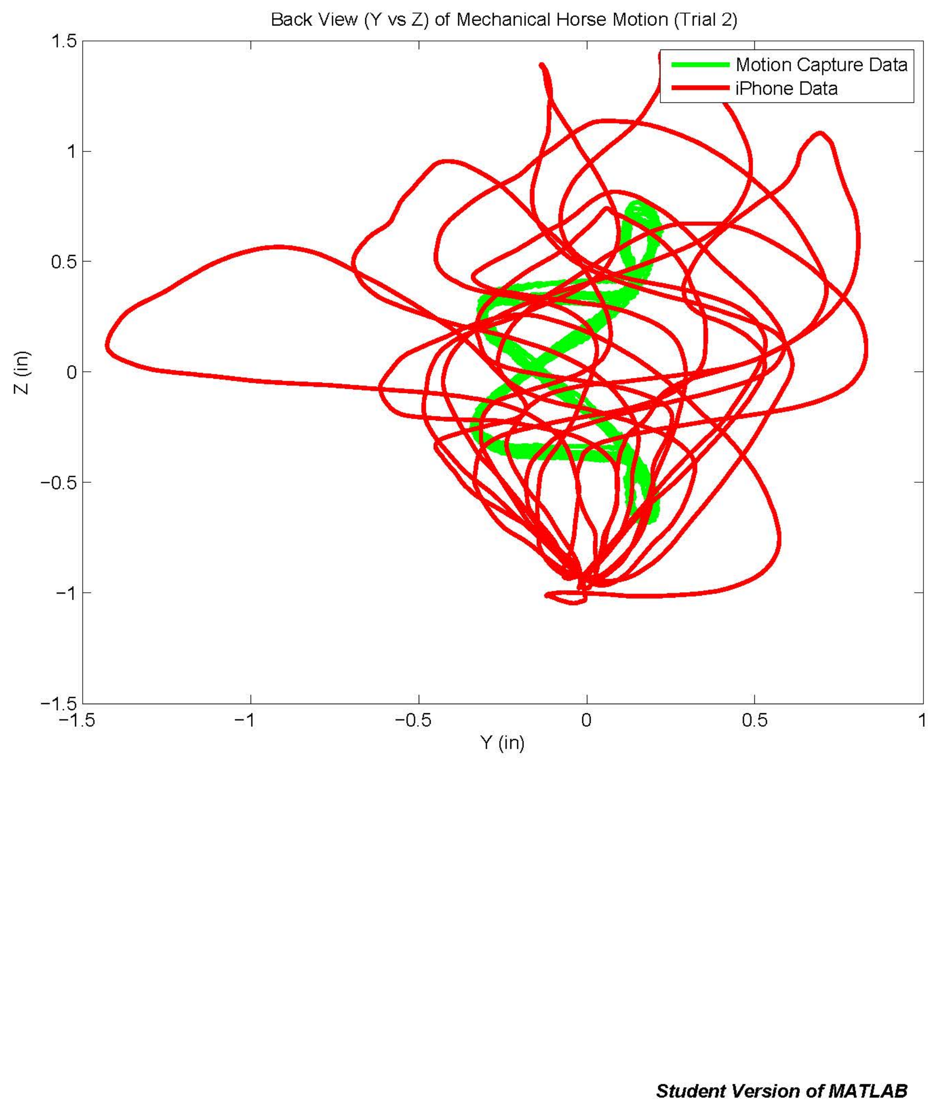
Back View (Y vs Z) of Mechanical Horse Motion (Trial 2)
Motion Capture Data
iPhone Data
Z (in)
Y (in)
1.5
1
0.5
0
−0.5
−1
−1.5
−1.5
−1
−0.5
0
0.5
1
Student Version of MATLAB

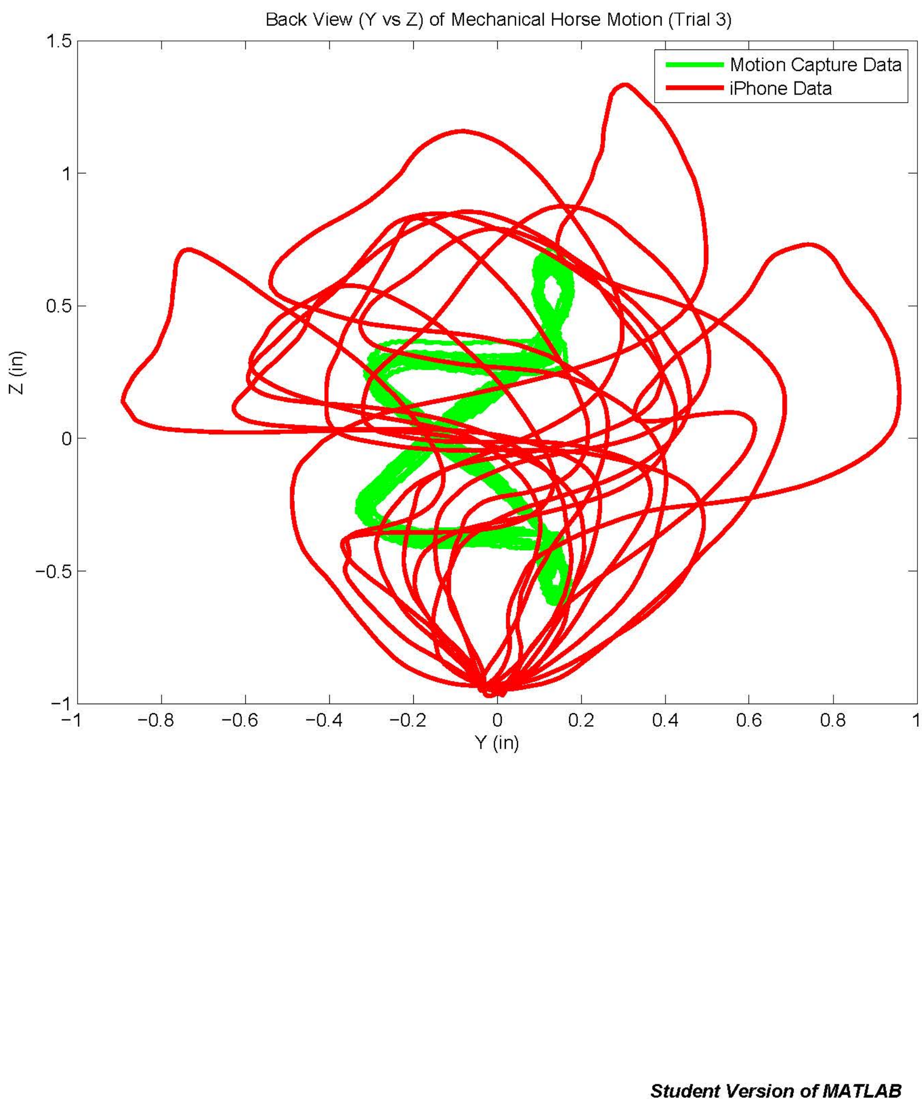

Back View (Y vs Z) of Mechanical Horse Motion (Trial 3)
Motion Capture Data
iPhone Data
Z (in)
Y (in)
1.5
1
0.5
0
−0.5
−1
−0.8
−0.6
−0.4
−0.2
0.2
0.4
0.6
0.8
Student Version of MATLAB

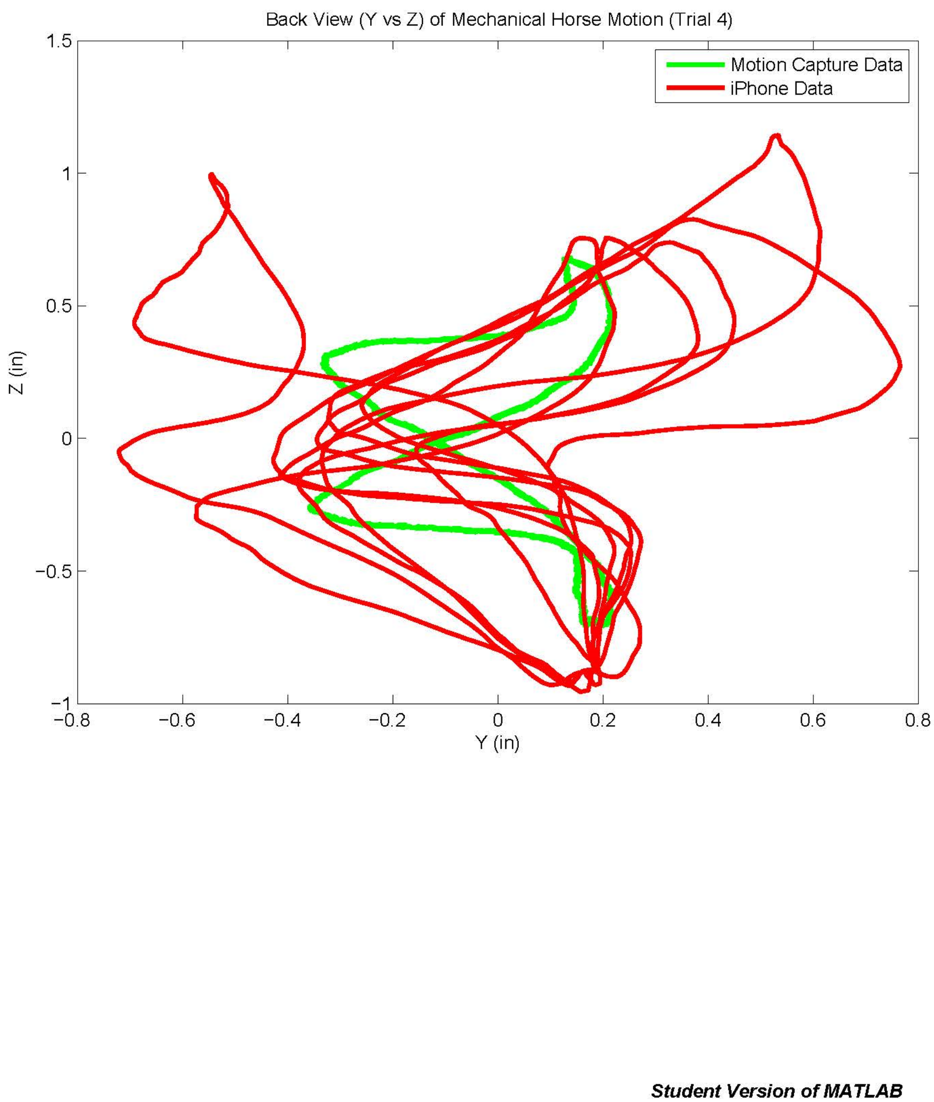

Back View (Y vs Z) of Mechanical Horse Motion (Trial 4)
Motion Capture Data
iPhone Data
Z (in)
Y (in)
1.5
1
0.5
0
−0.5
−1
−0.8
−0.6
−0.4
−0.2
0
0.2
0.4
0.6
0.8
Student Version of MATLAB

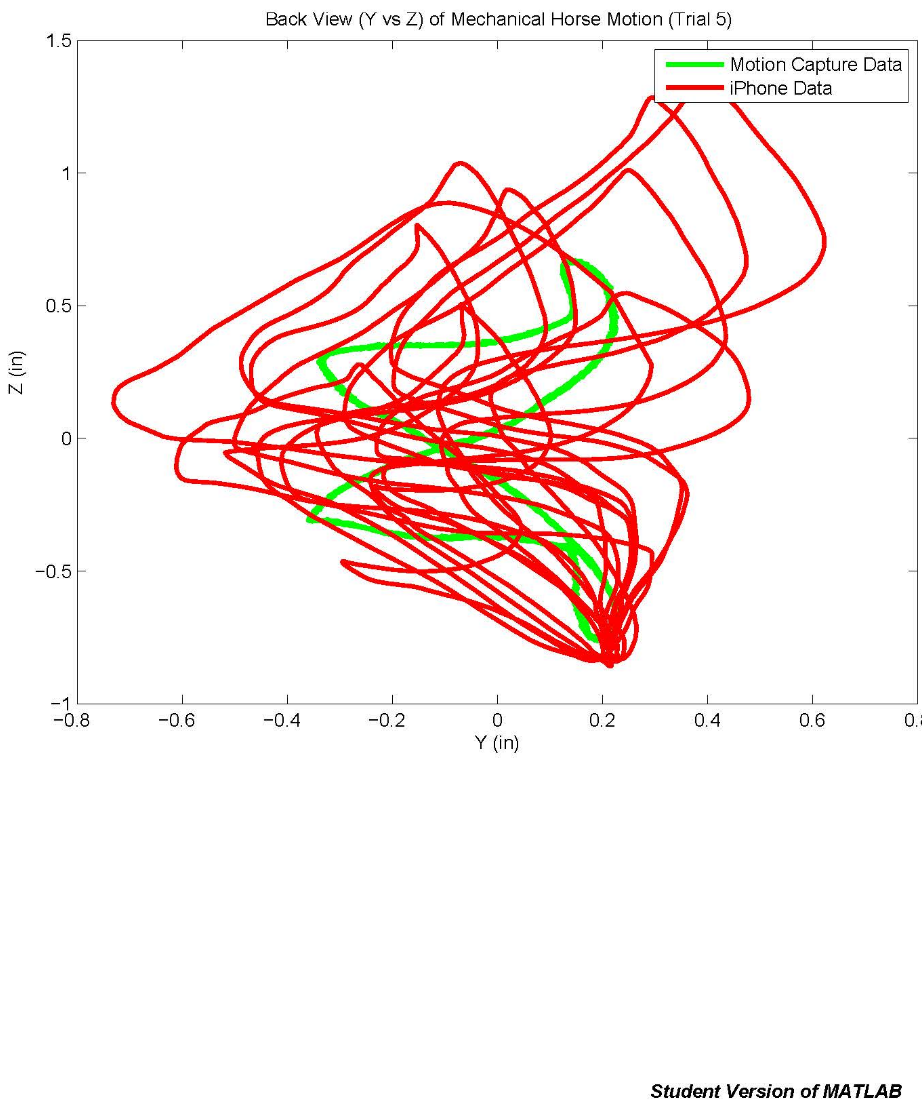
Back View (Y vs Z) of Mechanical Horse Motion (Trial 5)
Motion Capture Data
iPhone Data
Z (in)
Y (in)
1.5
1
0.5
0
−0.5
−1
−0.8
−0.6
−0.4
−0.2
0
0.2
0.4
0.6
0.8
Student Version of MATLAB

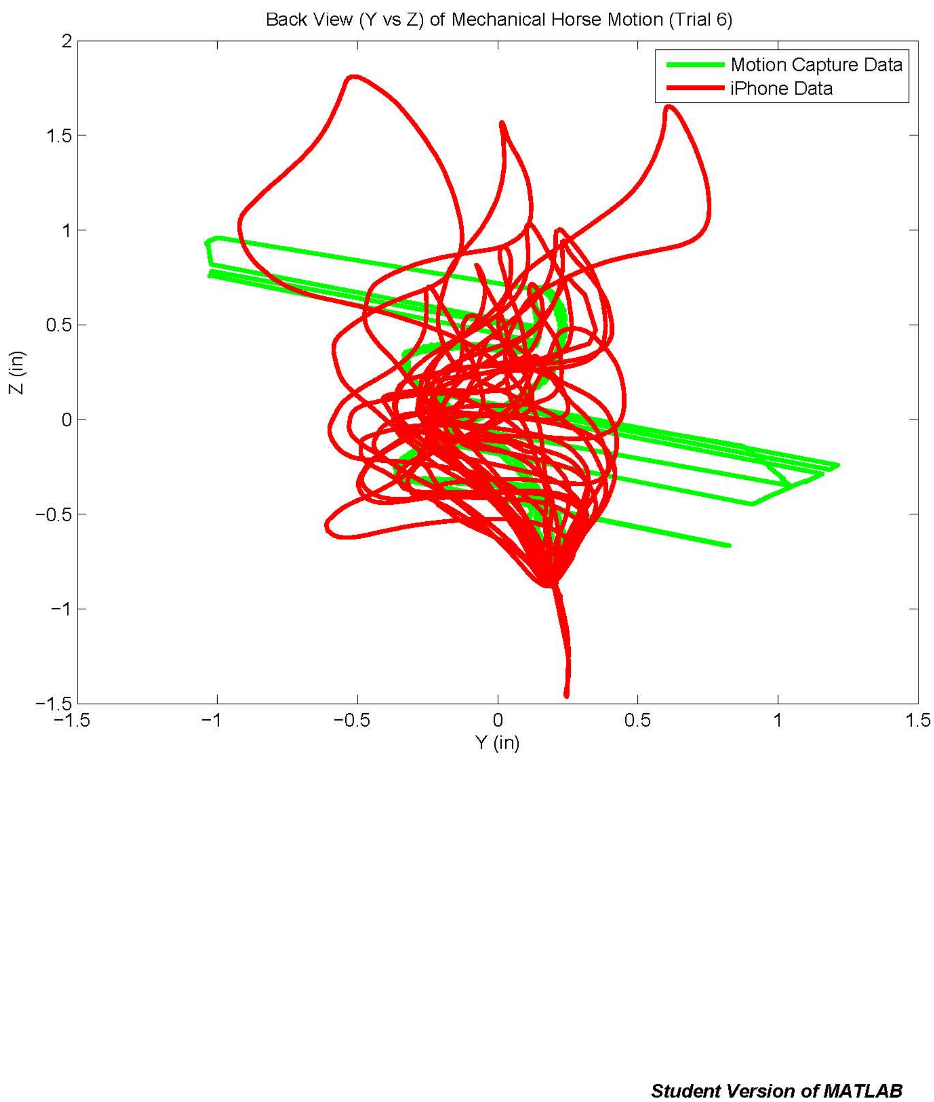
Back View (Y vs Z) of Mechanical Horse Motion (Trial 6)
Motion Capture Data
iPhone Data
Z (in)
Y (in)
2
1.5
1
0.5
0
−0.5
−1
−1.5
−1.5
−1
−0.5
0
0.5
1
1.5
Student Version of MATLAB

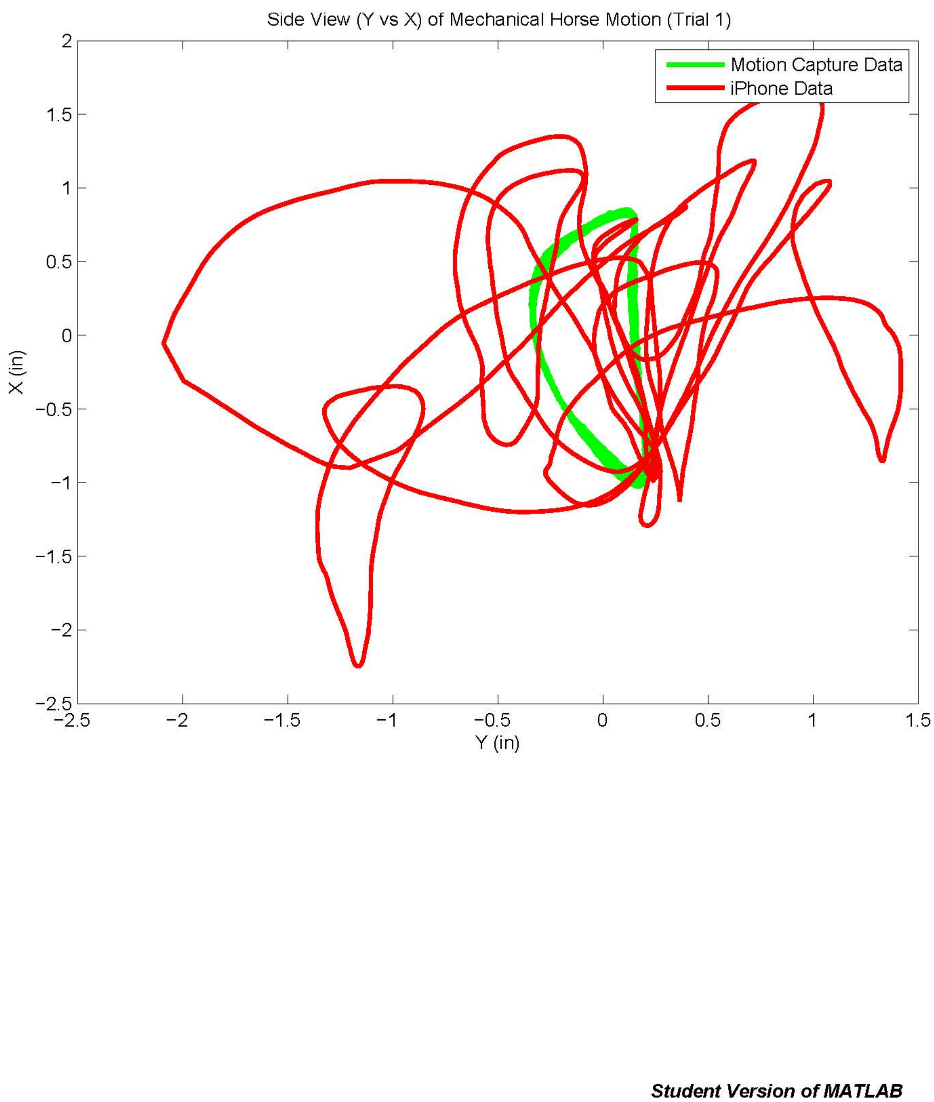
Side View (Y vs X) of Mechanical Horse Motion (Trial 1)
Motion Capture Data
iPhone Data
X (in)
Y (in)
2
1.5
1
0.5
0
−0.5
−1
−1.5
−2
−2.5
−2.5
−2
−1.5
−1
−0.5
0
0.5
1
1.5
Student Version of MATLAB

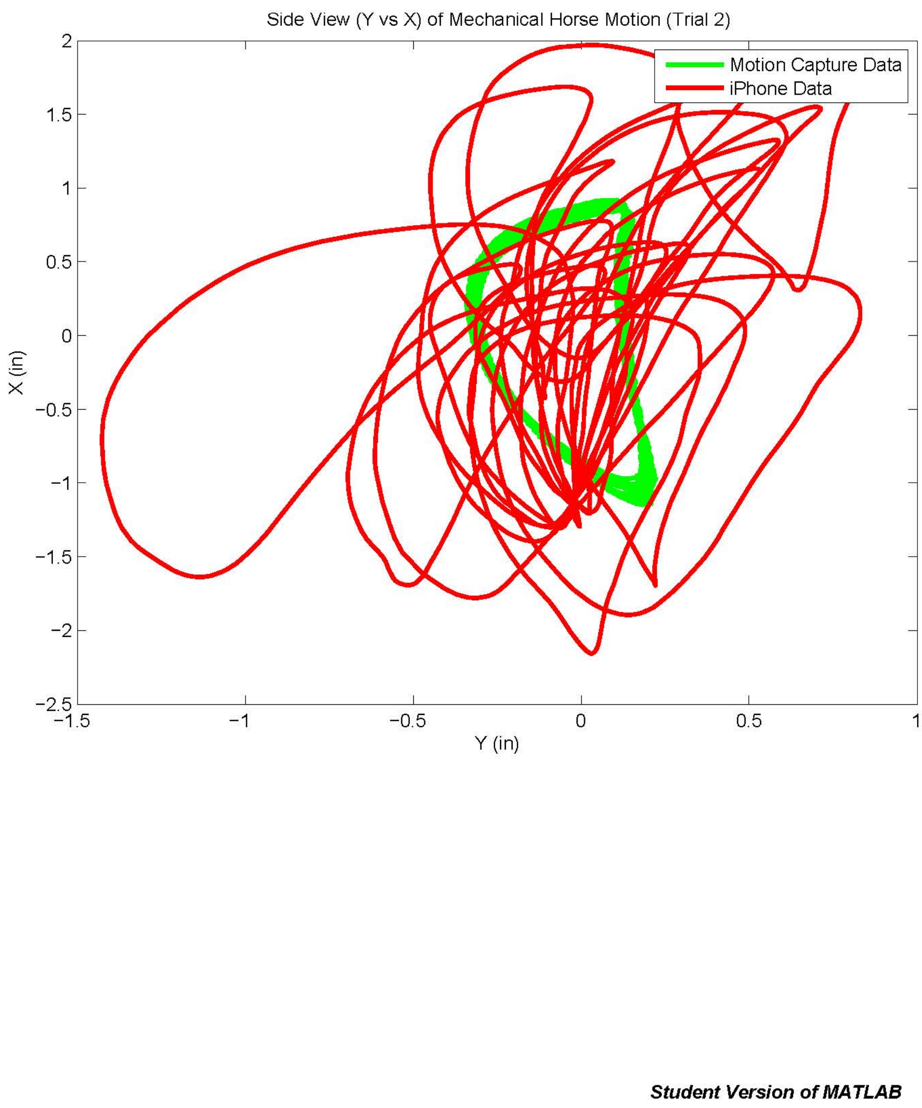
Side View (Y vs X) of Mechanical Horse Motion (Trial 2)
Motion Capture Data
iPhone Data
X (in)
Y (in)
2
1.5
1
0.5
0
−0.5
−1
−1.5
−2
−2.5
−1.5
−1
−0.5
0
0.5
1
Student Version of MATLAB

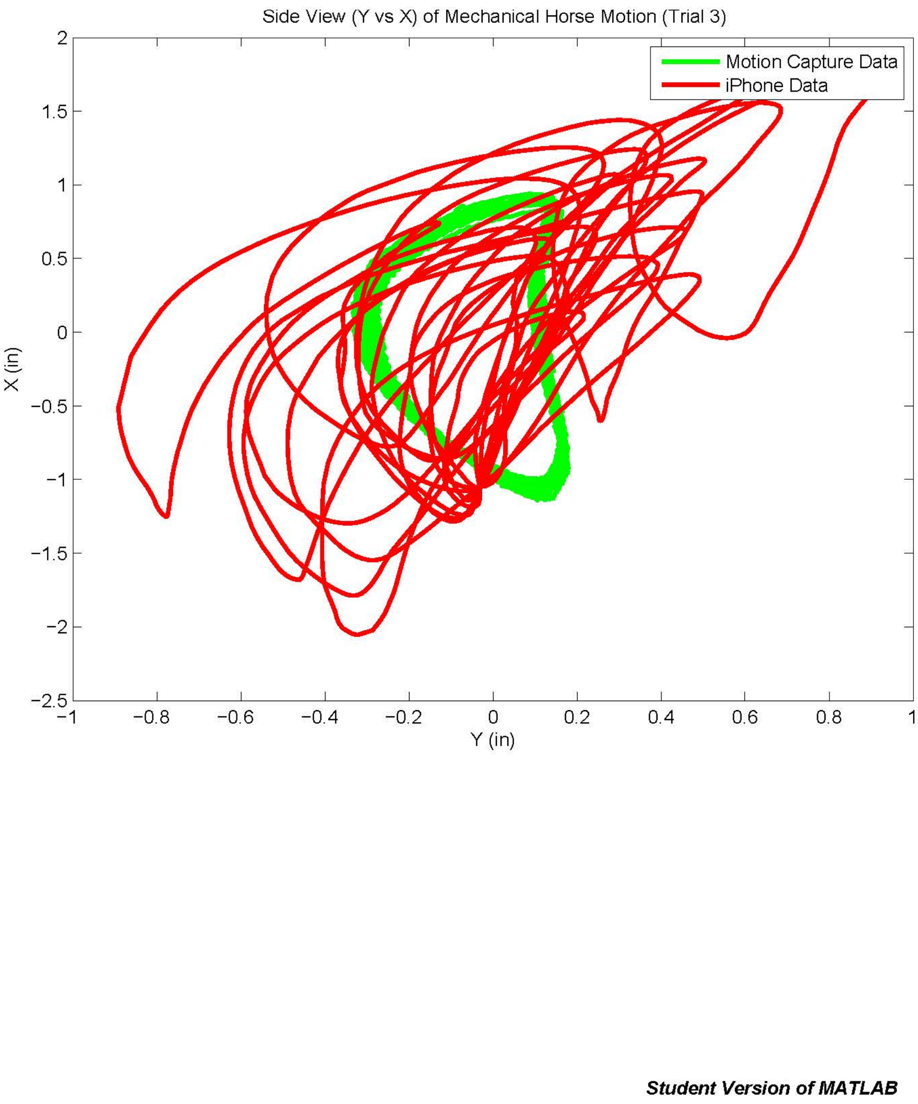
Side View (Y vs X) of Mechanical Horse Motion (Trial 3)
Motion Capture Data
iPhone Data
X (in)
Y (in)
2
1.5
1
0.5
0
−0.5
−1
−1.5
−2
−2.5
−1
−0.8
−0.6
−0.4
−0.2
0
0.2
0.4
0.6
0.8
1
Student Version of MATLAB

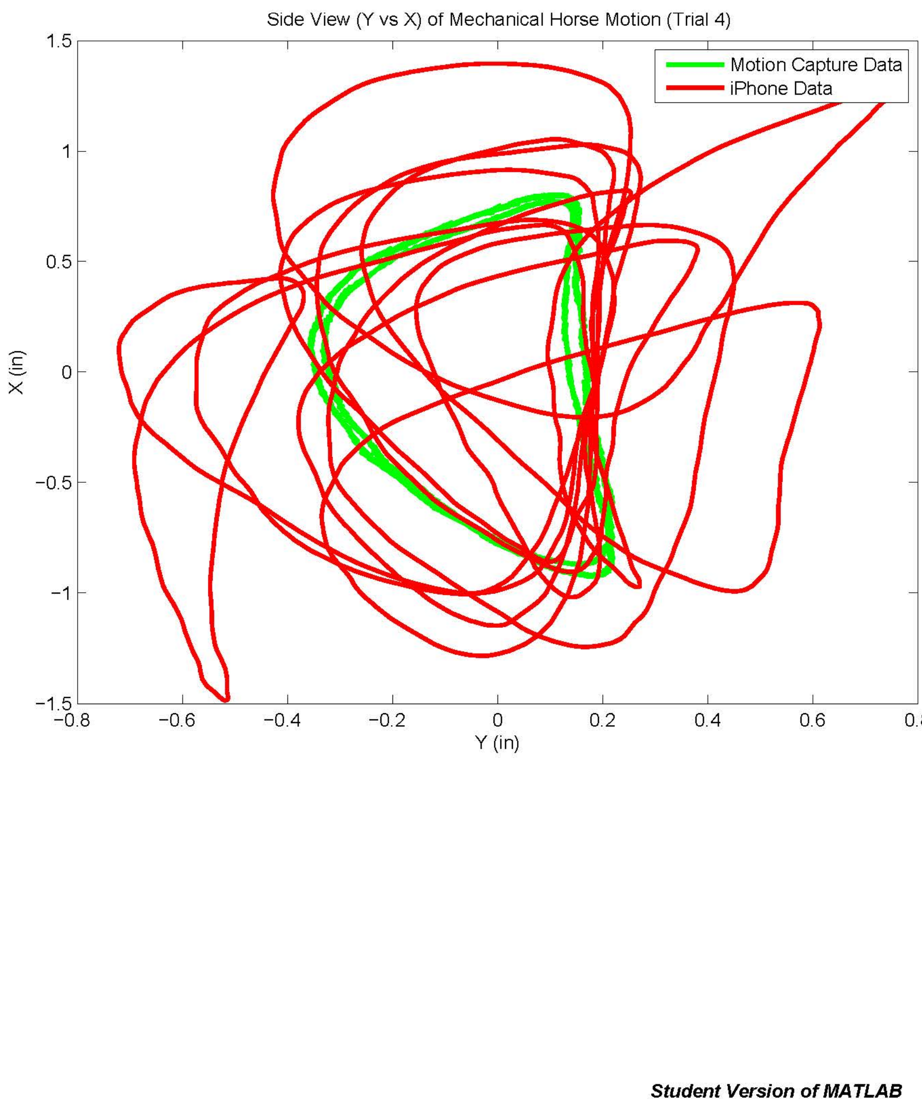
Side View (Y vs X) of Mechanical Horse Motion (Trial 4)
Motion Capture Data
iPhone Data
X (in)
Y (in)
1.5
1
0.5
0
−0.5
−1
−1.5
−0.8
−0.6
−0.4
−0.2
0
0.2
0.4
0.6
0.8
Student Version of MATLAB

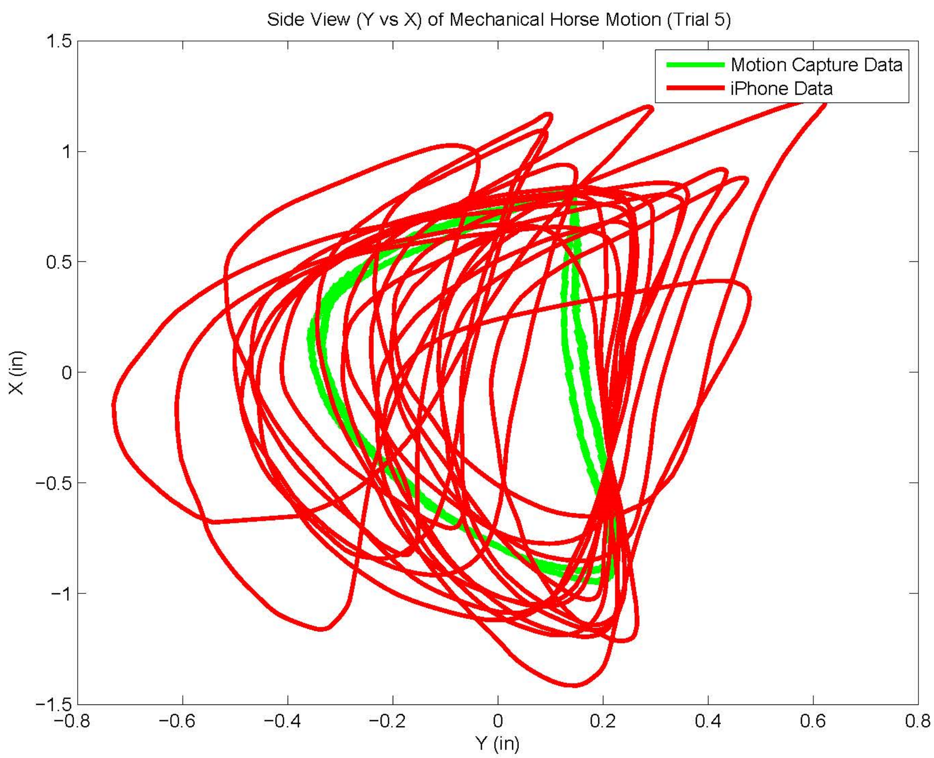

Student Version of MATLAB

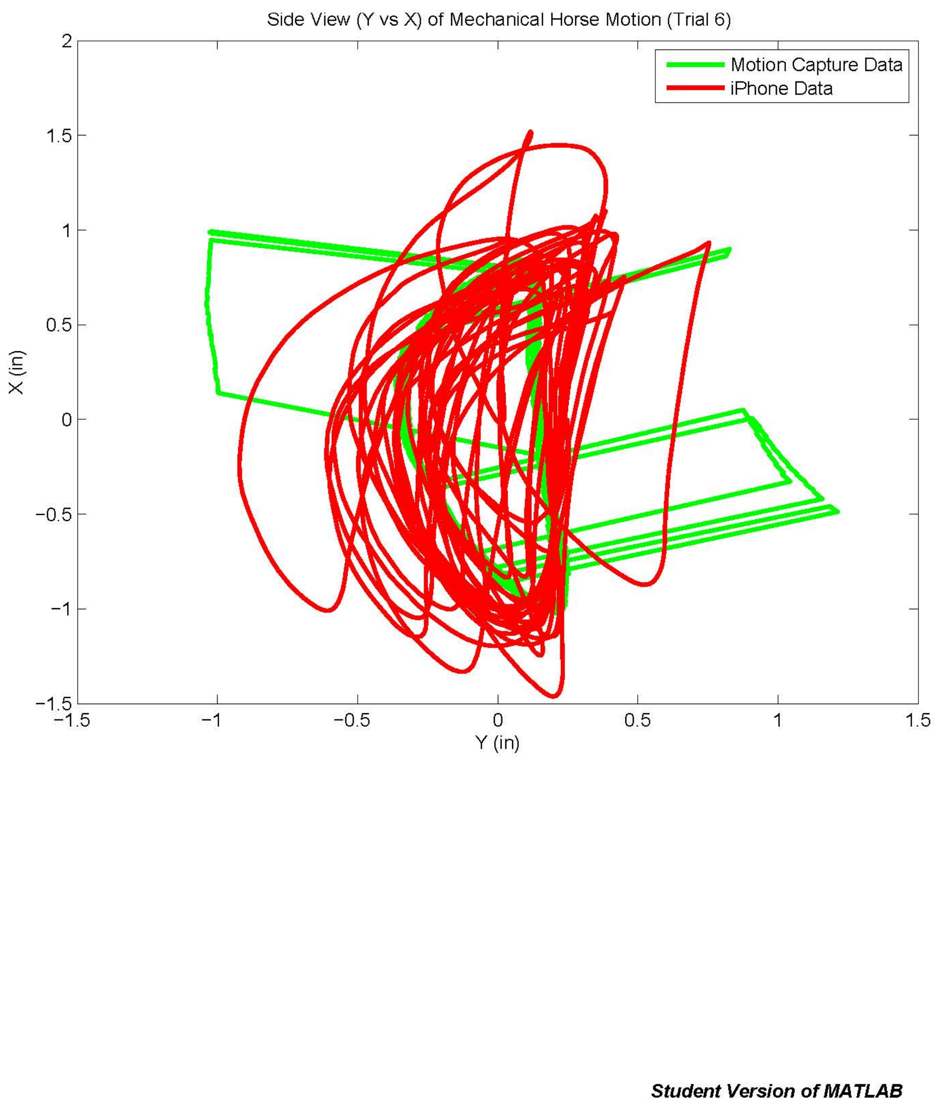
Side View (Y vs X) of Mechanical Horse Motion (Trial 6)
Motion Capture Data
iPhone Data
X (in)
Y (in)
2
1.5
1
0.5
0
−0.5
−1
−1.5
−1.5
−1
−0.5
0
0.5
1
1.5
Student Version of MATLAB

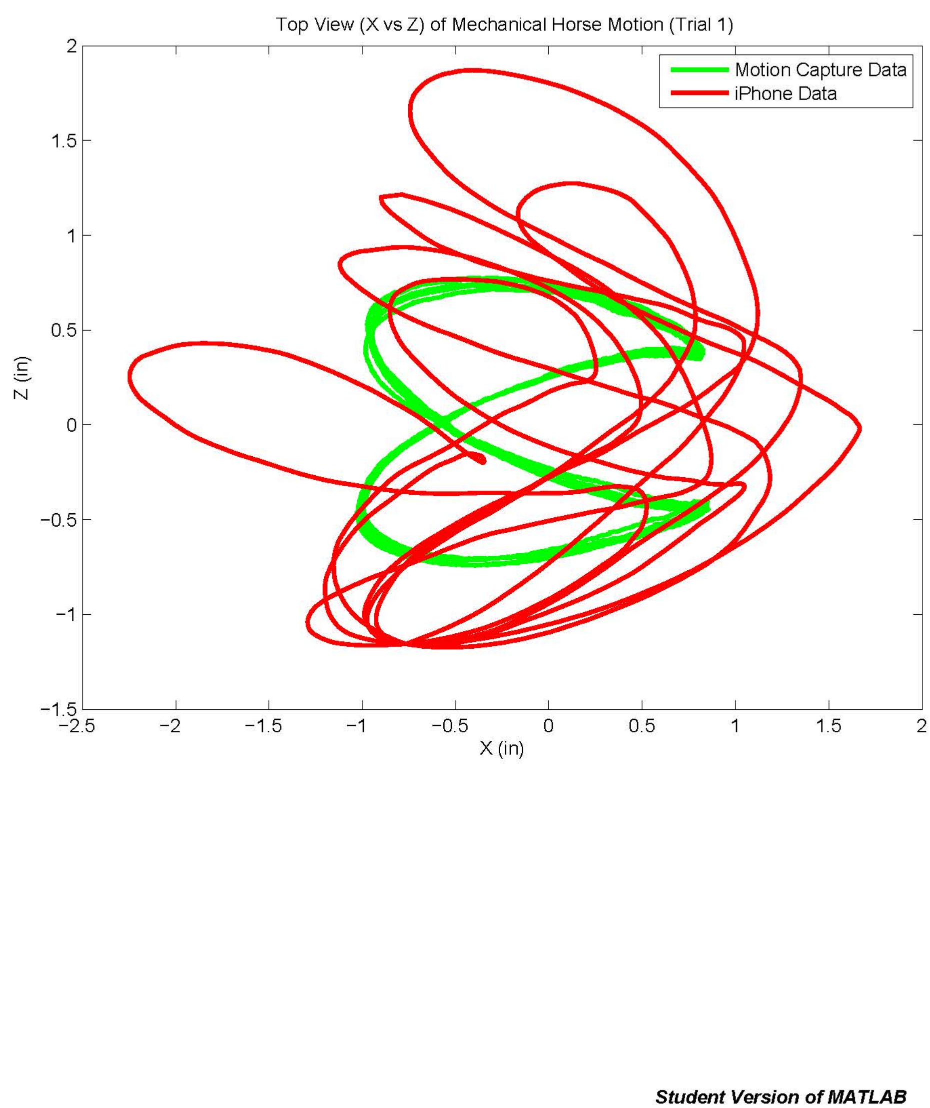
Top View (X vs Z) of Mechanical Horse Motion (Trial 1)
Motion Capture Data
iPhone Data
Z (in)
X (in)
2
1.5
1
0.5
0
−0.5
−1
−1.5
−2.5
−2
−1.5
−1
−0.5
0
0.5
1
1.5
2
Student Version of MATLAB

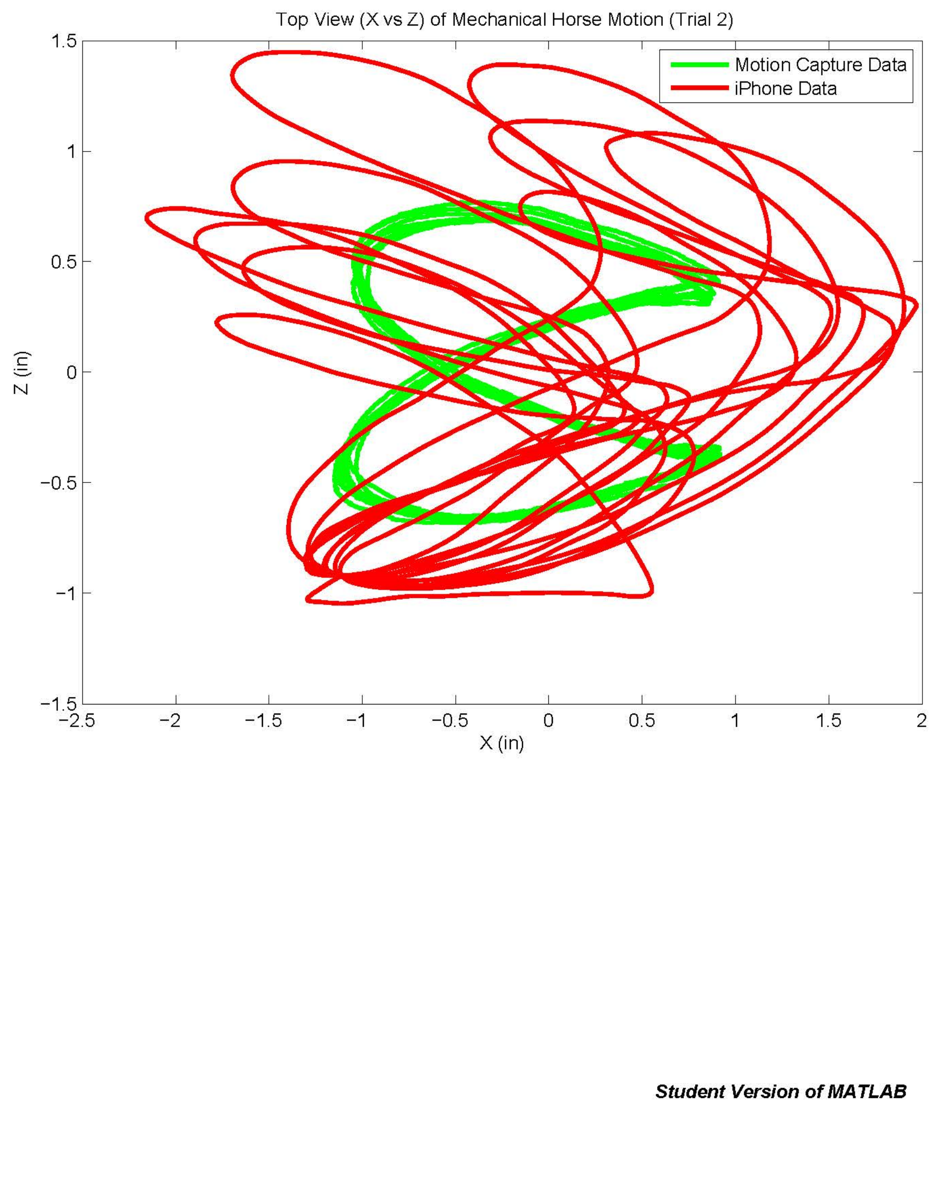
Top View (X vs Z) of Mechanical Horse Motion (Trial 2)
Motion Capture Data
iPhone Data
Z (in)
X (in)
1.5
1
0.5
0
−0.5
−1
−1.5
−2.5
−2
−1.5
−1
−0.5
0
0.5
1
1.5
2
Student Version of MATLAB

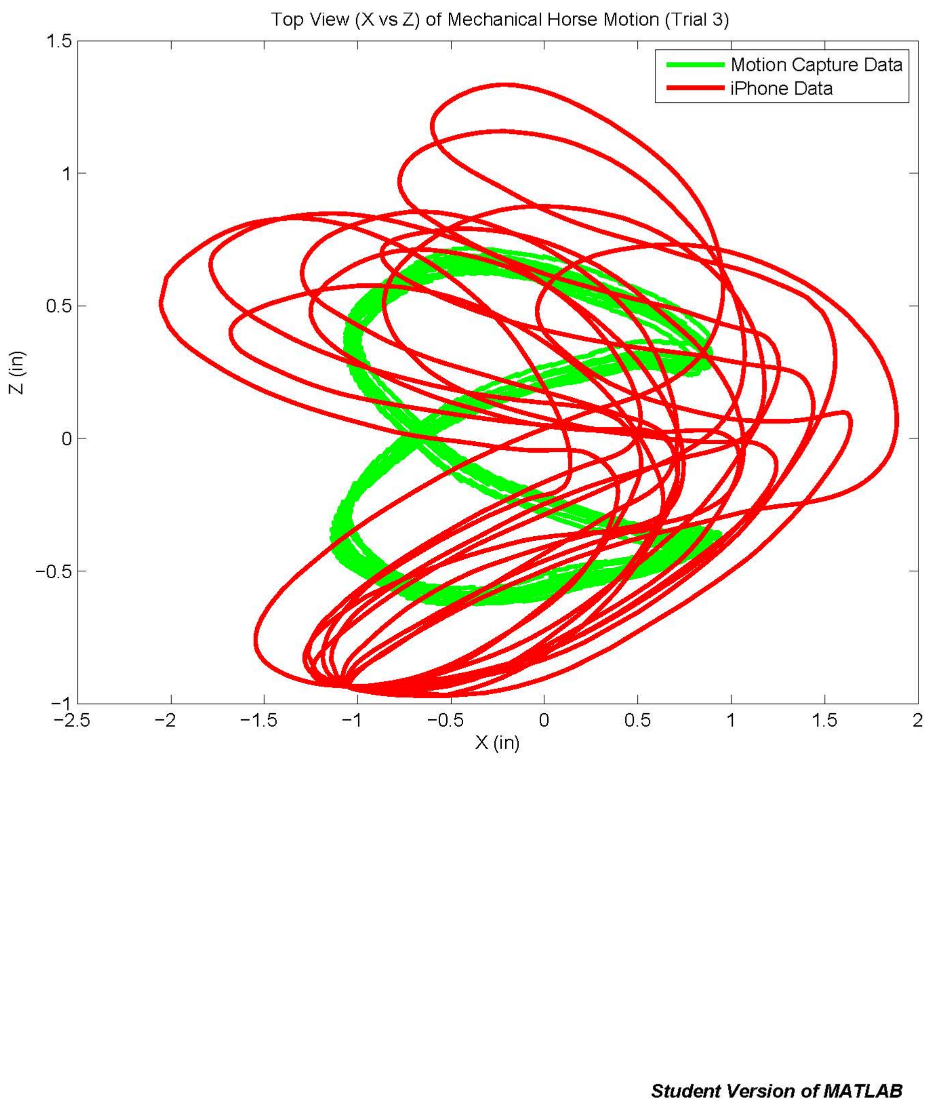

Top View (X vs Z) of Mechanical Horse Motion (Trial 3)
Motion Capture Data
iPhone Data
Z (in)
X (in)
1.5
1
0.5
0
−0.5
−1
−2.5
−2
−1.5
−1
−0.5
0
0.5
1
1.5
2
Student Version of MATLAB

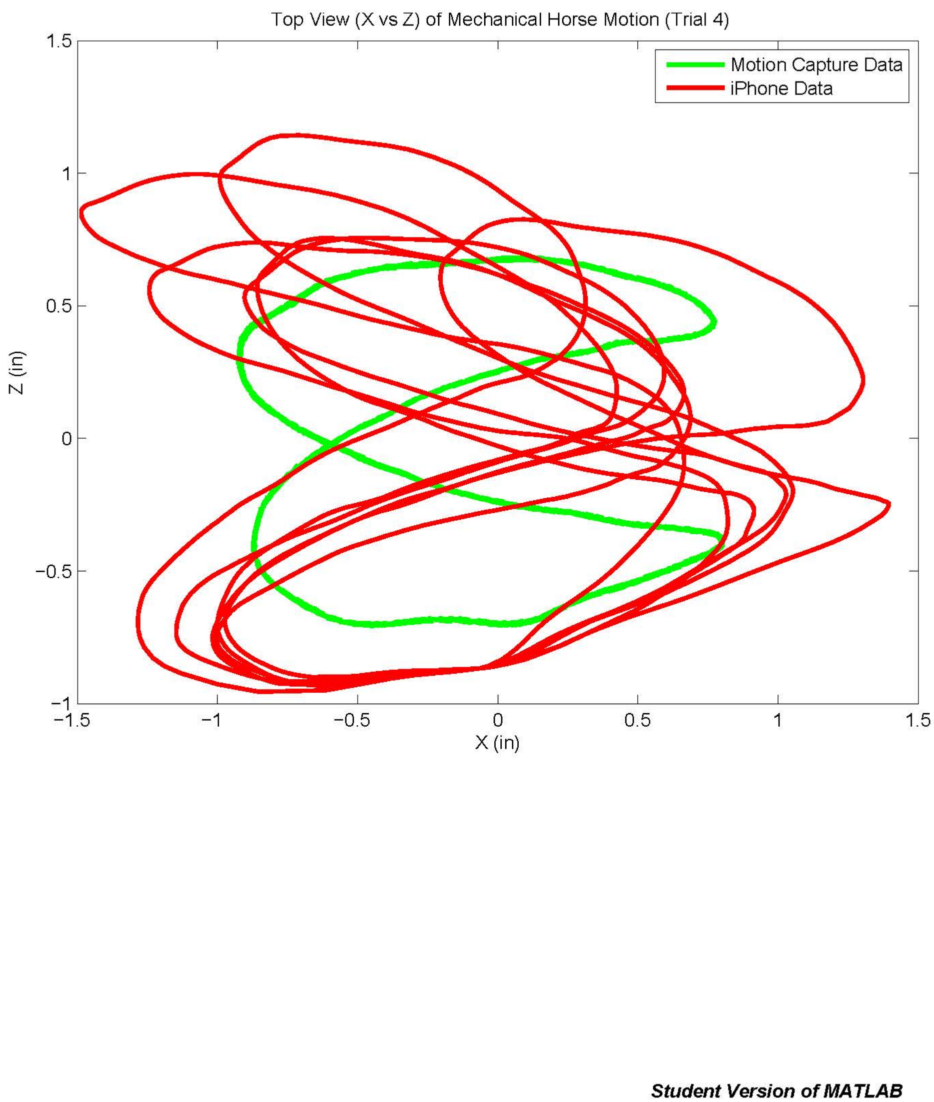
Top View (X vs Z) of Mechanical Horse Motion (Trial 4)
Motion Capture Data
iPhone Data
Z (in)
X (in)
1.5
1
0.5
0
−0.5
−1
−1.5
Student Version of MATLAB

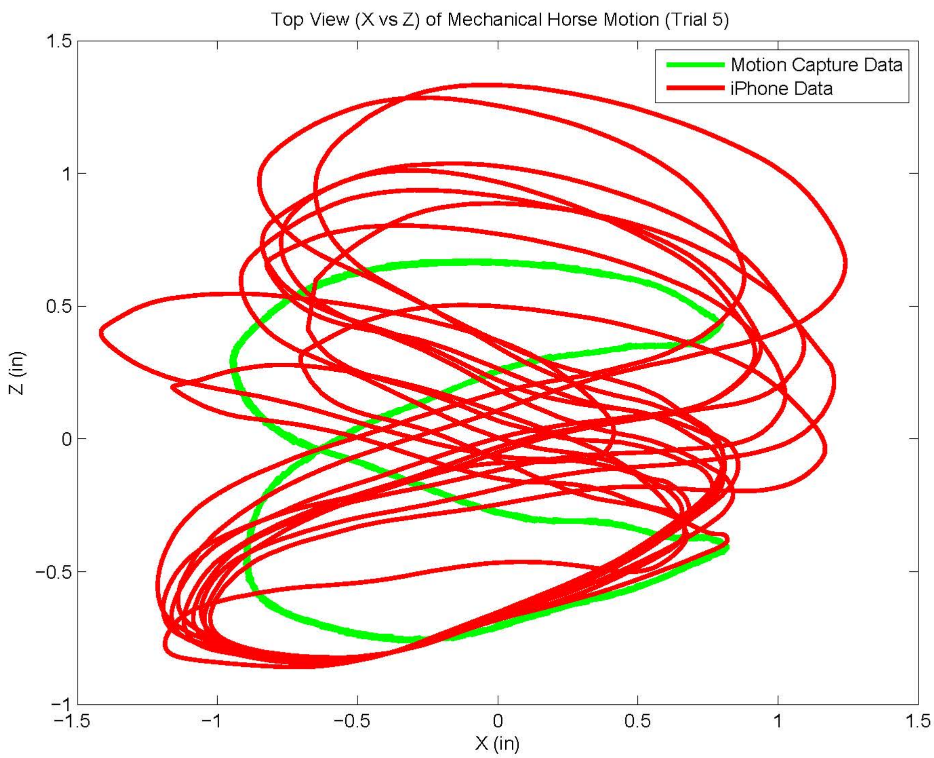

Student Version of MATLAB

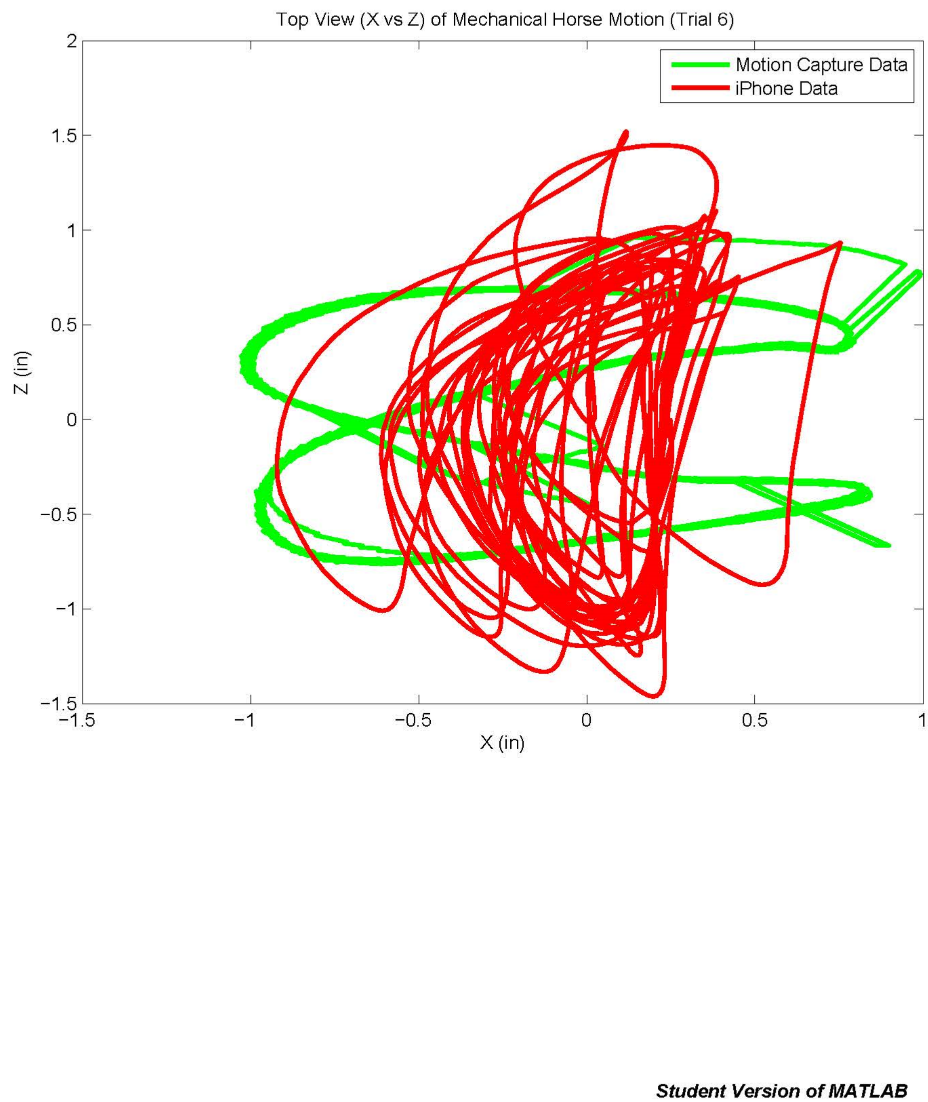
Top View (X vs Z) of Mechanical Horse Motion (Trial 6)
Motion Capture Data
iPhone Data
Z (in)
X (in)
2
1.5
1
0.5
0
−0.5
−1
−1.5
−1.5
−1
−0.5
0
0.5
1
Student Version of MATLAB

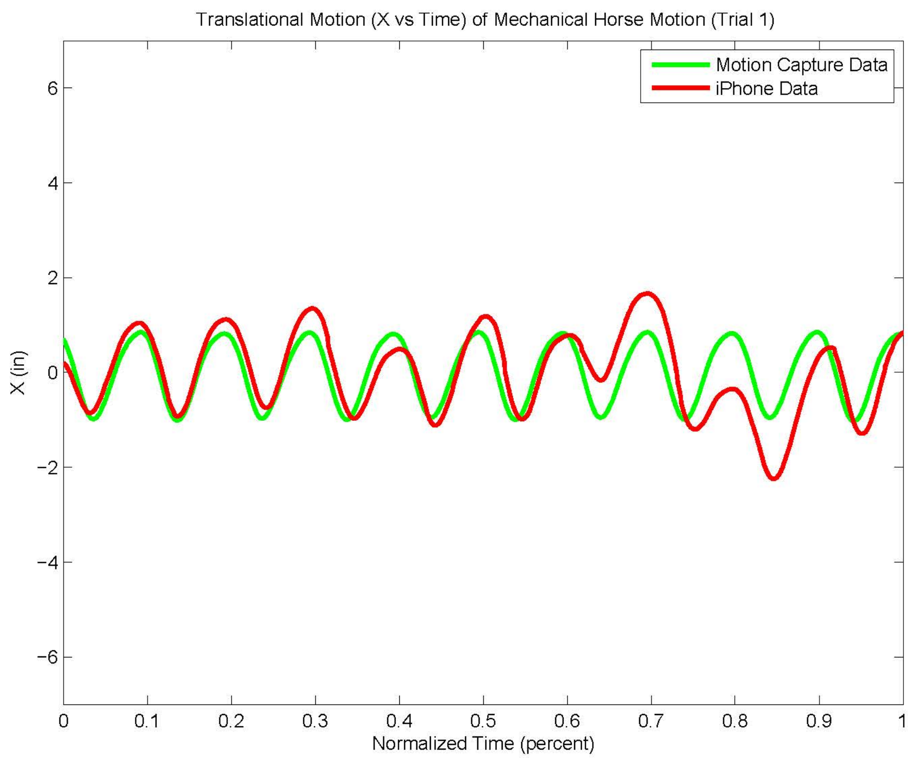

Student Version of MATLAB

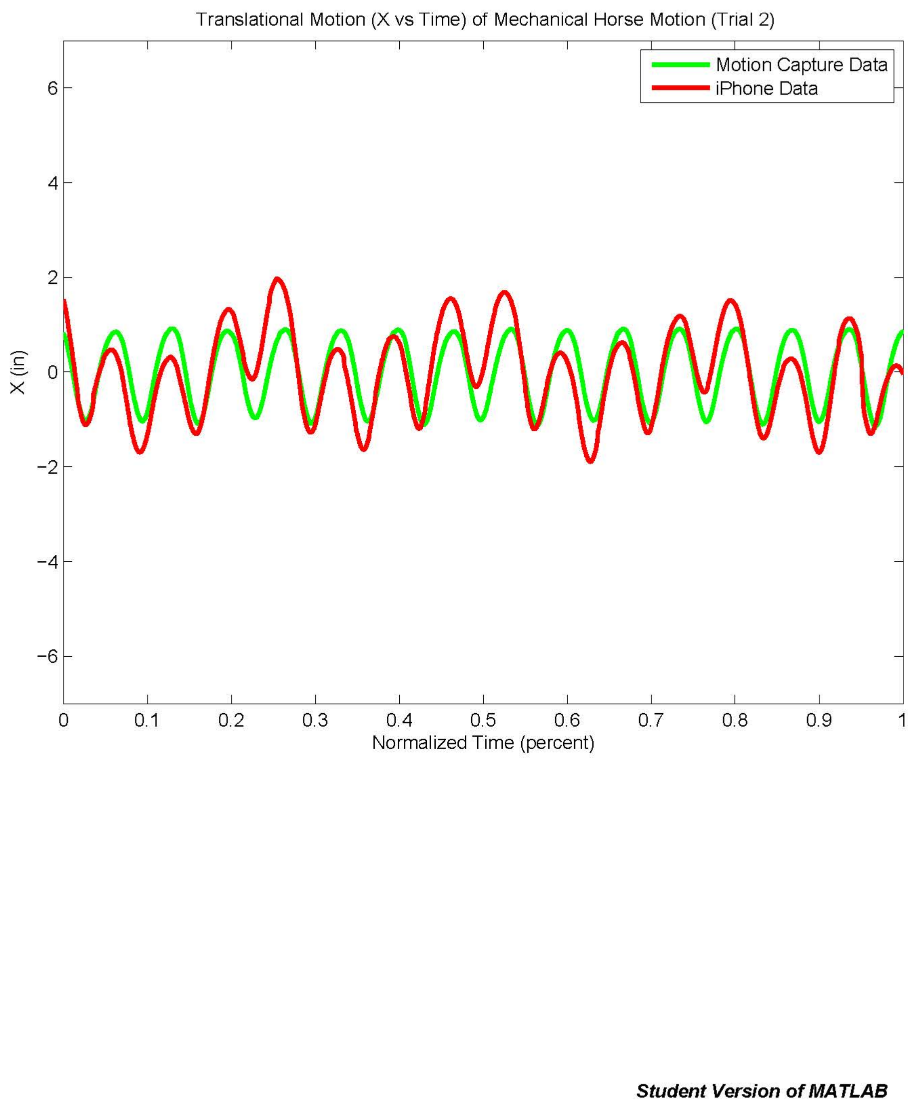
Translational Motion (X vs Time) of Mechanical Horse Motion (Trial 2)
Motion Capture Data
iPhone Data
X (in)
6
4
2
0
−2
−4
−6
0
0.1
0.2
0.3
0.4
0.5
0.6
0.7
0.8
0.9
1
Normalized Time (percent)
Student Version of MATLAB

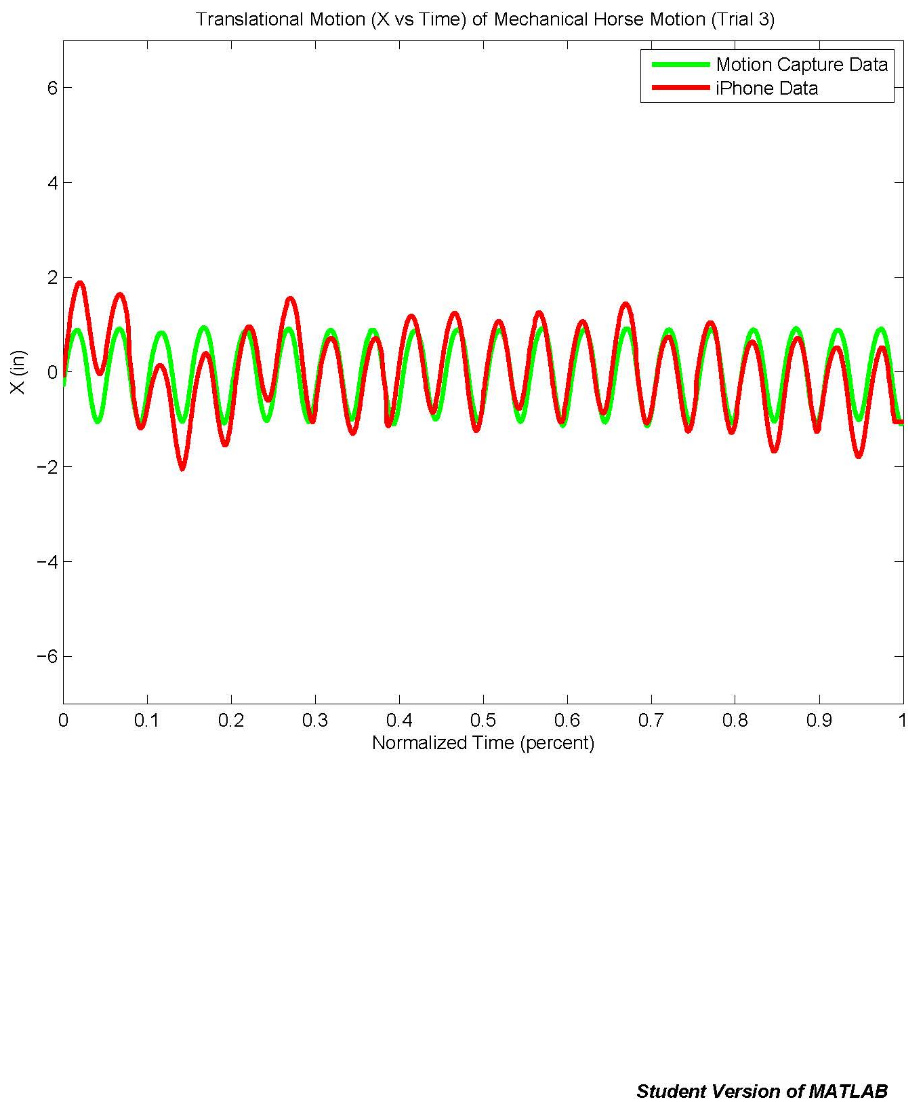
Translational Motion (X vs Time) of Mechanical Horse Motion (Trial 3)
Motion Capture Data
iPhone Data
X (in)
6
4
2
0
−2
−4
−6
0
0.1
0.2
0.3
0.4
0.5
0.6
0.7
0.8
0.9
1
Normalized Time (percent)
Student Version of MATLAB

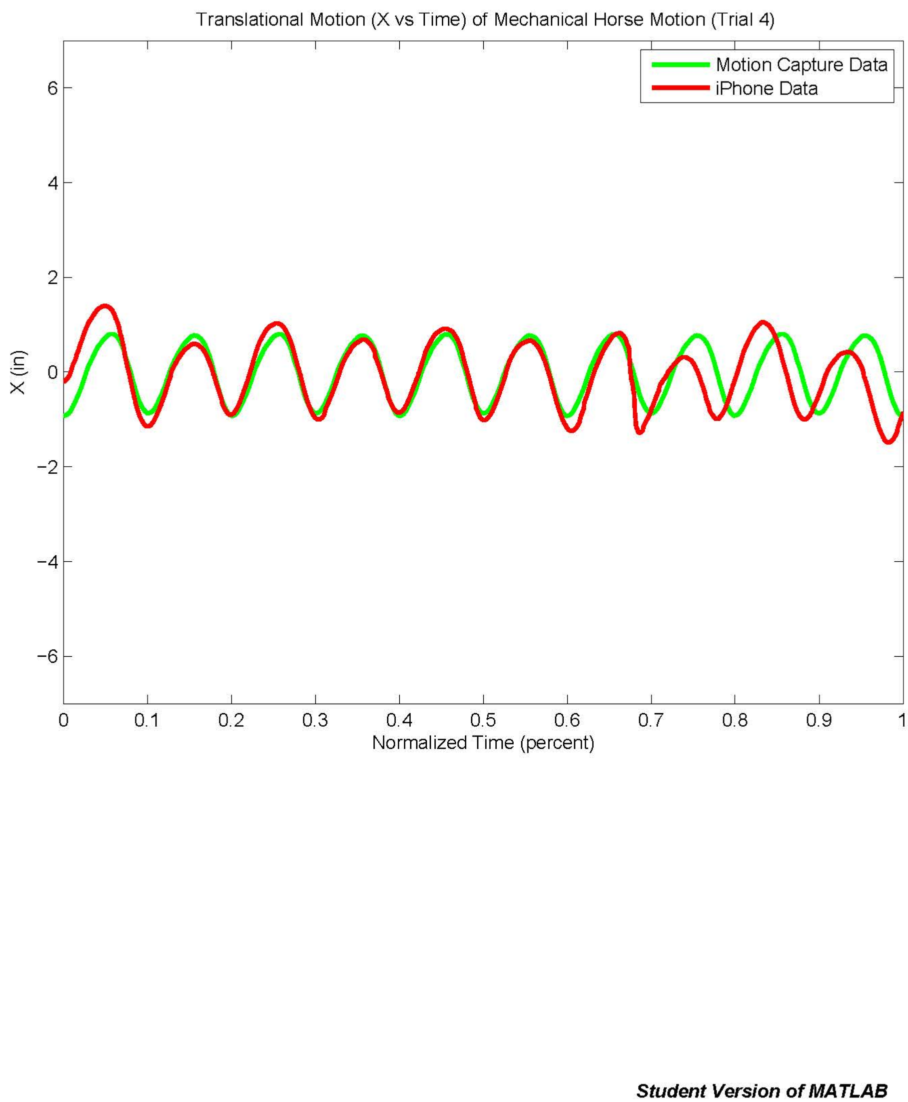
Translational Motion (X vs Time) of Mechanical Horse Motion (Trial 4)
Motion Capture Data
iPhone Data
X (in)
Normalized Time (percent)
6
4
2
0
−2
−4
−6
0
0.1
0.2
0.3
0.4
0.5
0.6
0.7
0.8
0.9
1
Student Version of MATLAB

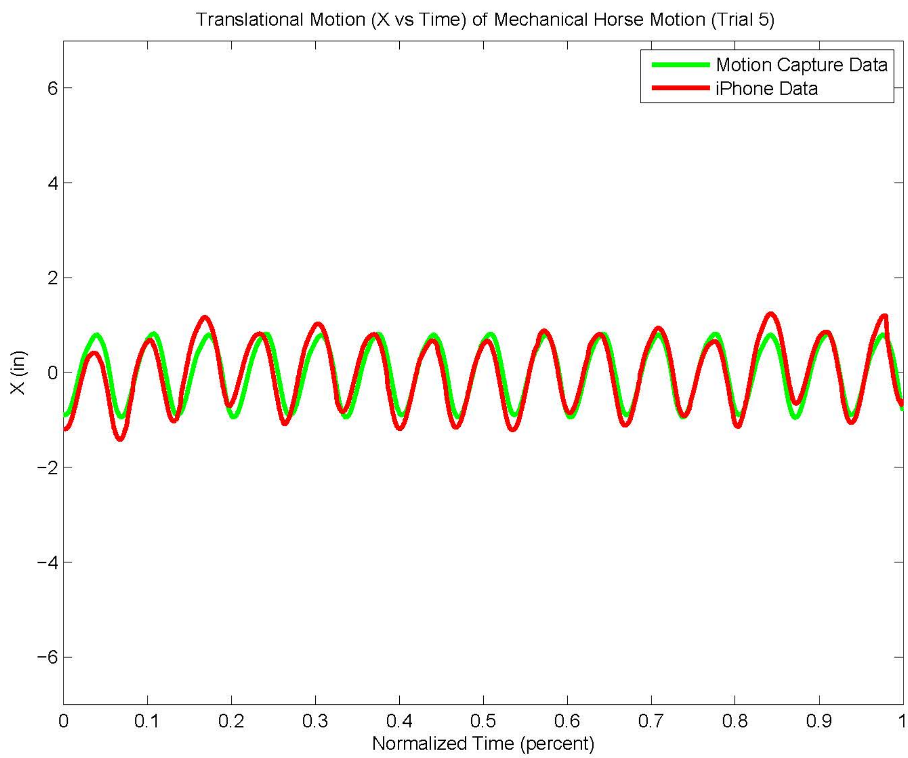

Student Version of MATLAB

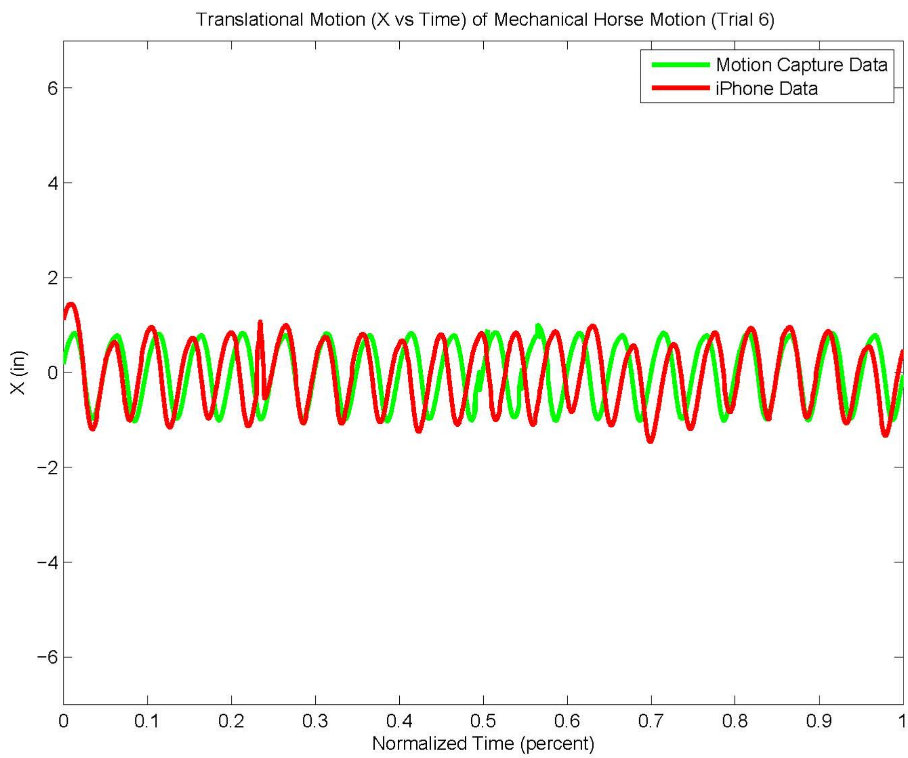

Student Version of MATLAB

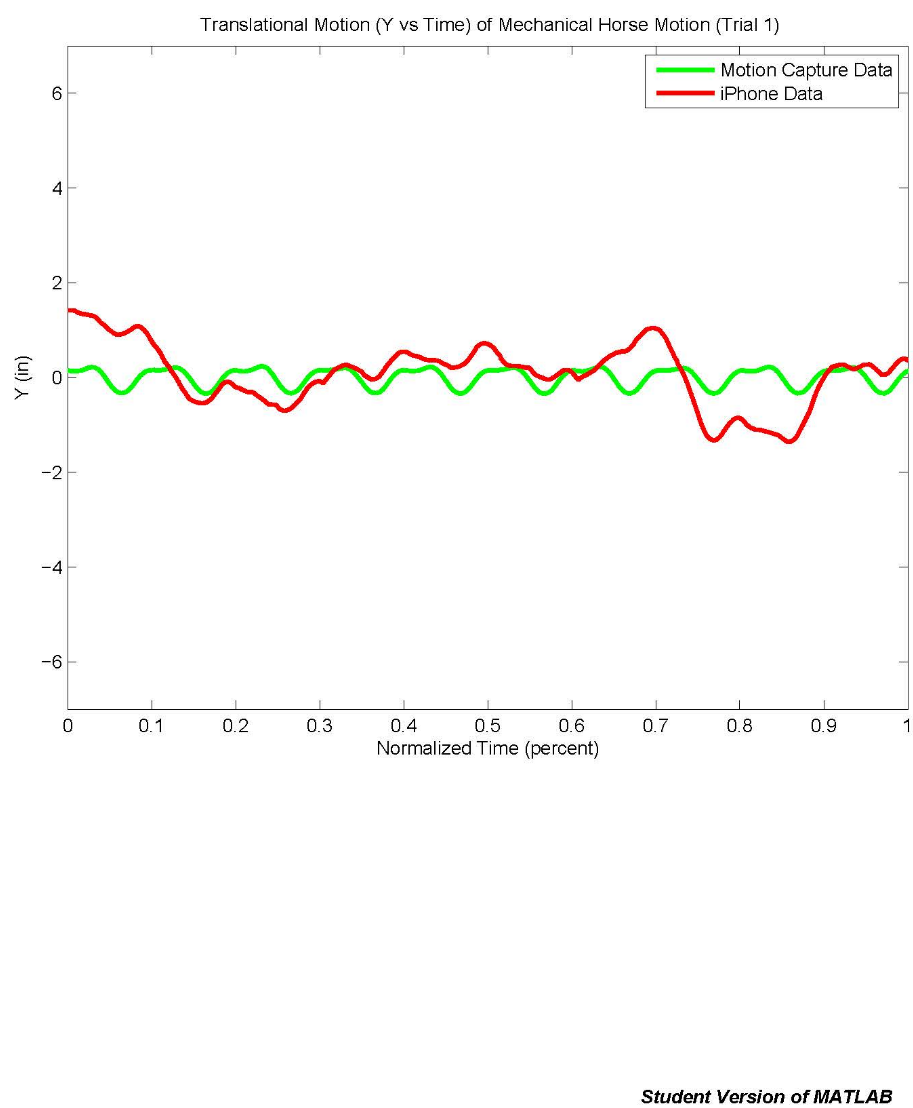
Translational Motion (Y vs Time) of Mechanical Horse Motion (Trial 1)
Motion Capture Data
iPhone Data
Y (in)
6
4
2
0
−2
−4
−6
0
0.1
0.2
0.3
0.4
0.5
0.6
0.7
0.8
0.9
1
Normalized Time (percent)
Student Version of MATLAB

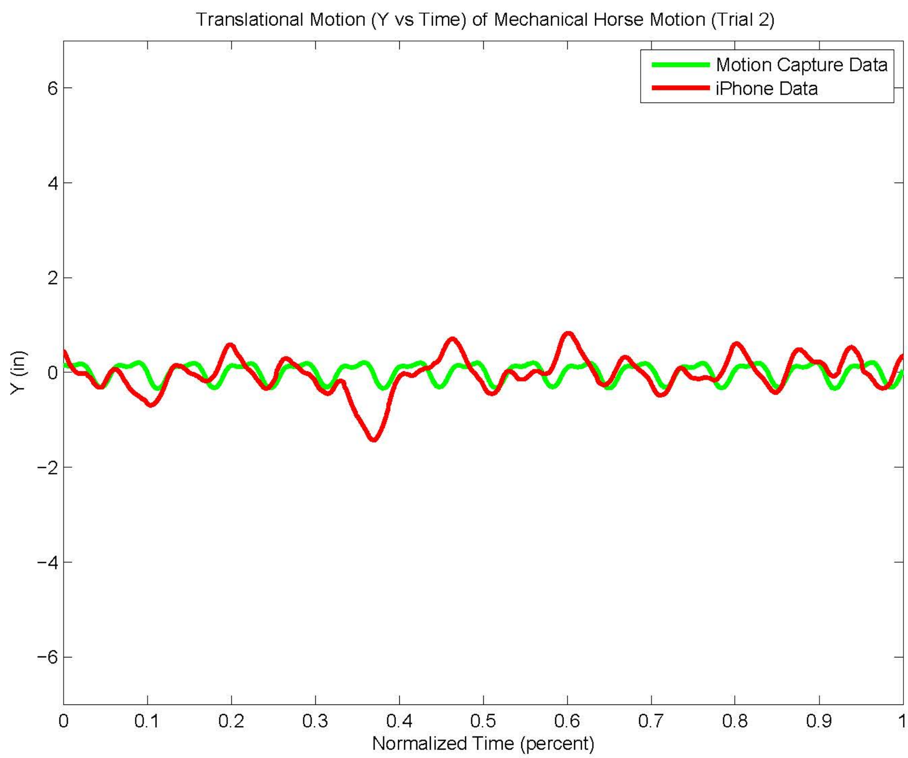

Student Version of MATLAB

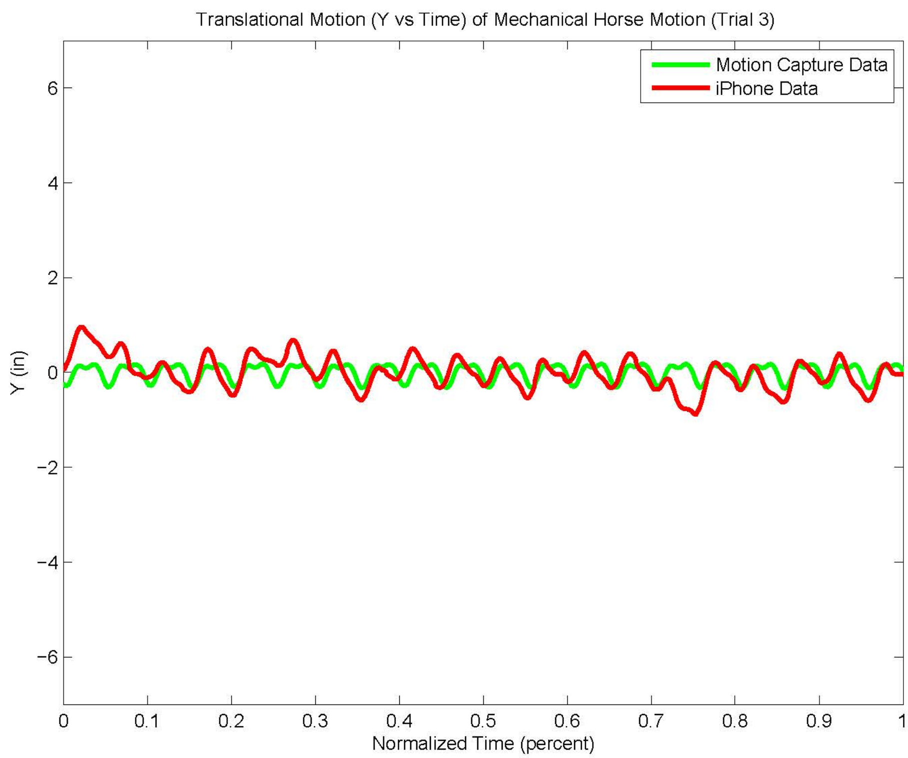

Student Version of MATLAB

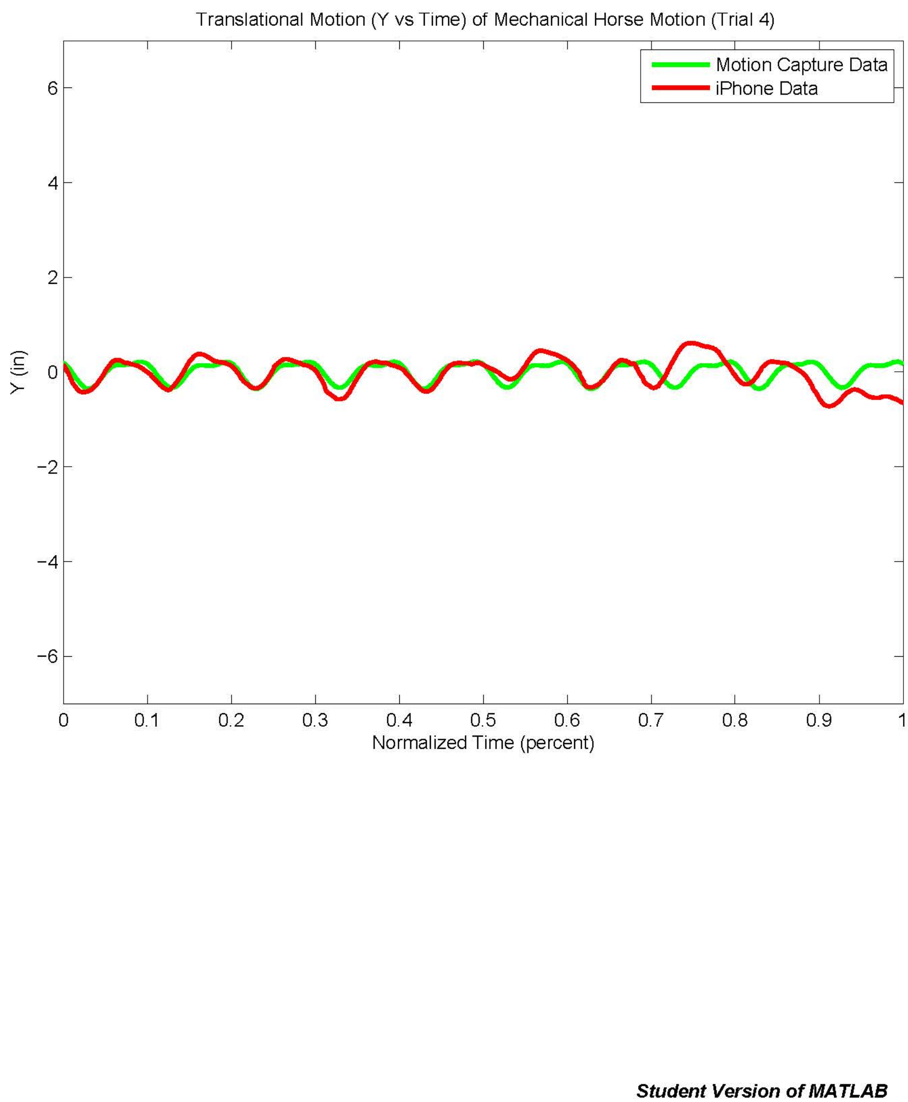
Translational Motion (Y vs Time) of Mechanical Horse Motion (Trial 4)
Motion Capture Data
iPhone Data
6
4
2
0
−2
−4
−6
Y (in)
0
0.1
0.2
0.3
0.4
0.5
0.6
0.7
0.8
0.9
1
Normalized Time (percent)
Student Version of MATLAB

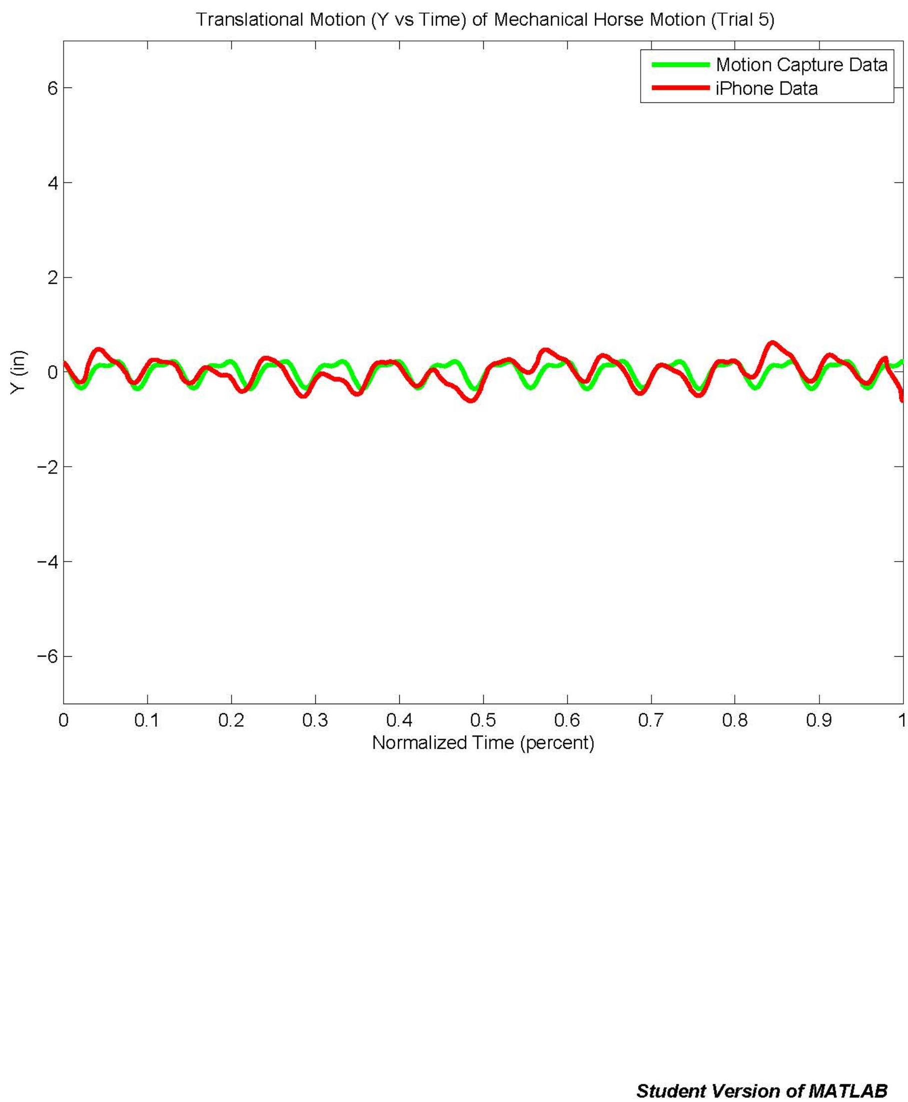

Translational Motion (Y vs Time) of Mechanical Horse Motion (Trial 5)
Motion Capture Data
iPhone Data
Y (in)
6
4
2
0
−2
−4
−6
0
0.1
0.2
0.3
0.4
0.5
0.6
0.7
0.8
0.9
1
Normalized Time (percent)
Student Version of MATLAB

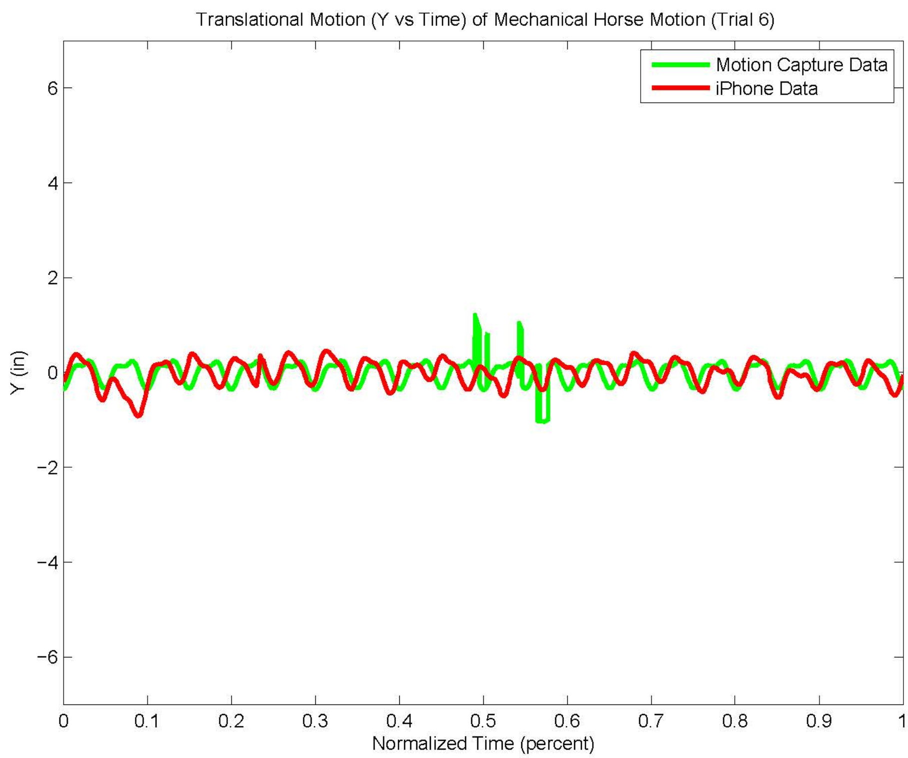

Student Version of MATLAB

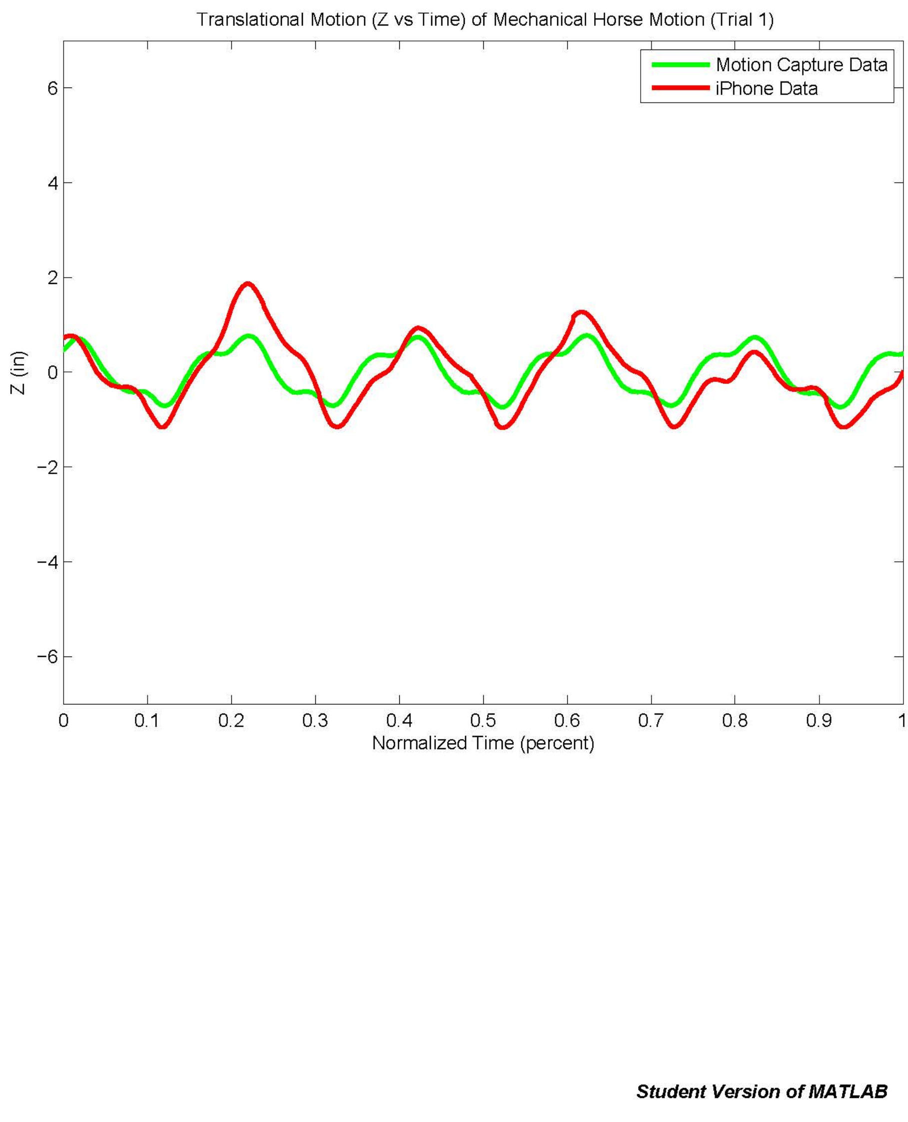
Translational Motion (Z vs Time) of Mechanical Horse Motion (Trial 1)
Motion Capture Data
iPhone Data
Z (in)
6
4
2
0
−2
−4
−6
0
0.1
0.2
0.3
0.4
0.5
0.6
0.7
0.8
0.9
1
Normalized Time (percent)
Student Version of MATLAB

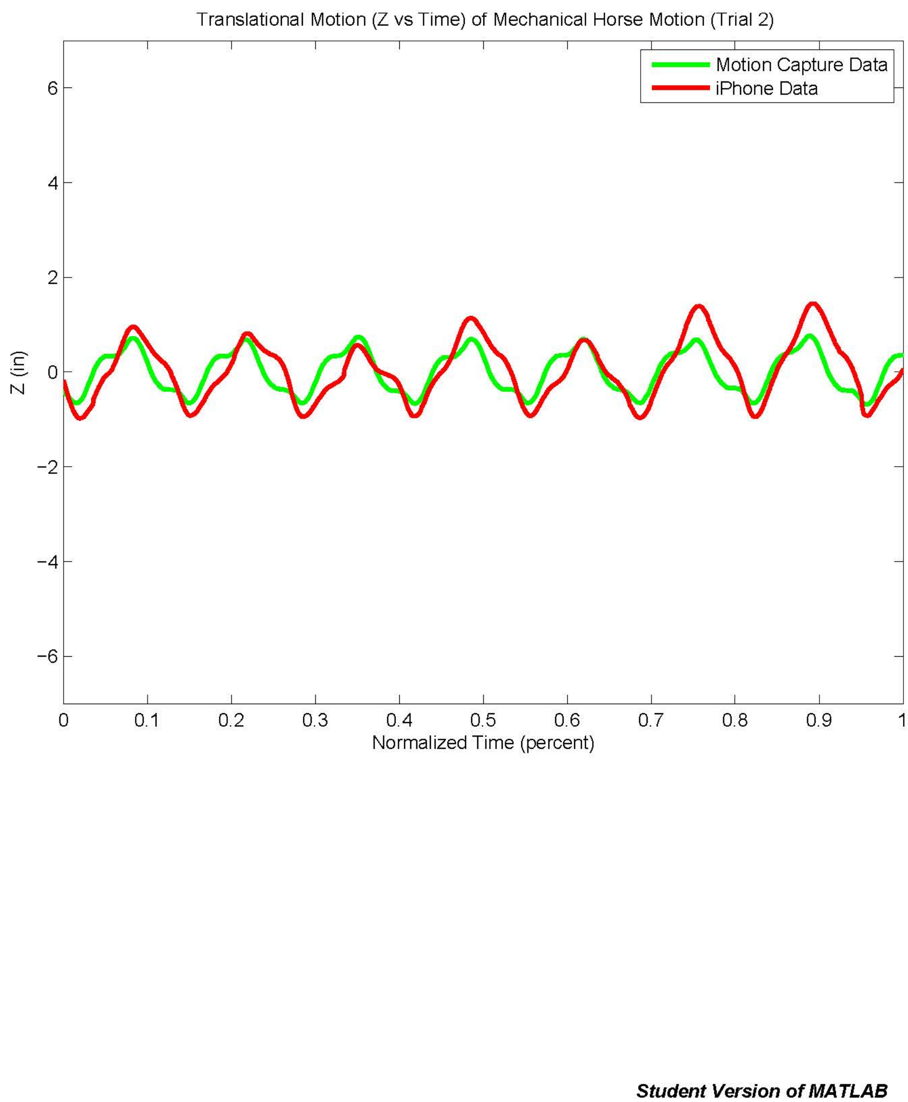

Translational Motion (Z vs Time) of Mechanical Horse Motion (Trial 2)
Motion Capture Data
iPhone Data
Z (in)
6
4
2
0
−2
−4
−6
0
0.1
0.2
0.3
0.4
0.5
0.6
0.7
0.8
0.9
1
Normalized Time (percent)
Student Version of MATLAB

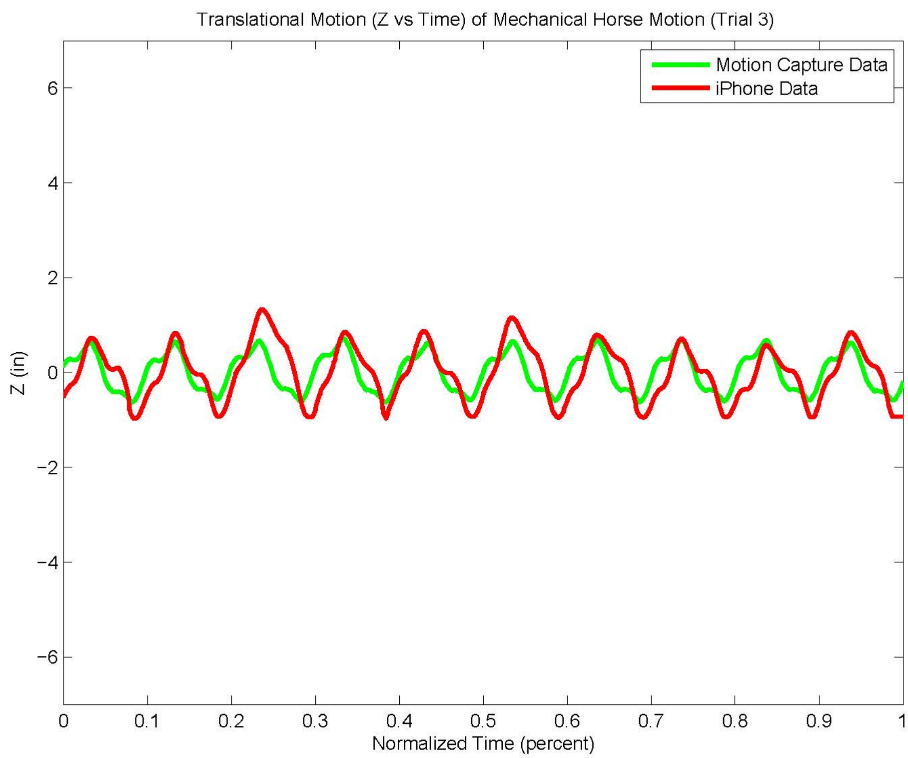

Student Version of MATLAB

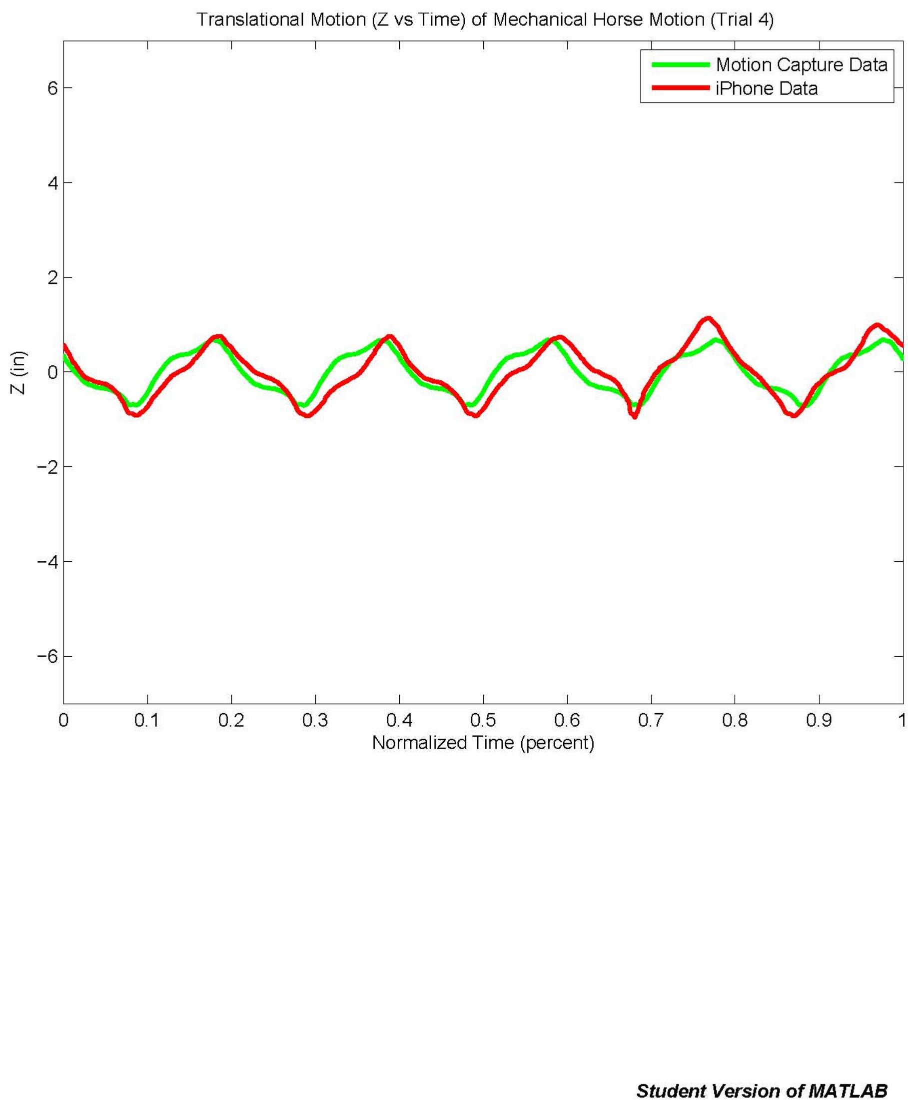

Translational Motion (Z vs Time) of Mechanical Horse Motion (Trial 4)
Motion Capture Data
iPhone Data
Z (in)
6
4
2
0
−2
−4
−6
0
0.1
0.2
0.3
0.4
0.5
0.6
0.7
0.8
0.9
1
Normalized Time (percent)
Student Version of MATLAB

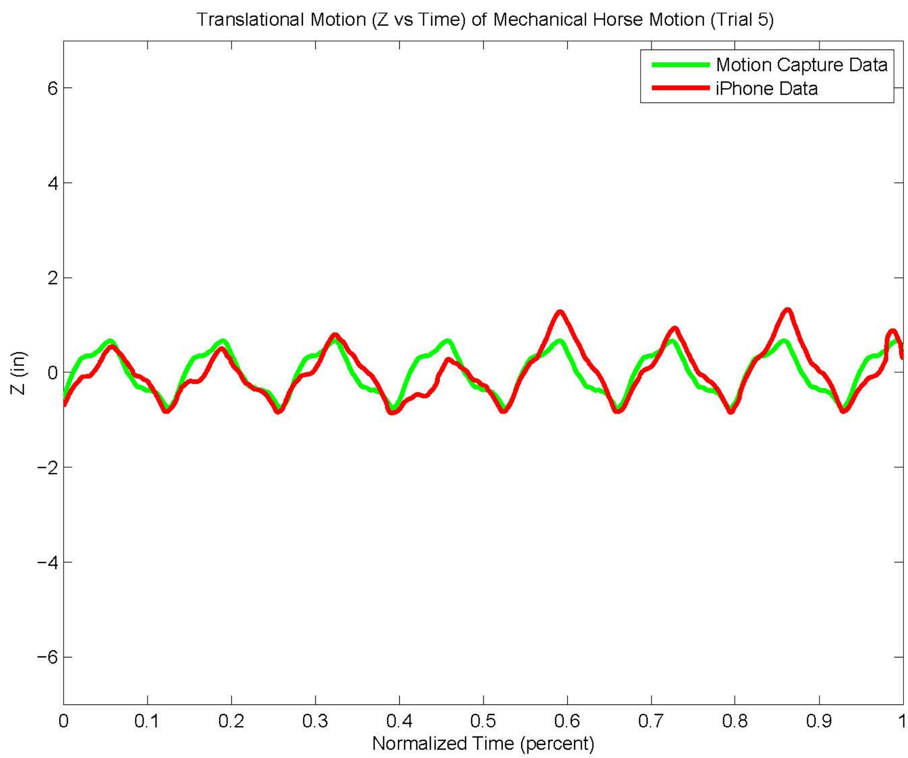

Student Version of MATLAB

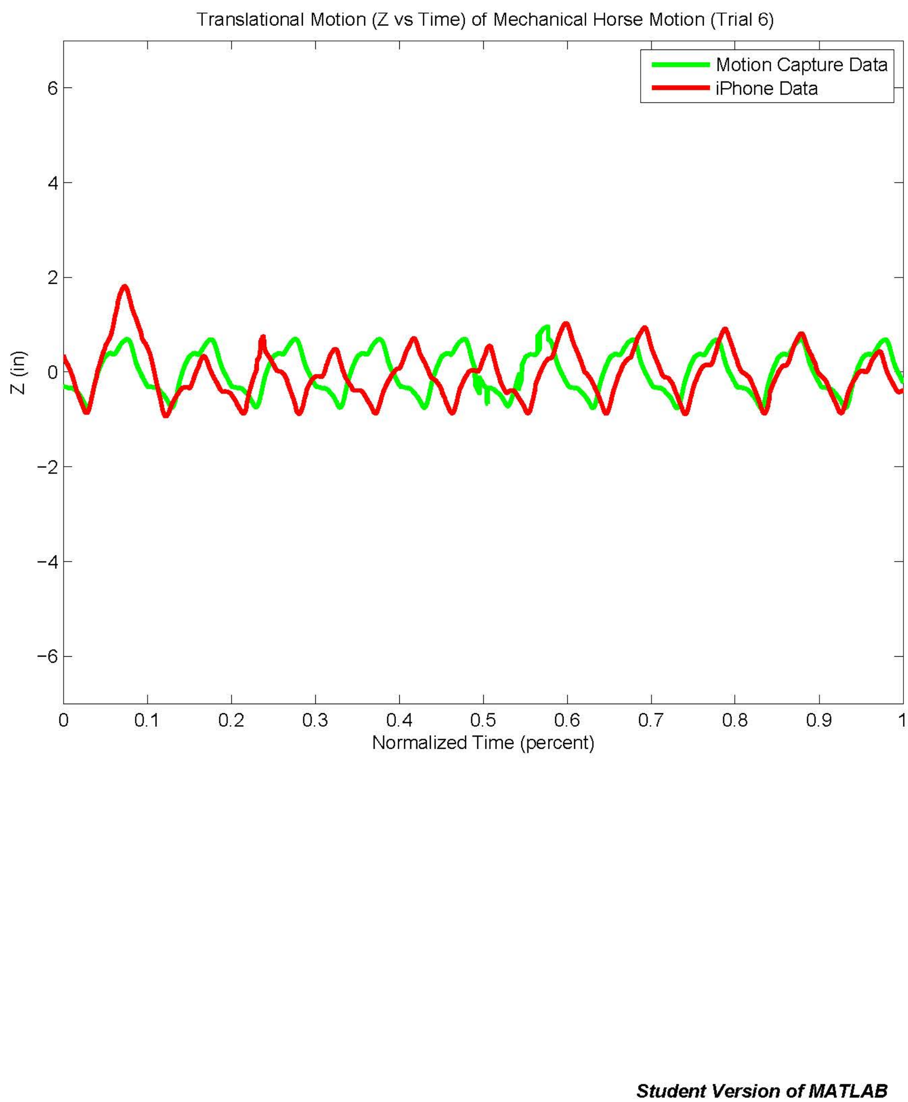
Translational Motion (Z vs Time) of Mechanical Horse Motion (Trial 6)
Motion Capture Data
iPhone Data
Z (in)
Normalized Time (percent)
6
4
2
0
−2
−4
−6
0
0.1
0.2
0.3
0.4
0.5
0.6
0.7
0.8
0.9
1
Student Version of MATLAB

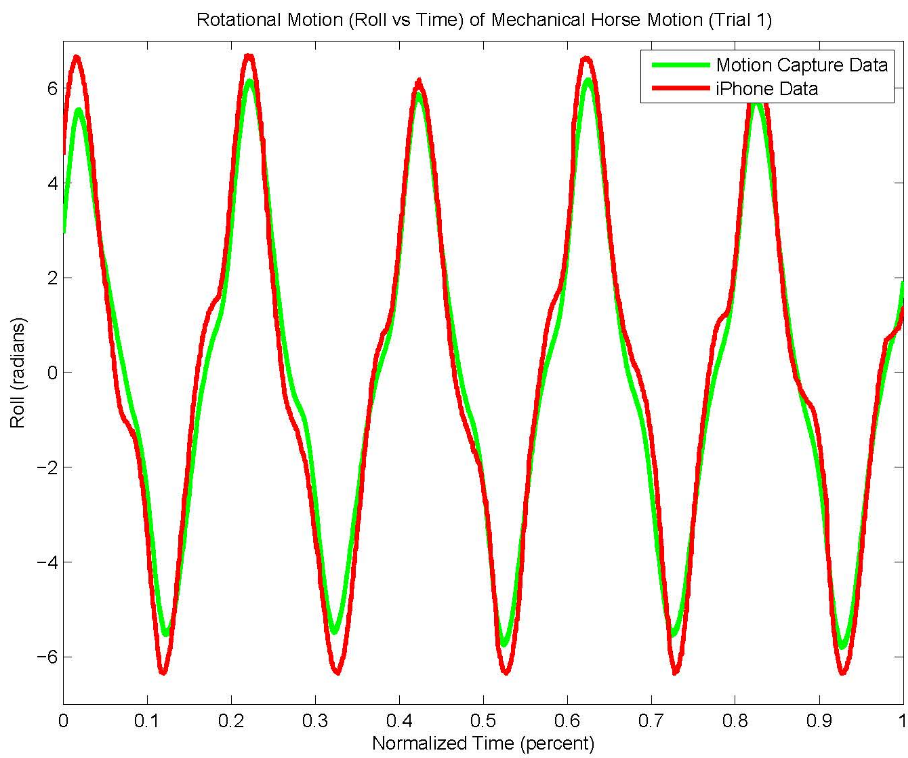

Student Version of MATLAB

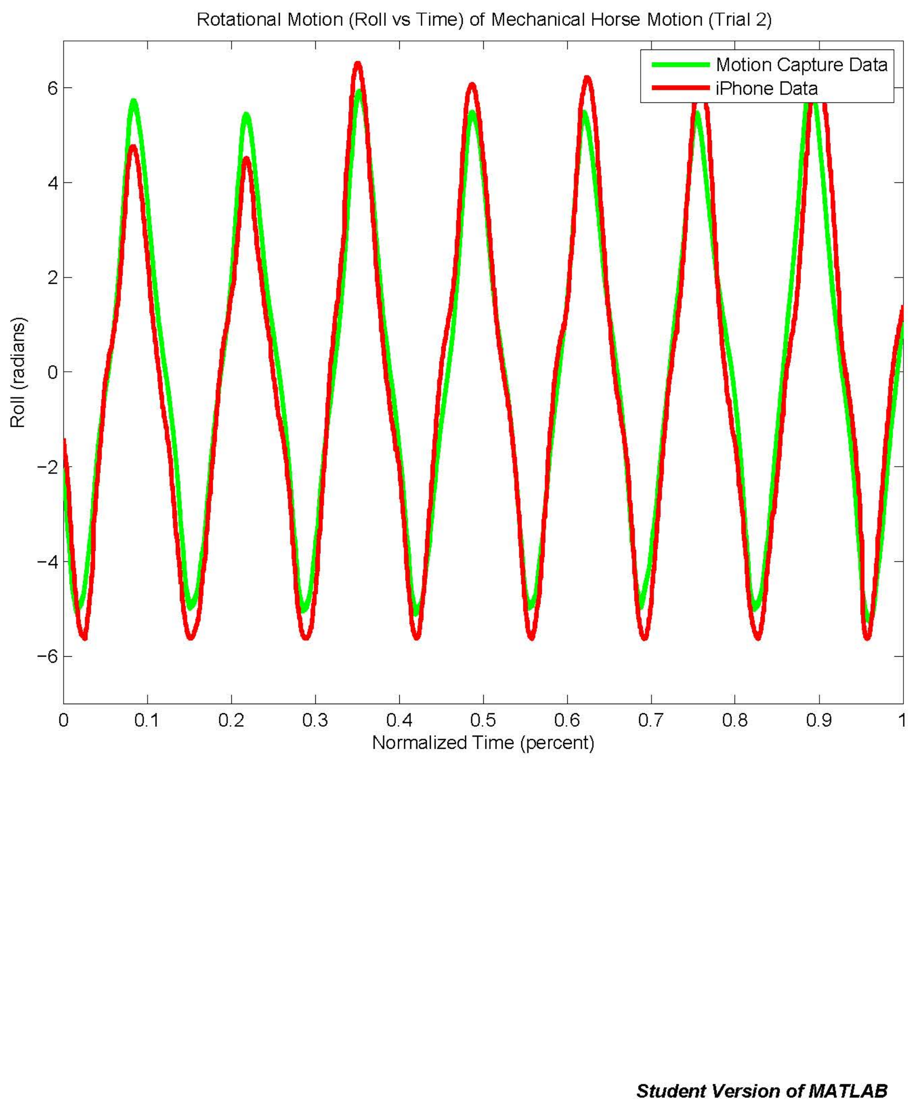
Rotational Motion (Roll vs Time) of Mechanical Horse Motion (Trial 2)
Motion Capture Data
iPhone Data
Roll (radians)
Normalized Time (percent)
6
4
2
0
−2
−4
−6
0
0.1
0.2
0.3
0.4
0.5
0.6
0.7
0.8
0.9
1
Student Version of MATLAB

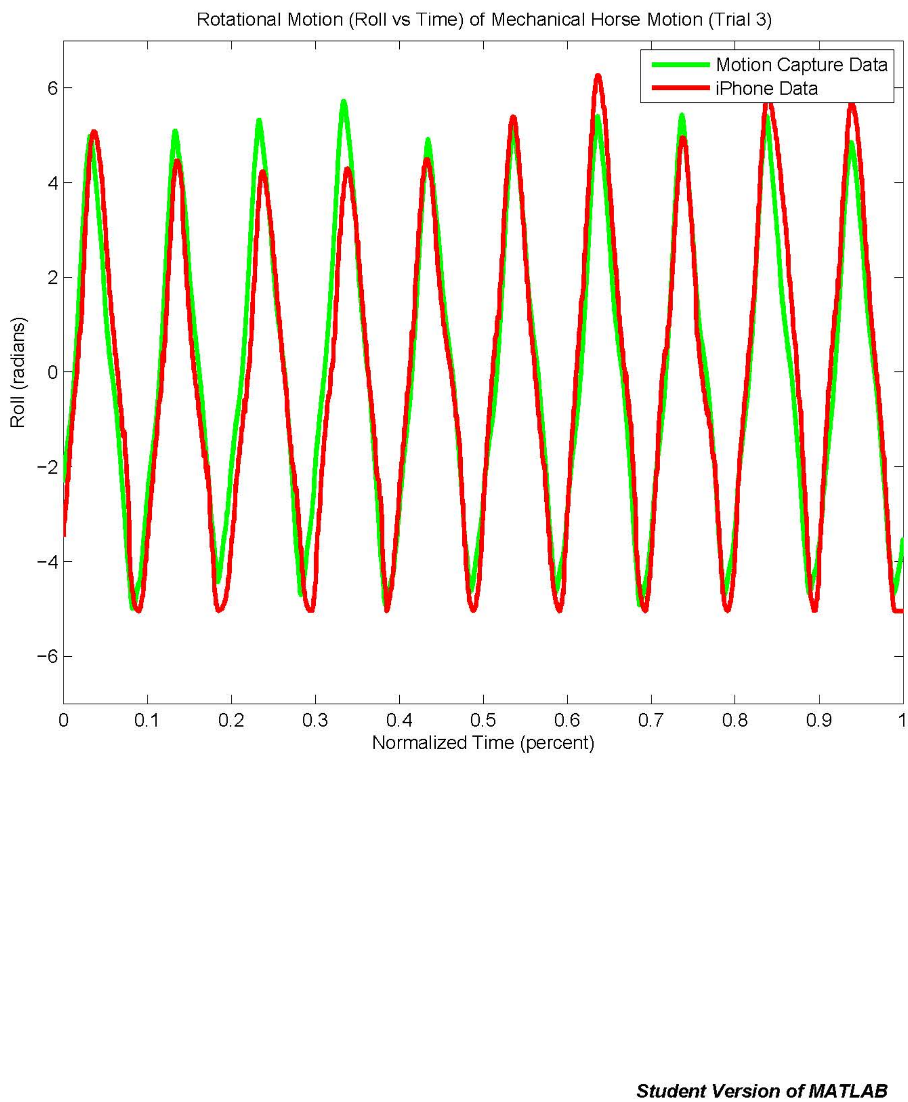
Rotational Motion (Roll vs Time) of Mechanical Horse Motion (Trial 3)
Motion Capture Data
iPhone Data
Roll (radians)
Normalized Time (percent)
6
4
2
0
−2
−4
−6
0
0.1
0.2
0.3
0.4
0.5
0.6
0.7
0.8
0.9
1
Student Version of MATLAB

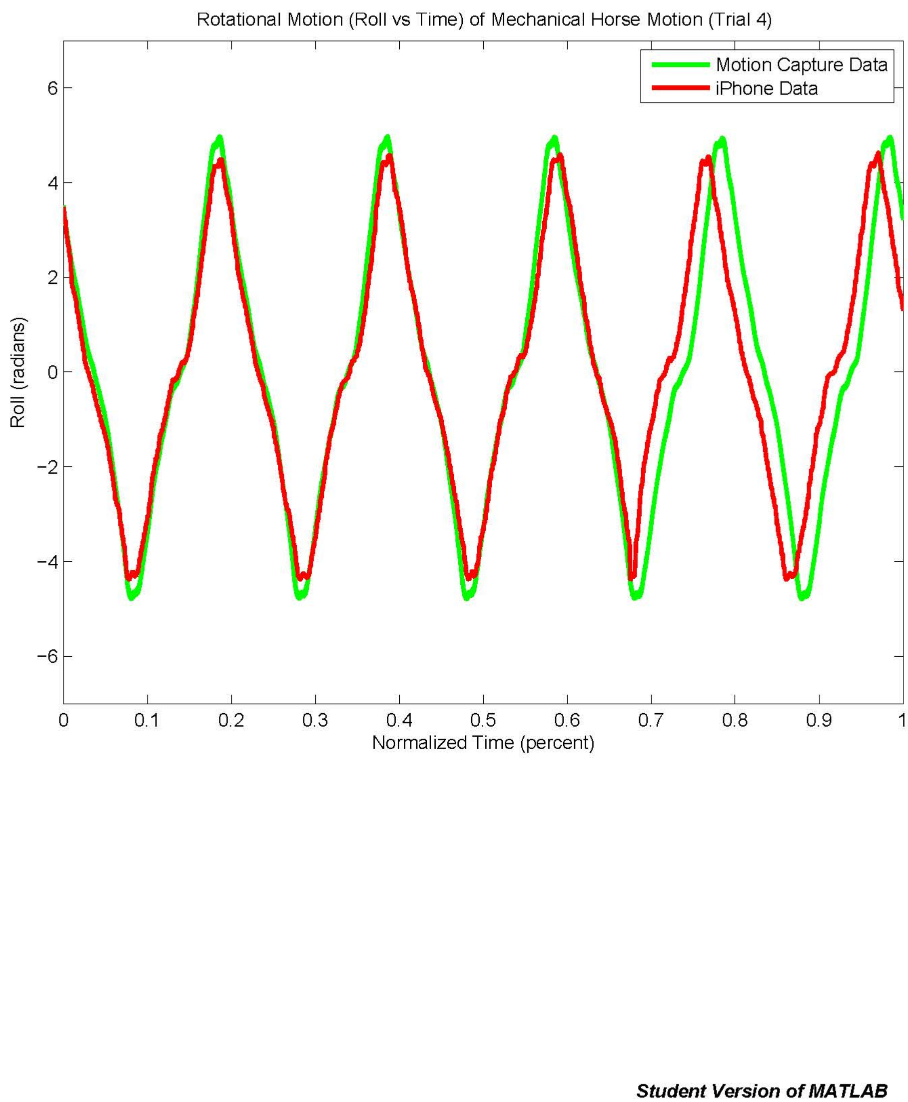

Rotational Motion (Roll vs Time) of Mechanical Horse Motion (Trial 4)
Motion Capture Data
iPhone Data
Roll (radians)
Normalized Time (percent)
6
4
2
0
−2
−4
−6
0
0.1
0.2
0.3
0.4
0.5
0.6
0.7
0.8
0.9
1
Student Version of MATLAB

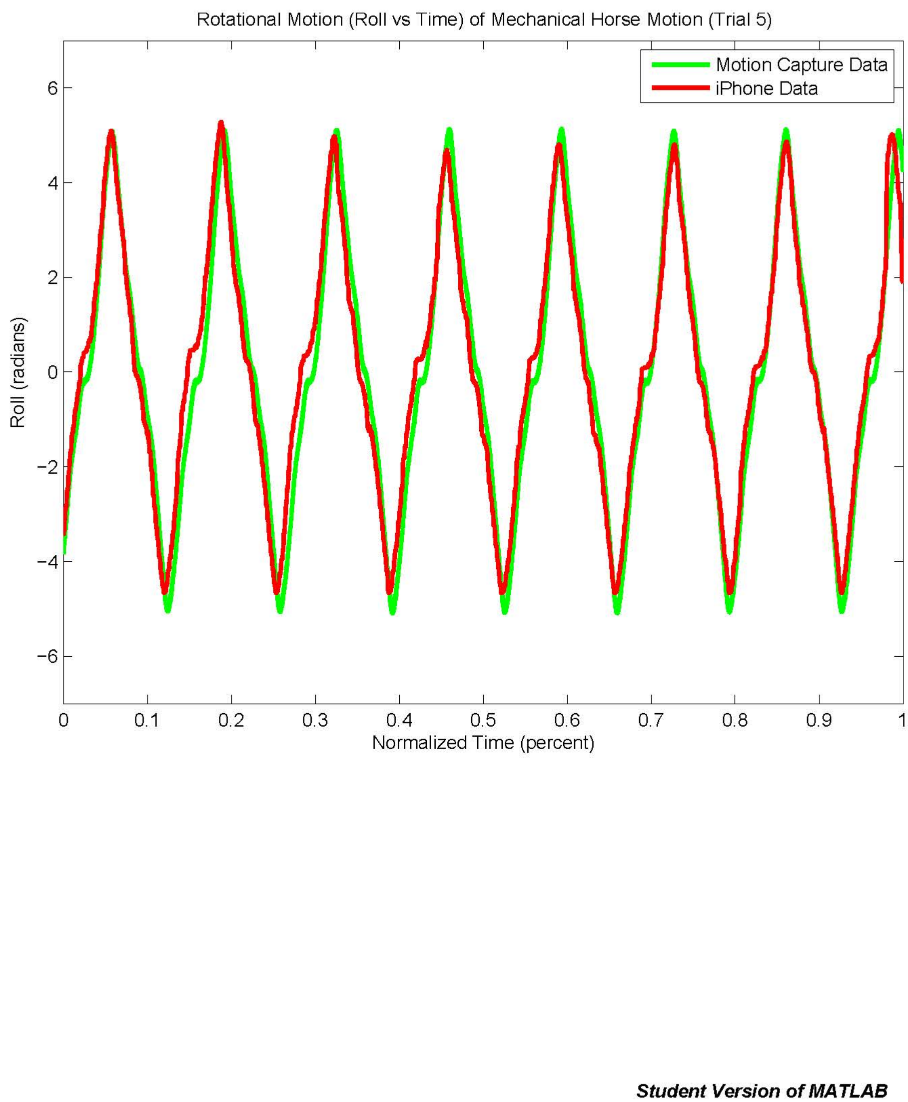
Rotational Motion (Roll vs Time) of Mechanical Horse Motion (Trial 5)
Motion Capture Data
iPhone Data
Roll (radians)
Normalized Time (percent)
6
4
2
0
−2
−4
−6
0
0.1
0.2
0.3
0.4
0.5
0.6
0.7
0.8
0.9
1
Student Version of MATLAB

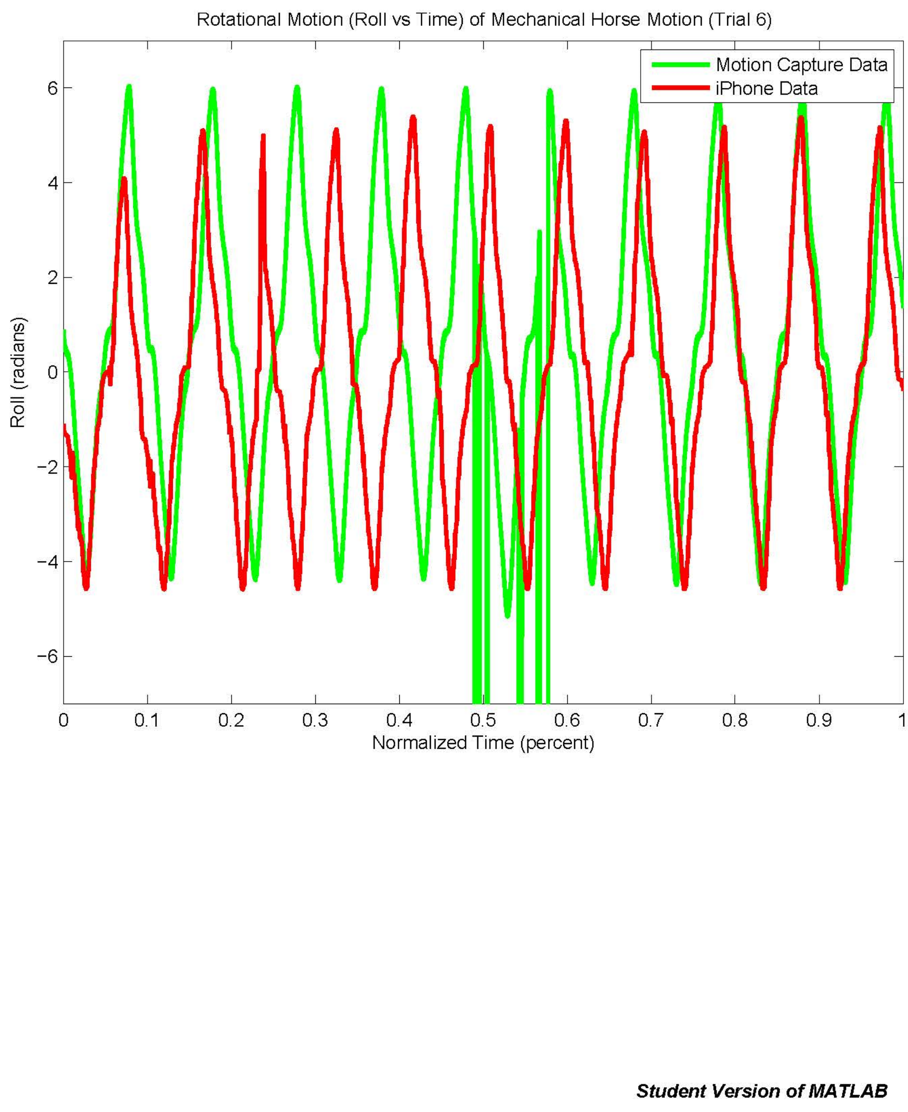

Rotational Motion (Roll vs Time) of Mechanical Horse Motion (Trial 6)
Motion Capture Data
iPhone Data
Roll (radians)
Normalized Time (percent)
6
4
2
0
−2
−4
−6
0
0.1
0.2
0.3
0.4
0.5
0.6
0.7
0.8
0.9
1
Student Version of MATLAB

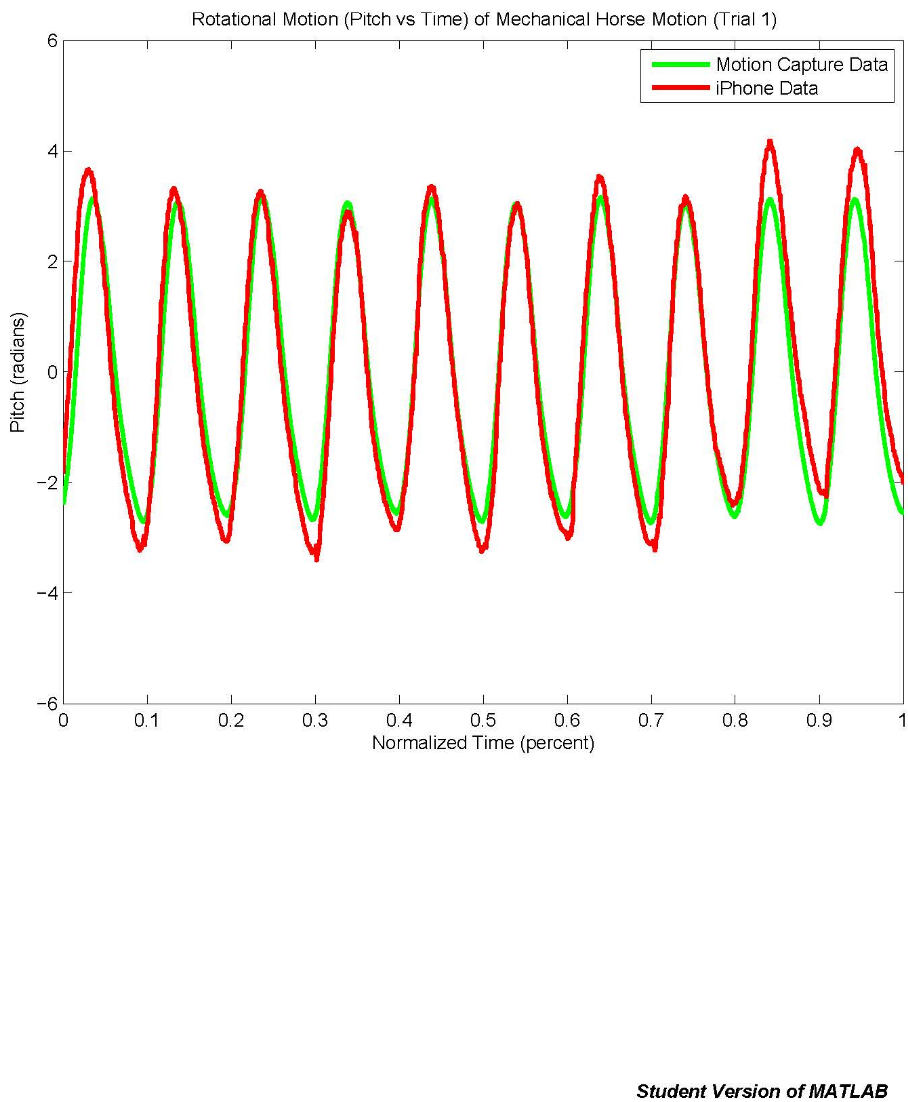
Rotational Motion (Pitch vs Time) of Mechanical Horse Motion (Trial 1)
Motion Capture Data
iPhone Data
Pitch (radians)
Normalized Time (percent)
6
4
2
0
-2
-4
-6
0
0.1
0.2
0.3
0.4
0.5
0.6
0.7
0.8
0.9
1
Student Version of MATLAB

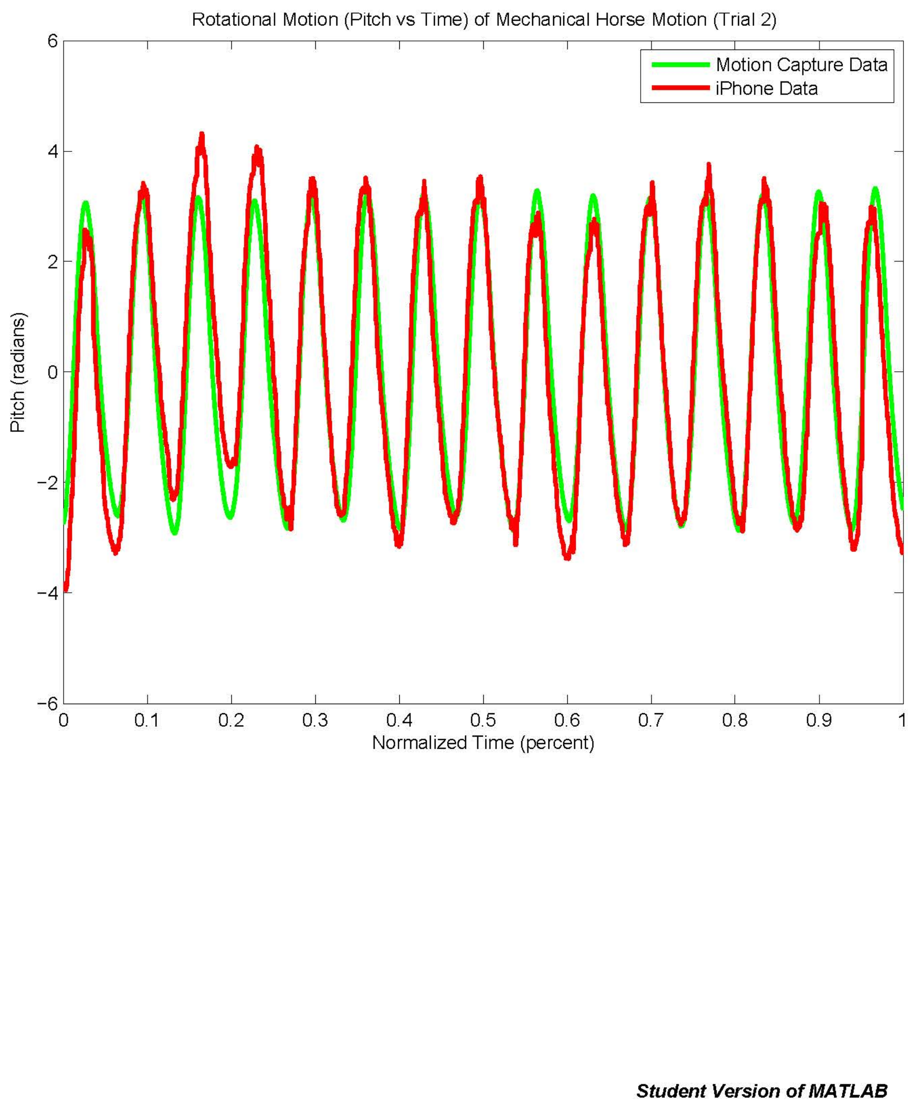
Rotational Motion (Pitch vs Time) of Mechanical Horse Motion (Trial 2)
Motion Capture Data
iPhone Data
Pitch (radians)
Normalized Time (percent)
6
4
2
0
-2
-4
-6
0
0.1
0.2
0.3
0.4
0.5
0.6
0.7
0.8
0.9
1
Student Version of MATLAB

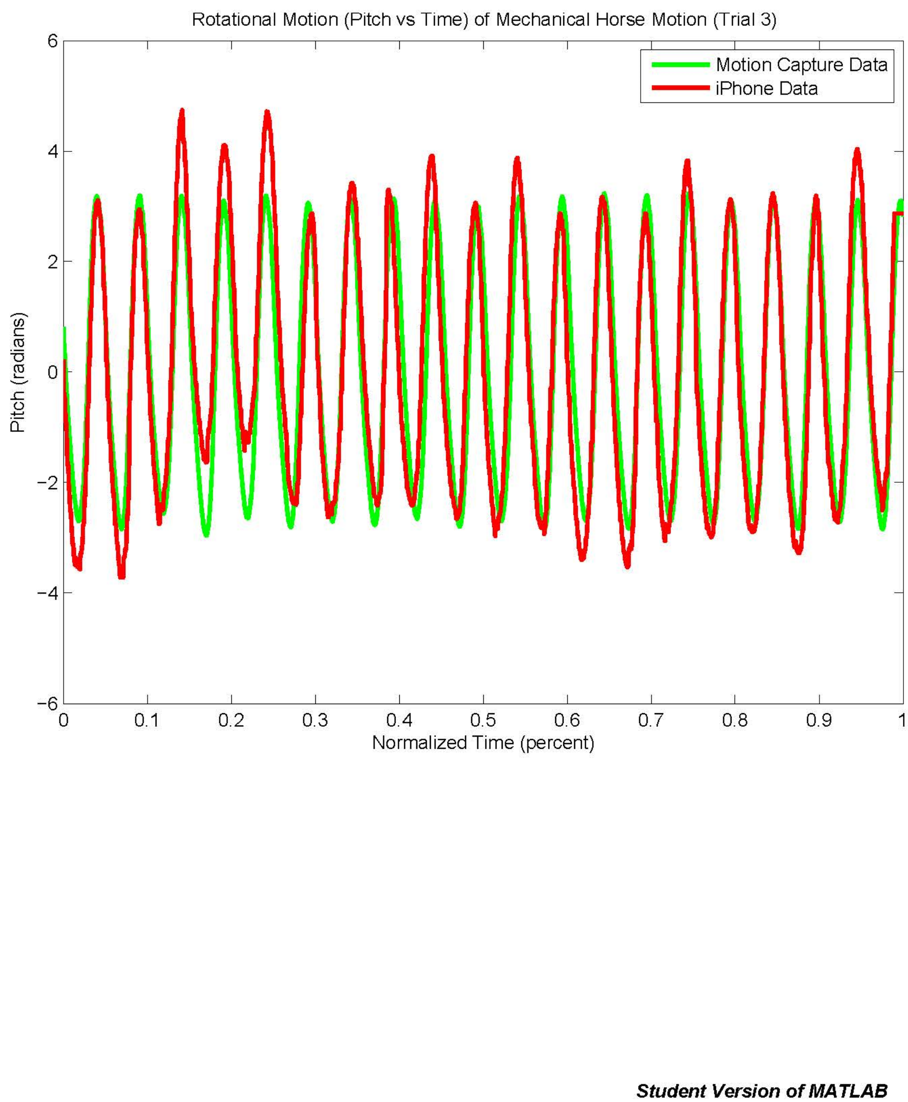
Rotational Motion (Pitch vs Time) of Mechanical Horse Motion (Trial 3)
Motion Capture Data
iPhone Data
Pitch (radians)
Normalized Time (percent)
6
4
2
0
-2
-4
-6
0
0.1
0.2
0.3
0.4
0.5
0.6
0.7
0.8
0.9
1
Student Version of MATLAB

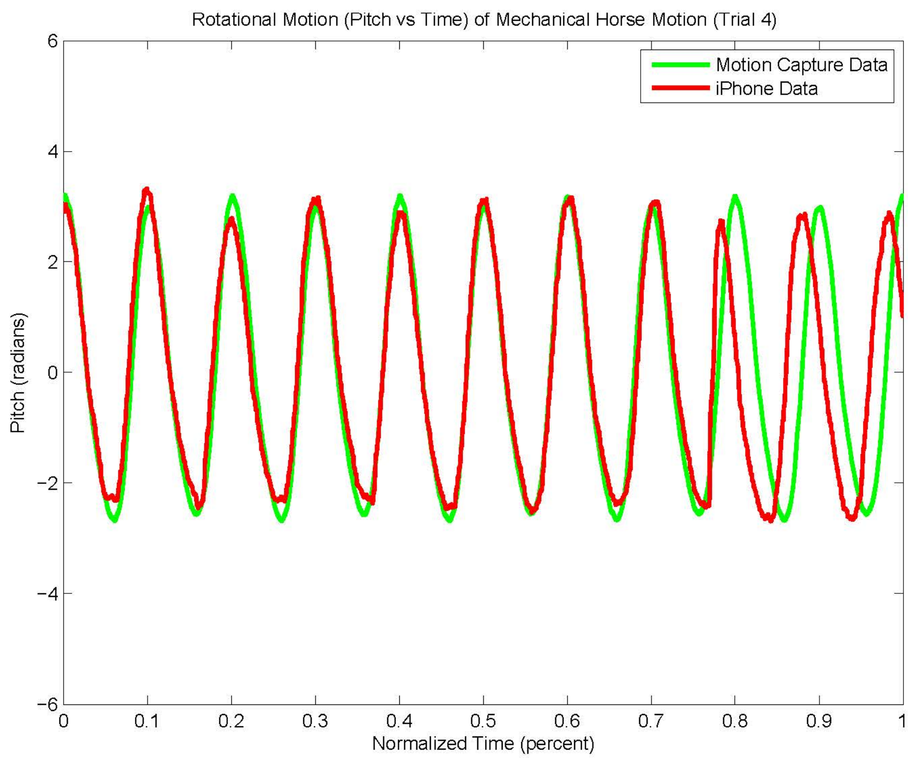

Student Version of MATLAB

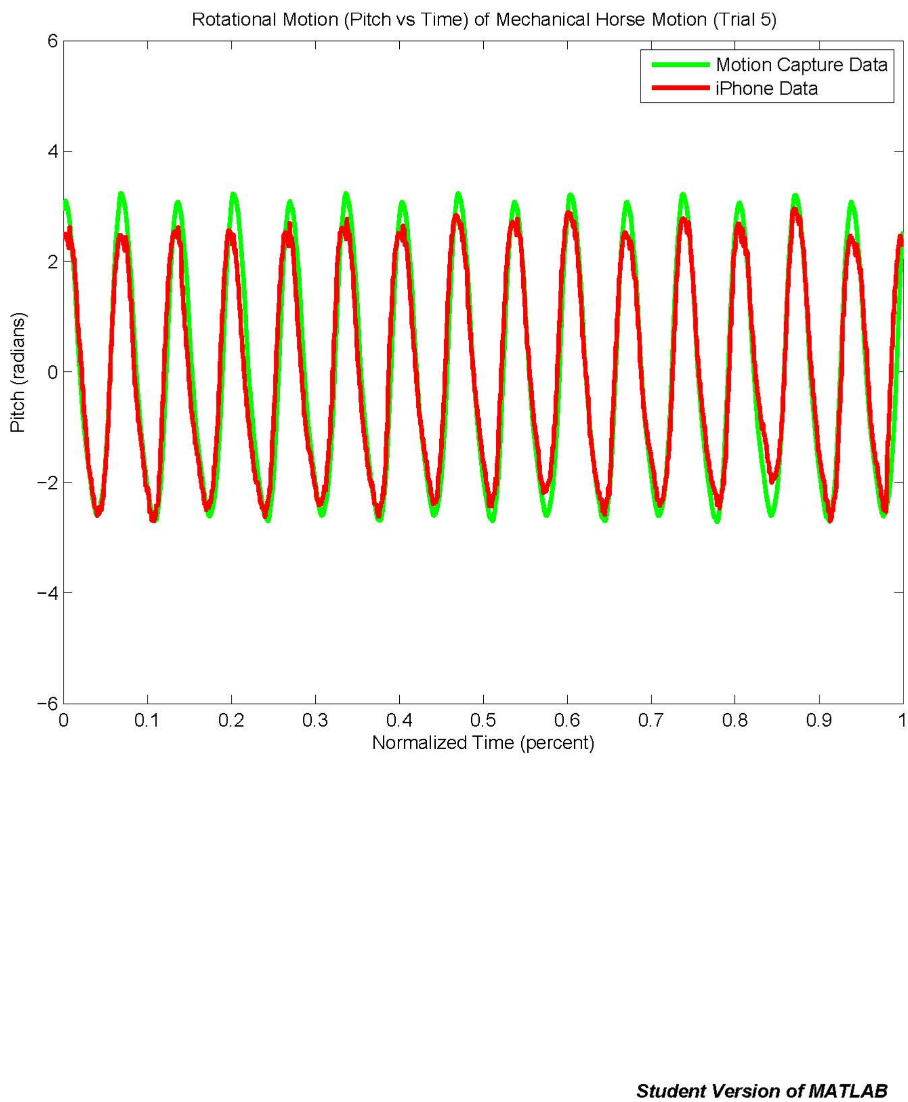
Rotational Motion (Pitch vs Time) of Mechanical Horse Motion (Trial 5)
Motion Capture Data
iPhone Data
Pitch (radians)
Normalized Time (percent)
6
4
2
0
−2
−4
−6
0
0.1
0.2
0.3
0.4
0.5
0.6
0.7
0.8
0.9
1
Student Version of MATLAB

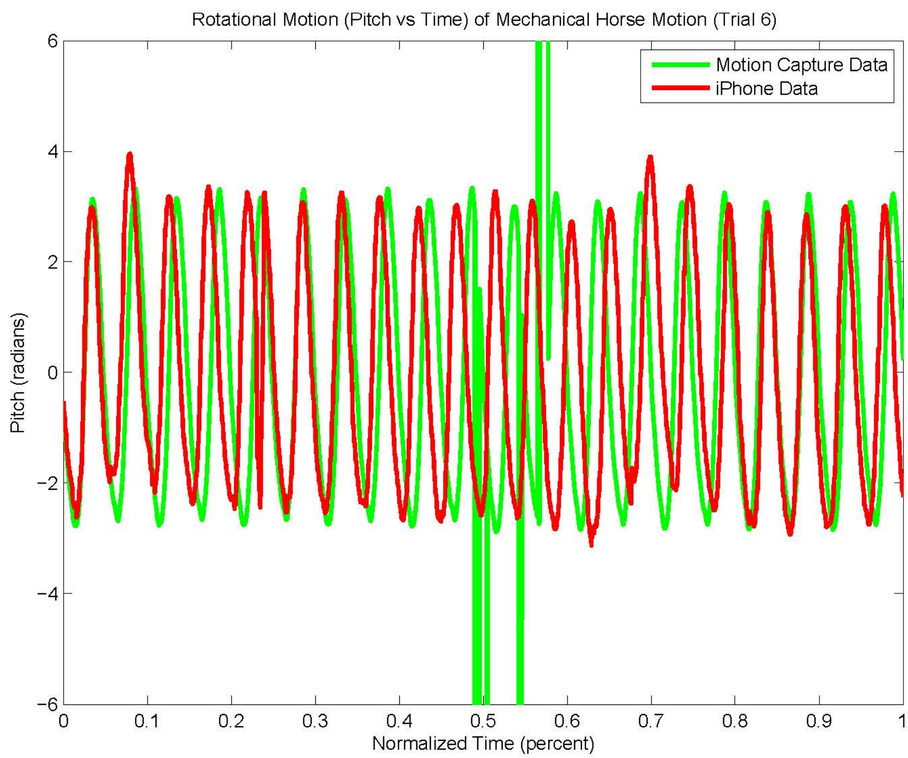

Student Version of MATLAB

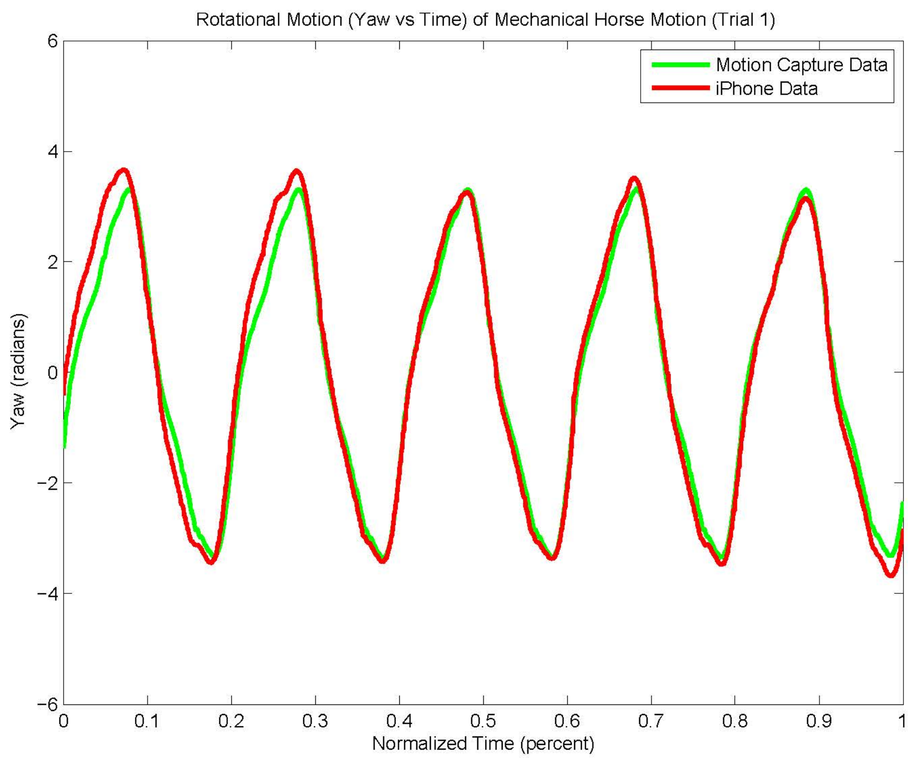

Student Version of MATLAB

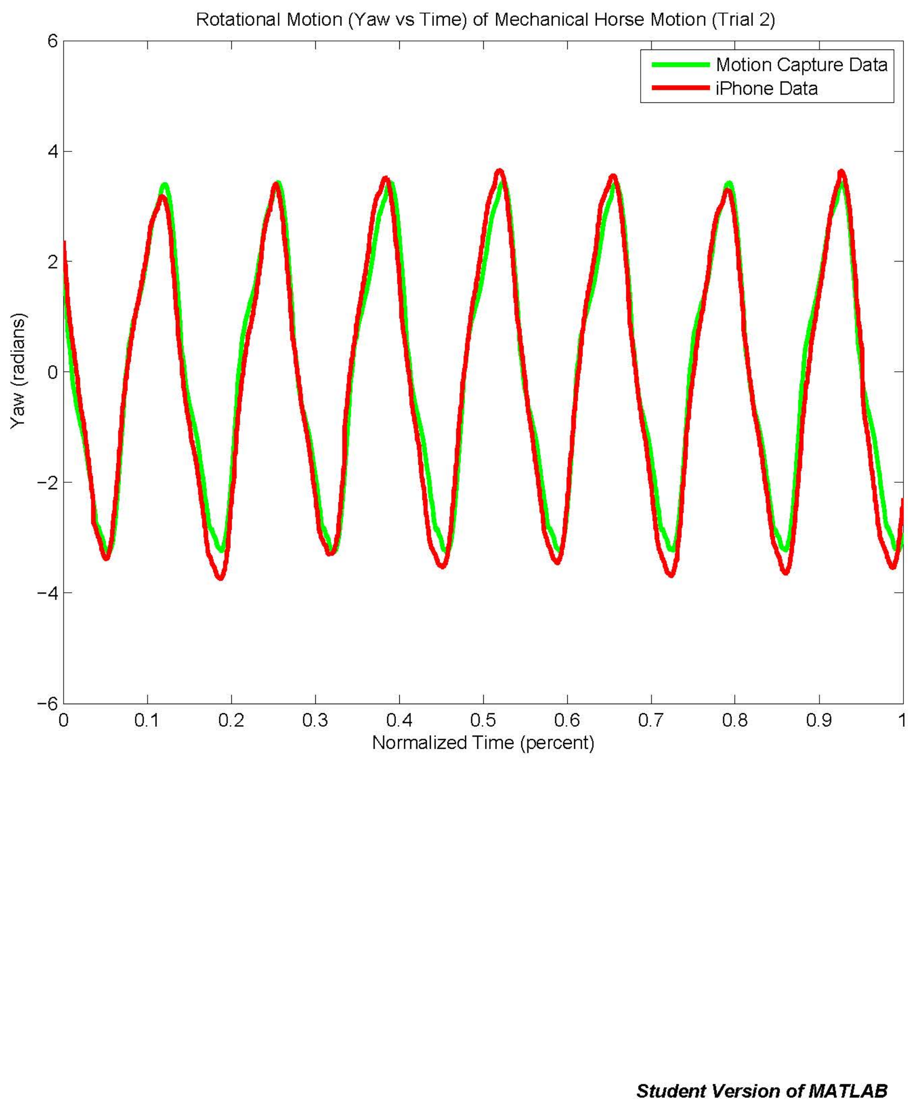
Rotational Motion (Yaw vs Time) of Mechanical Horse Motion (Trial 2)
Motion Capture Data
iPhone Data
Yaw (radians)
Normalized Time (percent)
6
4
2
0
-2
-4
-6
0
0.1
0.2
0.3
0.4
0.5
0.6
0.7
0.8
0.9
1
Student Version of MATLAB

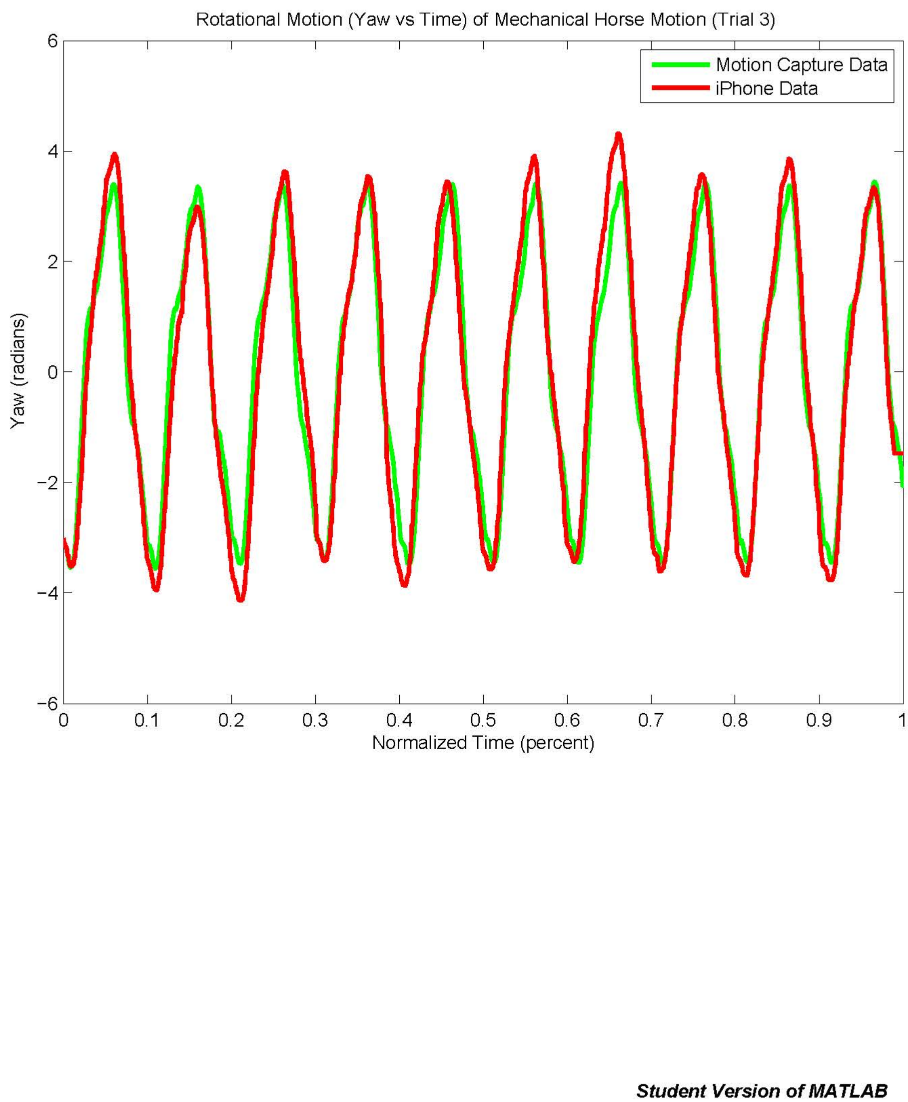
Rotational Motion (Yaw vs Time) of Mechanical Horse Motion (Trial 3)
Motion Capture Data
iPhone Data
Yaw (radians)
Normalized Time (percent)
6
4
2
0
-2
-4
-6
0
0.1
0.2
0.3
0.4
0.5
0.6
0.7
0.8
0.9
1
Student Version of MATLAB

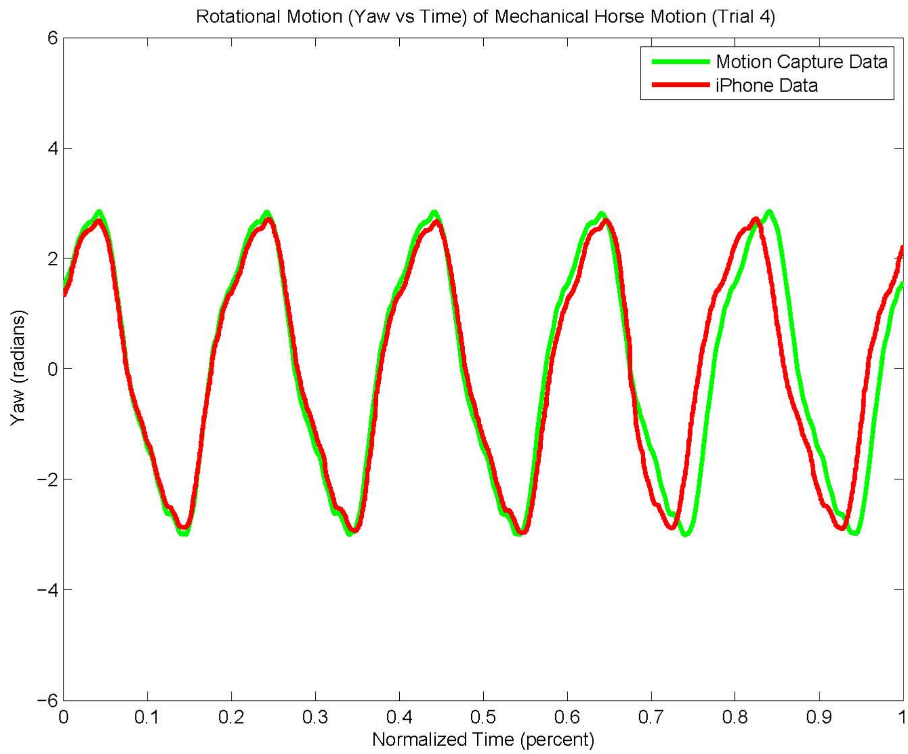

Student Version of MATLAB

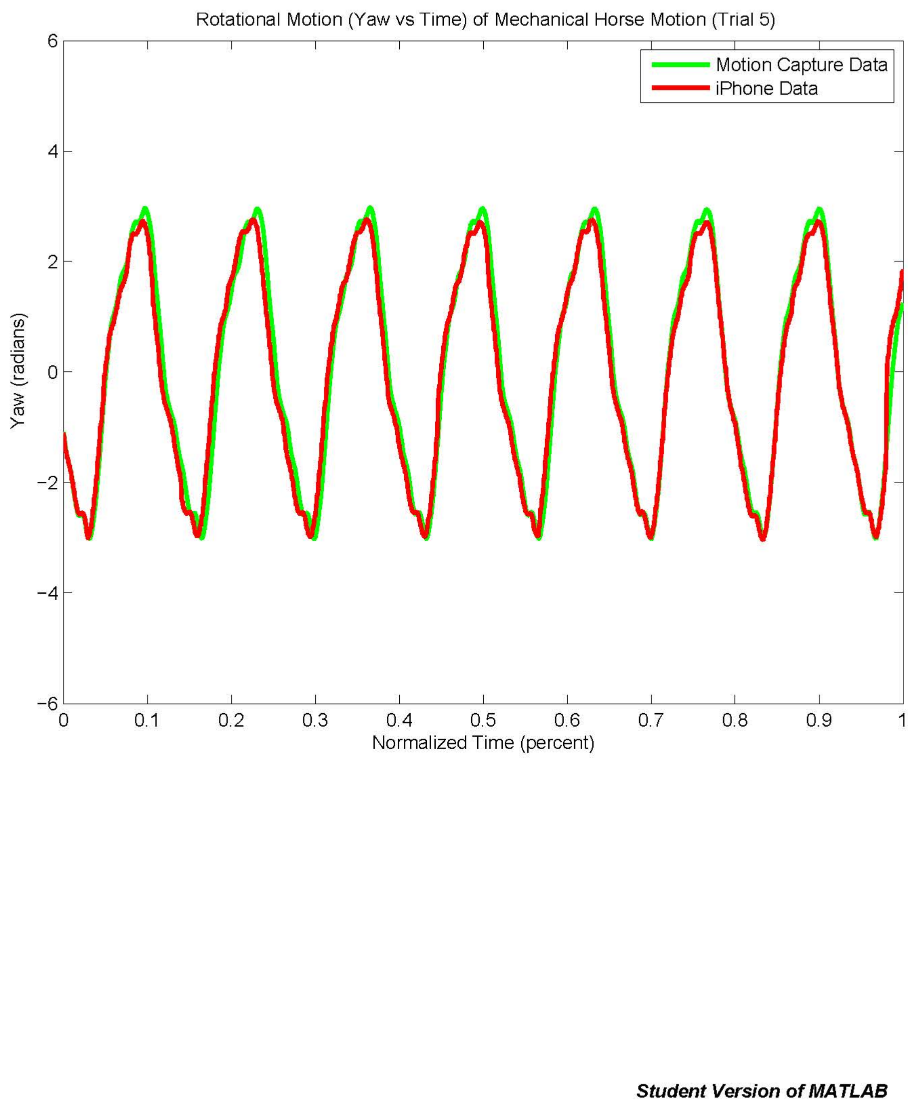
Rotational Motion (Yaw vs Time) of Mechanical Horse Motion (Trial 5)
Motion Capture Data
iPhone Data
Yaw (radians)
Normalized Time (percent)
6
4
2
0
-2
-4
-6
0
0.1
0.2
0.3
0.4
0.5
0.6
0.7
0.8
0.9
1
Student Version of MATLAB

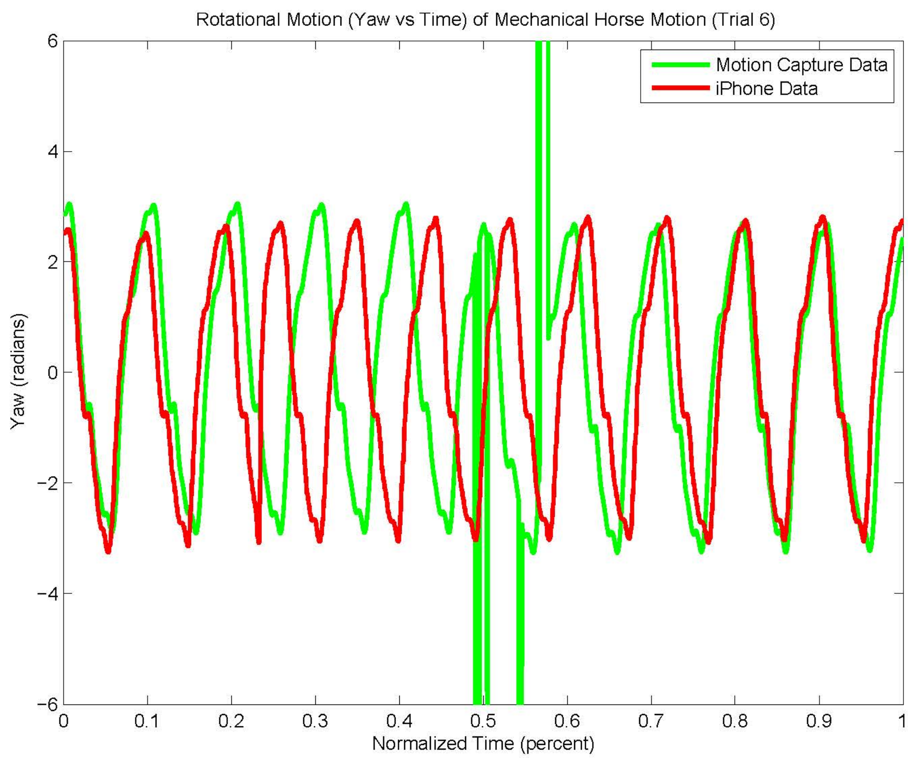

Student Version of MATLAB

BIBLIOGRAPHY

Augustynek, M., M. Penhaker, and D. Korpas. "Controlling Peacemakers by Accelerometers." *2010 Second International Conference on Computer Engineering and Applications (ICCEA)*. Vol. 2. N. p., 2010. 161–163. *IEEE Xplore*. Web.

Bai, Ying-Wen, Siao-Cian Wu, and Cheng-Lung Tsai. "Design and Implementation of a Fall Monitor System by Using a 3-Axis Accelerometer in a Smart Phone." *IEEE Transactions on Consumer Electronics* 58.4 (2012): 1269–1275. *IEEE Xplore*. Web.

Chiu, Chih-Yi et al. "Content-Based Retrieval for Human Motion Data." *Journal of Visual Communication and Image Representation* 15.3 (2004): 446–466. *ScienceDirect*. Web. 28 Oct. 2013.

Cho, Hyunju et al. "Motion Recognition with Smart Phone Embedded 3-Axis Accelerometer Sensor." *2012 IEEE International Conference on Systems, Man, and Cybernetics (SMC)*. N. p., 2012. 919–924. *IEEE Xplore*. Web.

Ellison, Jennifer Barbee, Steven J. Rose, and Shirley A. Sahrmann. "Patterns of Hip Rotation Range of Motion: A Comparison Between Healthy Subjects and Patients with Low Back Pain." *Physical Therapy* 70.9 (1990): 537–541. Print.

Fuentes, D. et al. "Online Motion Recognition Using an Accelerometer in a Mobile Device." *Expert Systems with Applications* 39.3 (2012): 2461–2465. *ScienceDirect*. Web. 28 Oct. 2013.

Grimnes, M. et al. "Velocity and Position Approximations from Left Ventricular 3D Accelerometer Data." *Bioengineering Conference, 2004. Proceedings of the IEEE 30th Annual Northeast*. N. p., 2004. 25–26. *IEEE Xplore*. Web.

Li, Xiangrong, Yi Lu, and YuMing Zhang. "Accelerometer-Based Position and Speed Sensing for Manual Pipe Welding Process." *The International Journal of Advanced Manufacturing Technology* 69.1-4 (2013): 705–713. *link.springer.com*. Web. 18 Feb. 2014.

Mann, Rena K. et al. "Comparing Movement Patterns Associated with Huntington's Chorea and Parkinson's Dyskinesia." *Experimental Brain Research* 218.4 (2012): 639–654. *link.springer.com*. Web. 18 Feb. 2014.

Mesbah, M. et al. "Accelerometer-Based Fetal Movement Detection." *2011 Annual International Conference of the IEEE Engineering in Medicine and Biology Society,EMBC*. N. p., 2011. 7877–7880. *IEEE Xplore*. Web.

Meta Motion. "Magnetic Motion Capture." *Meta Motion*. N. p., 2013. Web. 27 Oct. 2013.

Milosevic, Mladen, Emil Jovanov, and Aleksandar Milenkovic. "Quantifying Timed-Up-and-Go Test: A Smartphone Implementation." *2013 IEEE International Conference on Body Sensor Networks (BSN)*. N. p., 2013. 1–6. *IEEE Xplore*. Web.

Roetenberg, Daniel, Henk Luinge, and Per Slycke. "Xsens MVN: Full 6DOF Human Motion Tracking Using Miniature Inertial Sensors." *XSENS TECHNOLOGIES* (2013): n. pag. Print.

Ryu, Mun-Ho et al. "Ambulatory Gait Analysis with Accelerometer on Smart Phone." *American Scientific Publishers* 10.5-6 (2012): 1137–1141. Print.

Slyper, Ronit, and Jessica K. Hodgins. "Action Capture with Accelerometers." *Proceedings of the 2008 ACM SIGGRAPH/Eurographics Symposium on Computer Animation*. Aire-la-Ville, Switzerland, Switzerland: Eurographics Association, 2008. 193–199. *ACM Digital Library*. Web. 18 Feb. 2014. SCA '08.

Tundo, M.D., E. Lemaire, and N. Baddour. "Correcting Smartphone Orientation for Accelerometer-Based Analysis." *2013 IEEE International Symposium on Medical Measurements and Applications Proceedings (MeMeA)*. N. p., 2013. 58–62. *IEEE Xplore*. Web.

Wavefront Labs. "Sensor Data." *Wavefront Labs*. N. p., 2010 2009. Web. 27 Oct. 2013.

Yao, Xu et al. "The Design of a Real-Time Accelerometer-Based Sleeping Position Monitoring System and Its Application on Obstructive Sleep Apnea Syndrome." *2012 International Conference on Systems and Informatics (ICSAI)*. N. p., 2012. 1061–1066. *IEEE Xplore*. Web.

Zhang, Shumei et al. "Activity Monitoring Using a Smart Phone's Accelerometer with Hierarchical Classification." *2010 Sixth International Conference on Intelligent Environments (IE)*. N. p., 2010. 158–163. *IEEE Xplore*. Web.